Xenogeneic silencing-mediated temperature- and salinity-dependent regulation of type III secretion system 2 in *Vibrio parahaemolyticus*

DOCTORAL DISSERTATION

Submitted as partial fulfillment of the requirement to obtain

Doctor of Philosophy Degree from Graduate School of

Frontier Biosciences, Osaka University, Japan

March 2022

Andre Pratama

32A19707

Prof. Tetsuya Iida

Supervisor

ABSTRACT

Xenogeneic silencing-mediated temperature- and salinity-dependent regulation of type III secretion system 2 in *Vibrio parahaemolyticus*

Andre Pratama

A marine bacterium *Vibrio parahaemolyticus* is a common seafood-borne pathogen that causes acute diarrhea in humans. A major virulence determinant of *V. parahaemolyticus* is the type III secretion system 2 (T3SS2) encoded on a pathogenicity island, Vp-PAI. The T3SS2 gene expression is affected by external environmental cues such as temperature and salinity: the expression is induced at 37°C and 0.1 M NaCl (a permissive condition) but is silenced at lower temperature or higher salinity (non-permissive conditions). However, the mechanism by which T3SS expression is regulated in a temperature- and salinity-dependent manner remains unknown. Here, I show that histone-like nucleoid-structuring protein (H-NS), a xenogeneic silencing protein, regulates T3SS2 gene expression by transcriptional silencing of VtrB, a master regulator of Vp-PAI, under the non-permissive conditions. H-NS bound to the *vtrB* promoter, and the binding sites partially overlapped with the binding sites of two positive regulators of *vtrB*, VtrA and ToxR, which may block transcriptional activation of *vtrB*. The H-NS family protein silences its target gene transcription by binding and subsequent multimerization to form filaments and/or bridges nucleoprotein complex. In *V. parahaemolyticus*, mutations at dimerization domain of H-NS impaired repression of VtrB production *in vivo* but retains its binding ability to the *vtrB* promoter *in vitro*, suggesting that H-NS multimerization is also crucial for silencing of *vtrB* transcription. Together, these findings demonstrate that H-NS mediated xenogeneic silencing is pivotal to the temperature- and salinity-dependent T3SS2 gene regulation, and expand our understanding of the virulence regulation in *V. parahaemolyticus*.

TABLE OF CONTENTS

LIST OF ABBREVIATIONS

6-FAM: 6-carboxyfluorescein

BSA: bovine serum albumin

CBB: coomassie brilliant blue

CRISPR: clustered regularly interspaced short palindromic

DNA: deoxyribonucleic acid

EDTA: ethylenediaminetetraacetic acid

EMSA: electrophoretic mobility shift assay

F-actin: filamentous actin

KP: Kanagawa phenomenon

LB: Luria-Bertani

MAPK: mitogen-activated protein kinase

NF-κB: nuclear factor-kappa B

PCR: polymerase chain reaction

PVDF: polyvinylidene difluoride

RNAP: ribonucleic acid polymerase

SDS: sodium dodecyl sulfate

SDS-PAGE: sodium dodecyl sulfate-polyacrylamide gel electrophoresis

T3SS: type III secretion system

TAKI: TGF-β-activated kinase 1

TBS: Tris-buffered saline

TRE: T-rich repetitive element

Vp-PAI: *V. parahaemolyticus* pathogenicity island

WT: wild type

qRT-PCR: quantitative real time polymerase chain reaction

LIST OF FIGURES

LIST OF TABLES

CHAPTER 1

GENERAL INTRODUCTION

1.1 *Vibrio parahaemolyticus* from origin to pandemic

Vibrio parahaemolyticus is a member of *Vibrionaceae* that are gram-negative, comma-shaped, motile, facultative anaerobic and fermentative γ-Proteobacteria inhabiting the marine and brackish environment (Thompson et al., 2004) (**Fig. 1**). This bacterium is also a major cause of seafood-borne illness in humans (Baker-Austin et al., 2018; Janda et al., 1988). Among the *Vibrionaceae* family that comprises six genera with over 100 species, *V. parahaemolyticus* is the most common human pathogen, along with *V. cholerae* that causes cholera, an acute severe diarrhea illness. Historically, this bacterium is part of Japanese researchers' significant findings in the field of infectious diseases. Dr. Tsunesaburo Fujino at the Research Institute for Microbial Diseases, Osaka University, first isolated this bacterium as the causative agent of a foodborne outbreak “Shirasu-food poisoning” (Shirasu is boiled and half-dried of whitebait or young sardine), which occurred in Osaka, Japan, in 1950, and resulted in 272 patients with acute gastroenteritis and 20 deaths (Fujino et al., 1953; Shinoda, 2011). *V. parahaemolyticus* infections typically cause acute gastroenteritis in humans. The transmission of *V. parahaemolyticus* to humans is mainly associated with the consumption of raw or undercooked fish and shellfish contaminated by this organism. The acute gastroenteritis symptoms include diarrhea, abdominal pain, fever, and vomiting after 8-24 hours of incubation. The outbreaks

often occur in Asia, including Japan, because eating raw fish is part of the cuisine and culture of this region. In Western countries such as the United States, the primary source of *V. parahaemolyticus* infections is the consumption of raw oysters, a delicacy food in this region.

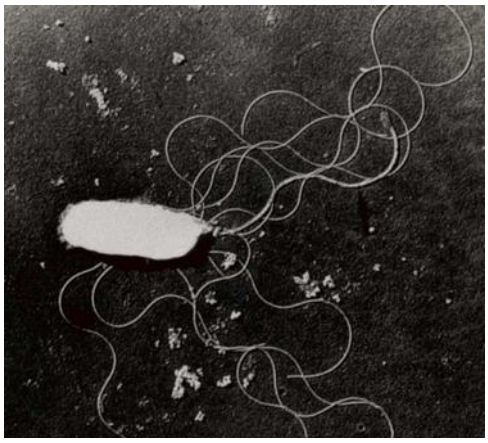

Figure 1. Electron micrograph of *Vibrio parahaemolyticus*.

Since its first identification, *V. parahaemolyticus*, also known as "chou-en vibrio" in Japanese, has long been one of the leading causes of bacterial food poisoning in Japan. *V. parahaemolyticus* has also caused outbreaks of seafood-associated gastroenteritis in many continents around the world: its infections have been reported in India (Chatterjee et al., 1970), Bangladesh (Hughes et al., 1978), Thailand (Echeverria et al., 1983; Sriratanaban & Reinprayoon, 1982), Malaysia (Jegathesan & Paramasivam, 1976), China (Hsu et al., 1977), Singapore (Goh & Lam, 1981), Australia (Ghosh & Bowen, 1980), Togo (Bockemühl et al., 1972), Bulgaria (Zakhariev, 1976), Mexico (Merson et al., 1976), Canada (Todd, 1981), Panama (Kourany & Vasquez, 1975), and United States (Barker et al., 1974; Bryan, 1980; Molenda et al., 1972) by 1996.

Starting from 1996, the infections by *V. parahaemolyticus* have become pandemic, which is still ongoing (Baker-Austin et al., 2018; Ansaruzzaman et al., 2005; Martinez-Urtaza et al., 2005; Hurley et al. 2006; Cabanillas-Beltrán et al., 2006; Ottaviani et al., 2008; Leal et al., 2008; Velazquez-Roman et al. 2014). One method often used in epidemiological studies is serotyping for surveillance of the spread of pathogenic microorganisms (Henriksen, 1978). The serotype determination in *V. parahaemolyticus* is judged based on the properties of the somatic (O) and capsular (K) antigens, which are then defined by the combination of O and K antigens. So far, 13 O serotypes and 69 K serotypes have been reported, and diverse serotypes are often found in *V. parahaemolyticus* isolates (Faruque & Nair, 2006; Iguchi et al., 1995). In 1996, there was a high incidence of *V. parahaemolyticus* infections in Calcutta, India, by the unique strains with a single O3:K6 serotype that dominated from February to August. Because those isolates showed nearly identical genotypes as judged by arbitrarily primed PCR, a genome typing method, the O3:K6 strains are considered to be emerged from a single clone and thus called as "the pandemic clone" (Okuda et al., 1997). In the same year, the O3:K6 strains appeared in Japanese gastroenteritis patients who traveled from Southeast Asian countries (Okuda et al., 1997). Since then, many reports on *V. parahaemolyticus* outbreaks worldwide are associated with the new O3:K6 strains: those were found in patients with gastroenteritis in other countries such as Bangladesh, Taiwan, Laos, Japan, Thailand, Korea, and the United States (Matsumoto et al., 2000), indicating the rapid and global spread of this serotype of *V.*

parahaemolyticus. The O3:K6 strains are classified into a single sequence type (ST3) by multilocus sequence typing, a gold standard method for the genome typing, based on the sequence variations of seven housekeeping genes of *V. parahaemolyticus* (Gonzalez-Escalona et al., 2017). Recently, another sequence type, ST36 (serotype O4:K12 or O4:KUT), is also involved in many *V. parahaemolyticus* outbreaks in the Pacific Northwest region of the United States and also spread to Spain and Peru (Martinez-Urtaza & Baker-Austin, 2020) (**Fig. 2**), suggesting the complex global expansion of *V. parahaemolyticus* is ongoing. In the United States, *V. parahaemolyticus* causes around 50,000 illnesses every year, while the actual number of *V. parahaemolyticus* infections is estimated to be ~140-fold greater (Martinez-Urtaza & Baker-Austin, 2020).

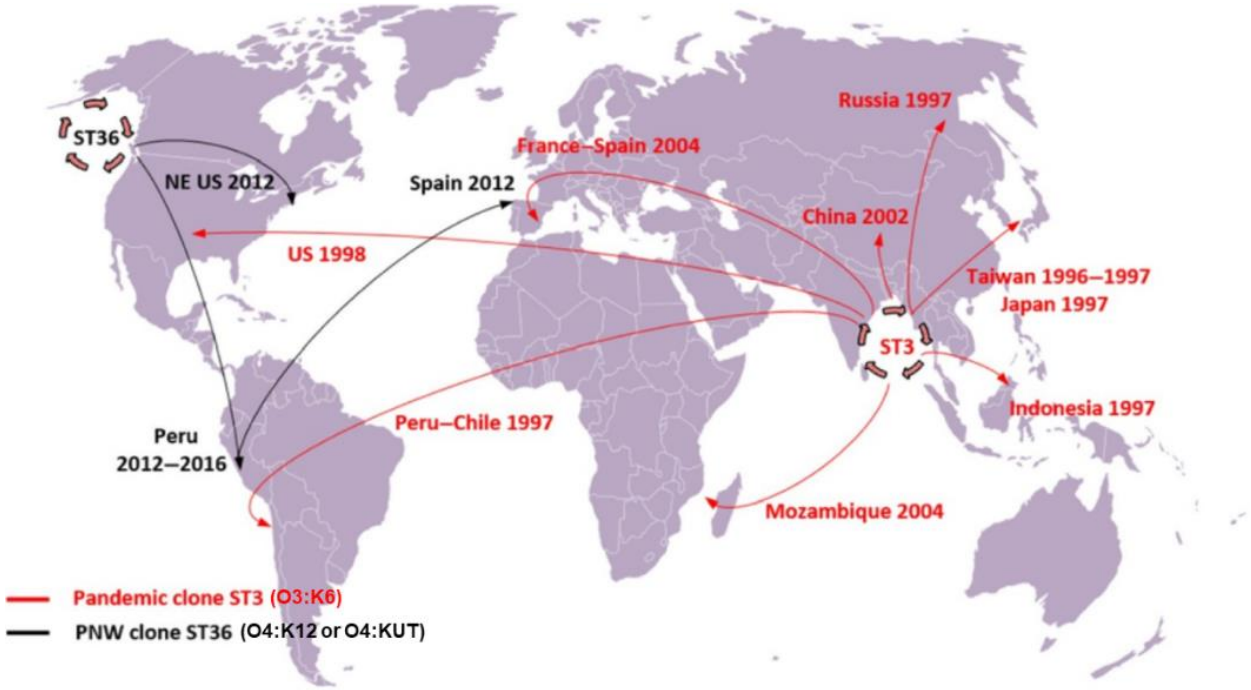

Figure 2. The global spread of *V. parahaemolyticus* pandemic clone ST3 (serotype O3:K6) and the Pacific Northwest clone ST36 (serotype O4:K12 or O4:KUT) (Adapted from Martinez-Urtaza and Baker-Austin, 2020).

1.2 Vibrio parahaemolyticus virulence factors

V. parahaemolyticus is a commensal bacterium in the ocean, and most strains isolated from the natural inhabit are not pathogenic to humans (Letchumanan et al., 2014). Conversely, only a minor proportion of *V. parahaemolyticus* is thought to be capable of causing gastroenteritis in humans. Pathogenic strains of *V. parahaemolyticus* show the β-hemolytic activity on blood agar medium (Miyamoto et al., 1969). This hemolytic activity is known as the "Kanagawa phenomenon" (KP), which is characterized by a clear hemolytic halo around the periphery of colonies on a specialized agar medium (Wagatsuma medium). The responsible factor for KP is the exotoxin called thermostable direct hemolysin (TDH) (Sakurai et al., 1973). TDH is a pore-forming toxin and shows various biological activities including hemolytic activity, cardiotoxicity, cytotoxicity and enterotoxicity (Honda et al., 1976; Honda et al., 1976; Sakurai et al., 1975, 1976). Even though most of the cases of *V. parahaemolyticus* infection are associated with KP-positive strains and most environment isolates are KP-negative strains, some cases can be caused by KP-negative strains (Honda et al., 1987). Such KP-negative strains possess another toxin called TDH-related hemolysin (TRH), which has similar but not identical in biological, immunological, and physiochemical properties to TDH (Honda et al., 1988; Honda & Iida, 1993). TDH and TRH are encoded by *tdh* and *trh* genes, respectively, which are used as an international standard (ISO 21872-1) to detect potential pathogenic *V. parahaemolyticus* in the food industry. These toxins have been considered as major virulence

factors associated with gastroenteritis outcome in *V. parahaemolyticus* infections due to their epidemiological association.

The advance of DNA sequencing technologies in the early 1990s enabled the whole genome sequencing of organisms (Fleischmann et al., 1995). The complete genome of *V. parahaemolyticus* strain RIMD2210633 (a KP-positive clinical isolate with serotype O3:K6) was sequenced in 2003 (Makino et al., 2003). This uncovered the presence of two gene clusters encoding two sets of type III secretion systems (T3SS) in *V. parahaemolyticus*, namely T3SS1 and T3SS2 (**Fig. 3A**). Although *V. parahaemolyticus* has two chromosomes, which is a common feature of *Vibrionaceae* (Okada et al., 2005), T3SS1 and T3SS2 are encoded on the chromosome 1 and 2, respectively.

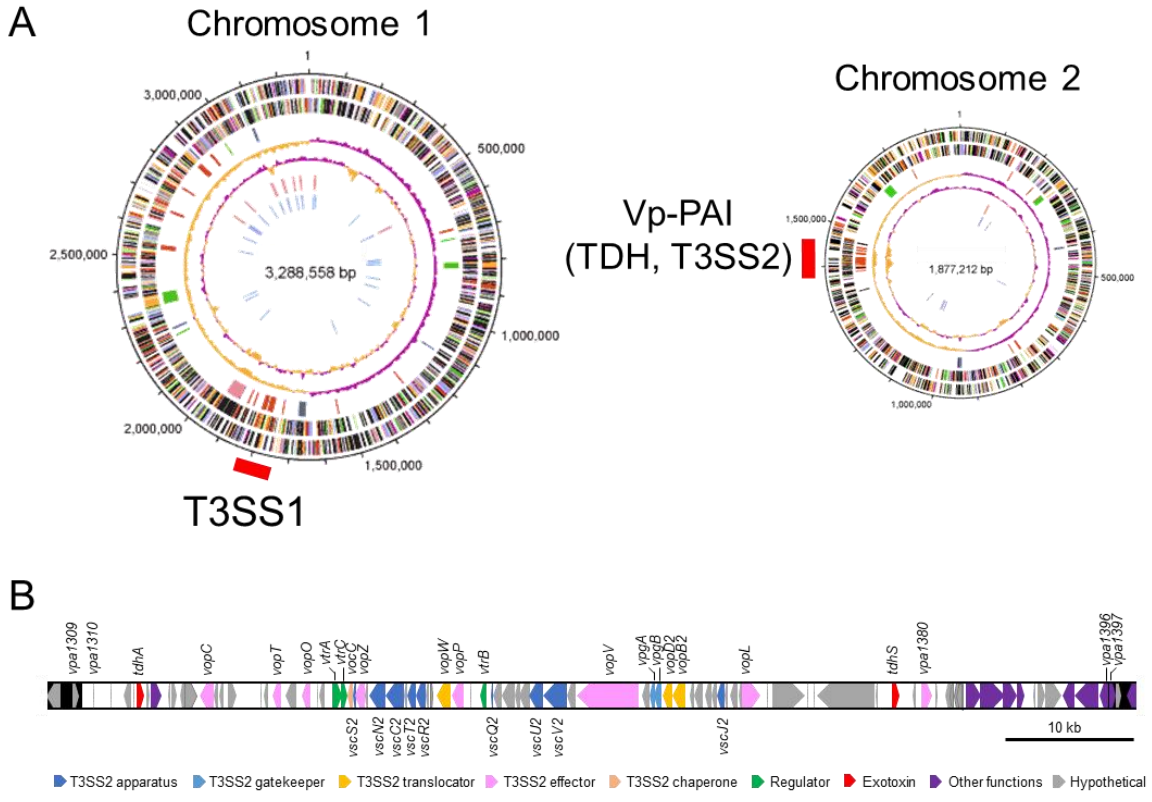

Figure 3. (**A**) The genome of *V. parahaemolyticus* strain RIMD2210633 (O3:K6), composed of two circular chromosomes (adapted from Makino et al., 2003 with modifications). The locations of genes for Type III secretion systems (T3SSs: T3SS1 and T3SS2) and TDH are indicated by red lines. (**B**) Genetic organization of Vp-PAI spanning open reading frames (ORFs) *vpa1310* to *vpa1396*. The Vp-PAI region is shown in white, and its neighboring regions are shown in black. Arrows indicate ORFs with their directions and functions and ORFs are color-coded according to their function; gene names and ORFs adjacent to the Vp-PAI border are shown above the arrows. The gene names annotated in the core structural components of T3SS are shown below the arrows (adapted from Makino et al., 2003 and Matsuda et al., 2020 with modification).

T3SSs are syringe-like protein export machinery that are widespread in Gram-negative pathogens and symbionts (Deng et al., 2017; Hueck, 1998; Radics et al., 2014). The T3SS apparatus is composed of over 20 proteins assembled from the basal body spanning bacterial envelope, the cytoplasmic components for the sorting platform, the needle protruding from bacteria, and the translocon at the tip of the needle (**Fig. 4A-C**). The T3SS exports protein substrates, so-called effectors, to extracellular milieu ("secretion") while injecting effectors into the host cells directly upon contact with host cells through the needle as a conduit and the translocon channel formed in the host cell plasma membrane ("translocation") (**Fig. 4C**). The translocated effectors then modify host cell functions and contribute to bacterial pathogenicity and symbiosis (Deng et al., 2017).

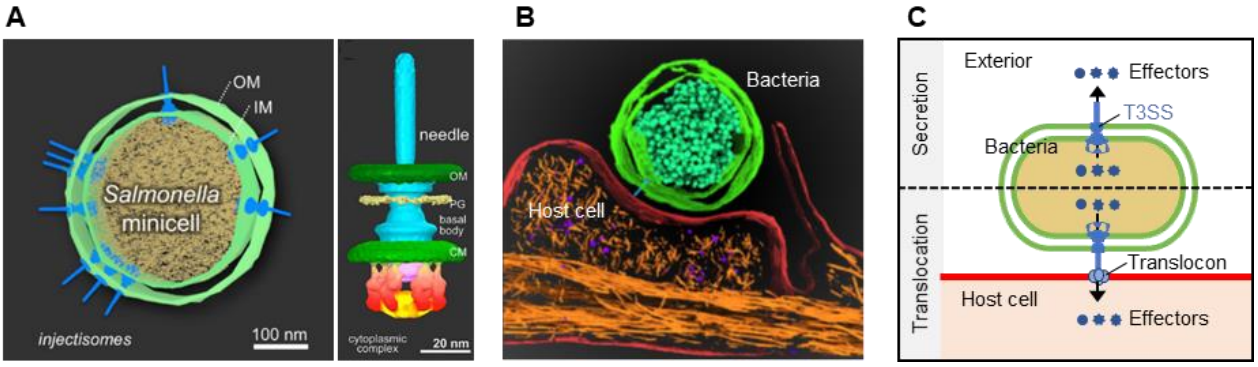

Figure 4. Cryo-electron microscopy images of the *Salmonella* T3SS structure embedded in the cell envelope (**A**) and the T3SS-mediated *Salmonella*-host interaction (**B**) (adapted from Hu et al., 2014; Hu et al., 2017; and Park et al., 2018 with modifications). (**C**) Schematic representation of effector export by the T3SS. Top (secretion): effectors are released to extracellular milieu. Bottom (translocation): upon contact with host cells, effectors are directly injected into host cells through the translocon channel formed in the host cell membranes. OM, outer membrane; IM, inner membrane.

Many enteric bacterial pathogens indeed rely on T3SSs for their pathogenicity inside the gastrointestinal tract during their enteric infections by modulating essential host cell functions (Pinaud et al., 2018). *Yersinia enterocolitica* and *Y. pseudotuberculosis,* which cause yersiniosis, employ the T3SS to evade the host immune system by modulating innate immune defense in phagocytes (Pha & Navarro, 2016). Enteropathogenic *Escherichia coli* (EPEC) and enterohemorrhagic *E. coli* (EHEC), both of which are diarrheagenic *E. coli*, utilize the T3SS to form attaching and effacing (A/E) lesion, which is a unique phenotype induced by these pathogens, characterized by the effacement of epithelial microvilli and the accumulation of F-actin beneath the adherent bacteria, for the colonization (Gaytán et al., 2016). *Salmonella enterica*, a facultative intracellular pathogen, employs two different T3SSs: to invade non-

phagocytic cells (T3SS-1 encoded on *Salmonella* pathogenicity island 1 or SPI-1) and to survive in *Salmonella*-containing vacuole (T3SS-2 encoded on *Salmonella* pathogenicity island 2 or SPI-2) (Jennings et al., 2017; D. Zhou & Galán, 2001). *Shigella*, the causative agent of shigellosis, delivers effectors into epithelial cells through the T3SS to promote membrane ruffling and bacterial entry (Muthuramalingam et al., 2021).

Virulence genes of pathogenic bacteria are often encoded on the pathogenicity island (PAI) in the chromosome (Hacker & Kaper, 2000). PAI is a large genomic region of 10-200 kilobases (kb) in size and a class of genomic island acquired by horizontal gene transfer events as characterized by the different nucleotide composition and codon usage bias between PAI and core genome as well as the association of PAI with mobile genetic elements (Gal-Mor & Finlay, 2006). The complete genome sequence of *V. parahaemolyticus* also revealed the presence of an 80-kb genomic island including *tdh* and the T3SS2 gene cluster on the chromosome 2 (**Fig. 3B**) (Makino et al., 2003). This genomic island spans the open reading frames (ORFs) *vpa1310* to *vpa1396* and is flanked by 5-bp direct repeats (Sugiyama et al., 2008). The lower guanine-cytosine (GC) content of this region (39.8%) compared to the average GC content of the entire genome (45.4%) and the presence of putative mobile elements suggest that this genomic island was acquired via horizontal gene transfer (Makino et al., 2003; Sugiyama et al., 2008). Based on these characteristics of foreign DNA and the presence of virulence genes, this region has been proposed to be a pathogenicity island and is referred to as *V. parahaemolyticus*

pathogenicity island (Vp-PAI) (Makino et al., 2003). The putative mobile elements in Vp-PAI belong to a particular class of the Tn7-like transposon with CRISPR-Cas system that enables guide RNA-directed DNA integration into the chromosome (Peters et al., 2017). The guide RNA element of *V. parahaemolyticus* matches the attachment site adjacent to *vpa1397* (Petassi et al., 2020), which may explain how the Vp-PAI was integrated into the region between ORFs *vpa1309* and *vpa1397* on the chromosome 2 (Izutsu et al., 2008).

The Vp-PAI has distributed among the pandemic KP-positive strains and the non-pandemic KP-positive strains with other serotypes but is absent in non-pathogenic strains (Izutsu et al., 2008). The KP-negative but *trh*-positive clinical isolates also harbor the Vp-PAI, which is similar but not identical to the Vp-PAI of KP-positive strains, and besides differences in toxin genes (*tdh* and/or *trh*), there are also variations in the T3SS2 gene cluster (Okada et al., 2009). Thus, T3SS2 gene cluster is divided into two different phylogroups, T3SS2α (KP-positive T3SS2) and T3SS2β (KP-negative T3SS2) (Okada et al., 2009). These two variants of T3SS2s are also distributed in other *Vibrio* species such as non-O1/non-O139 *V. cholerae* which lacks cholera toxin but often causes sporadic cases of diarrhea, indicating non-restrictive distribution of the T3SS2 gene cluster across the species levels in *Vibrio* (Okada et al., 2010).

As described earlier, until the discovery of T3SSs, TDH and TRH have been considered to be the most important virulence factors for the enterotoxicity of *V. parahaemolyticus*. However,

tdh or *trh* isogenic mutant of *V. parahaemolyticus* still retains enterotoxicity as judged by the rabbit ileal loop test, a gold standard method to evaluate the enterotoxicity of *V. parahaemolyticus*, suggesting that unknown factor(s) besides these toxins is involved in the enterotoxicity (Park et al., 2004; Xu et al., 1994). The finding that *V. parahaemolyticus* possesses two sets of T3SSs drove subsequent analysis to examine the contribution of T3SSs to the pathogenicity of *V. parahaemolyticus*. T3SS1 and T3SS2 are functionally independent secretory apparatus, each secreting its own effectors (Park et al., 2004). To experimentally verify the contribution of two T3SSs to the pathogenicity of *V. parahaemolyticus*, the strains in which each T3SS was inactivated by gene deletion were subjected to the rabbit ileal loop test, demonstrated that T3SS2 is important for the enterotoxicity of this organism (Hiyoshi et al., 2010). The role of T3SS2 for the enterotoxicity has also been examined in several other animal models, the infant rabbit model and the piglet model (Piñeyro et al., 2010; Ritchie et al., 2012).

T3SS itself is the secretion machinery exporting effectors that produce the effects on the host cells. So far, nine effectors have been identified as T3SS2-specific effectors (VopP, VopT, VopL, VopC, VopV, VopZ, VopO, VPA1380, and VPA1328), all of which are encoded in Vp-PAI (Matsuda et al., 2020; Plaza et al., 2021). Among them, VopV and VopZ have been reported to be crucial effectors for T3SS2-mediated enterotoxicity (Hiyoshi et al., 2011; Zhou et al., 2013, 2014). VopV binds to F-actin with a high affinity of Kd = 54.4 nM, and this F-actin binding activity of VopV is correlated with the VopV-dependent enterotoxicity *in vivo*

(Hiyoshi et al., 2011; Nishimura et al., 2015). VopZ modulates host immune response by preventing TAK1 and subsequent downstream NF-*κB* and MAPK signaling. Deletion of *vopZ* also abolishes the enterotoxicity of *V. parahaemolyticus* in the infant rabbit model, although its detailed mechanism is unknown (Zhou et al., 2013). In addition to those conventional effectors, a recent study has shown that T3SS2 conducts unconventional export of TDH, which mediates the TDH-dependent enterotoxicitiy of *V. parahaemolyticus* (Matsuda et al., 2019). TDH is an exotoxin which is once released from bacteria via the canonical general secretory pathway, but a portion of mature TDH can be exported by T3SS2. Together, T3SS2 plays a central role in the enterotoxicity of *V. parahaemolyticus* during enteric infection, by transporting these effectors and the toxin.

V. cholerae is a closely related pathogenic *Vibrio* species of *V. parahaemolyticus* and causes devastating disease of cholera for centuries. The virulence genes of *V. cholerae* have been found in the genetic islands acquired by horizontal gene transfer (Faruque & Mekalanos, 2003). These genetic islands are CTXΦ genetic island, which encodes the genes for the cholera toxin (*ctx*) as the main factor for the induction of severe diarrhea, and the pathogenicity island 1 (VPI-1), which encodes the toxin-coregulated pilus (TCP) as the essential factor for intestinal colonization of *V. cholerae* (Faruque & Mekalanos, 2003). Those virulence genes expression from two different genetic islands is regulated under one master regulator, ToxT (DiRita et al., 1991). The *toxT* expression requires two unique membrane-bound transcriptional activators,

TcpP and ToxR (DiRita et al., 1991; Häse & Mekalanos, 1998), which could sense external stimuli such as bile acids to induce their activity (Bina et al., 2021; Hung & Mekalanos, 2005; Yang et al., 2013). Interestingly, although the pathogenic mechanism of *V. parahaemolyticus*, which relies on the complex T3SS2 machinery, is quite distinct from that of *V. cholerae*, which is dependent on the single exotoxin cholera toxin, the regulation of T3SS2 genes expression in *V. parahaemolyticus* is regulated in a similar fashion in which membrane-bound transcriptional activators are the key on the T3SS2 gene regulations as described below.

1.3 T3SS2 genes regulation

Vp-PAI gene expression, including T3SS2-related genes, relies on a regulatory cascade consisting of two transcriptional activators, VtrA and VtrB, encoded within Vp-PAI (**Fig. 5**) (Kodama et al., 2010). VtrA and VtrB contain N-terminal regions sharing homology with winged-helix-turn-helix (wHTH) DNA-binding domains of OmpR-family proteins. VtrA forms a complex with VtrC, a co-transcribed protein with VtrA, and positively controls *vtrB* transcription by binding to the upstream region *vtrB* (Li et al., 2016; Okada et al., 2017). VtrA consists of three domains: the N-terminal DNA binding domain, the central transmembrane domain embedded in the inner membrane, and the C-terminal periplasmic domain (Okada et al., 2017). The periplasmic and transmembrane domains are responsible for the dimerization of VtrA, which is crucial for transcriptional activation of *vtrB*. The periplasmic domain of VtrA

is also thought to serve as the environmental sensor that senses bile acids, which may induce the oligomerization of VtrA and enhance its DNA-binding and transcriptional activation activity (Li et al., 2016; Okada et al., 2017). VtrB contains the N-terminal DNA-binding region with a putative transmembrane domain but lacks the periplasmic domain, unlike VtrA. Over 60 genes, most of which are encoded in Vp-PAI, are activated under the control of VtrB (Kodama et al., 2010). Although transcriptional activation of *vtrB* by VtrA is the fundamental step for the expression of the T3SS2 gene cluster, the VtrA binding region within the *vtrB* promoter is not yet known. The *vtrB* promoter contains T-rich repetitive elements (TRE), an essential region for *vtrB* transcription (Okada et al., 2017), but its exact role in transcriptional activation *vtrB* is also unknown.

Besides the VtrA-VtrB regulatory cascade, ToxR, a transmembrane transcriptional regulator homologous to *V. cholerae* ToxR (hereinafter, *V. parahaemolyticus* ToxR and *V. cholerae* ToxRs are called Vp-ToxR and Vc-ToxR, respectively, for distinction), is also involved in the T3SSS2 gene regulation through the transcriptional activation of *vtrB* (Hubbard et al., 2016). Although Vc-ToxR was initially found as toxin regulatory protein that activates *ctx* transcription in *V. cholerae* (Miller & Mekalanos, 1984), it also regulates several genes essential for virulence and survival inside the host. As described earlier, Vc-ToxR stimulates the *toxT* expression together with TcpP. The expression of outer membrane protein U (OmpU), which is vital for survival inside the host to resist bile acids and host-derived

antimicrobial peptides, is also controlled by Vc-ToxR (Crawford et al., 1998; Zingl et al., 2020; Provenzano et al., 2000). In *V. parahaemolyticus,* Vp-ToxR positively regulates TDH production (Lin et al., 1993) and OmpU expression as well to resist bile acids and low pH stresses (Provenzano et al., 2000; Whitaker et al., 2012). These observations indicate that Vp-ToxR also plays a critical role in virulence gene expression in *V. parahaemolyticus*, as well as the Vc-ToxR in *V. cholerae*. However, the precise role of Vp-ToxR in *vtrB* transcription, including whether its effect is direct or indirect, remains unclear.

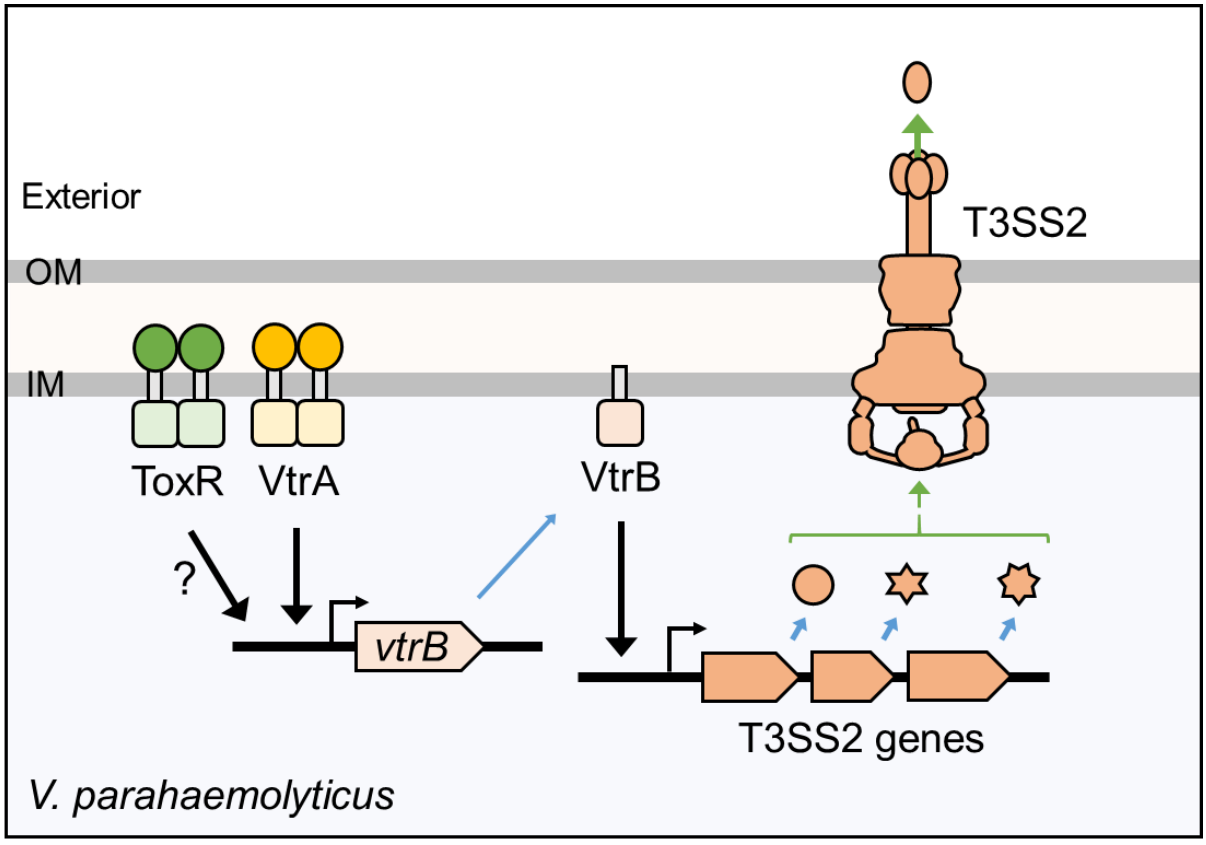

Figure 5. Regulation of T3SS2 gene expression. A membrane-bound transcriptional activator VtrA (gold) binds to *vtrB* promotor and activates *vtrB* transcription. Another known regulator, Vp-ToxR (green), stimulates the *vtrB* transcription by a yet to be determined mechanism. Consequently, VtrB (light orange) activates the T3SS2 gene cluster (orange). OM, outer membrane; IM, inner membrane.

Pathogenic bacteria sense and respond to various physical and chemical cues for virulence and adaptation to their host environment during infection (Fang et al., 2016; Guiney, 1997). The expression of virulence factors in bacteria are generally transcriptionally regulated as a function of the environmental and host factors, including temperature, pH and host-derived molecules (Böhme et al., 2012; Carlson-Banning & Sperandio, 2018; Lustri et al., 2017; Pienkoß et al., 2021; Yother et al., 1986; Yu et al., 2010). Indeed, the T3SS2 protein production in *V. parahaemolyticus* also varies with external conditions such as physical changes in temperature and salinity (Gotoh et al., 2010). When *V. parahaemolyticus* is grown in LB medium (containing 0.1 M NaCl) at various temperatures, T3SS2-related proteins are expressed above 37°C but not below 30°C. On the other hand, when *V. parahaemolyticus* is cultured in LB medium with various concentrations of NaCl at a fixed temperature of 37°C, the production of T3SS2-related proteins is observed at NaCl concentration of 0.1 M, but not at concentrations above 0.3 M. Thus, T3SS2 expression is permitted at 37°C and NaCl concentration of 0.1 M (hereinafter referred to as the permissive condition) but is silenced at lower temperatures or higher NaCl concentrations (hereinafter referred to as the non-permissive conditions). In general, a human body temperature of 37°C is greater than the temperature of the marine environment (below 30°C), while the salinity in the human body is extremely lower than that of the marine environment (equivalent to about 0.5 M NaCl). Therefore, the phenomenon that T3SS2 expression is regulated in a temperature- and salinity-

dependent manner may reflect adaptation of *V. parahaemolyticus* from its natural habitat to the host environment during its infection, but the underlying mechanism has been yet to be defined.

1.4 Xenogeneic silencer of H-NS involved in T3SS2 gene regulation

As described above, gene expression in bacteria is regulated in response to environmental conditions, which is essential for bacterial fitness and survival. Bacterial gene expression can be divided into two steps: transcription (DNA to RNA) and translation (RNA to polypeptide chain). In transcription, the RNA polymerase (RNAP) is responsible to synthesize messenger RNA (mRNA) from DNA, which occurs in three steps: initiation, elongation and termination (Fig. 6). Besides RNAP, the transcription initiation involves sigma (σ) factor and promoter elements, such as −35 and −10. The RNAP holoenzyme with σ factor initially recognizes and binds to the promoter elements in a closed complex, then triggers conformational changes that create an open complex. The addition of nucleoside triphosphates (NTPs) enables synthesizing RNA transcripts in the initiating complex state.

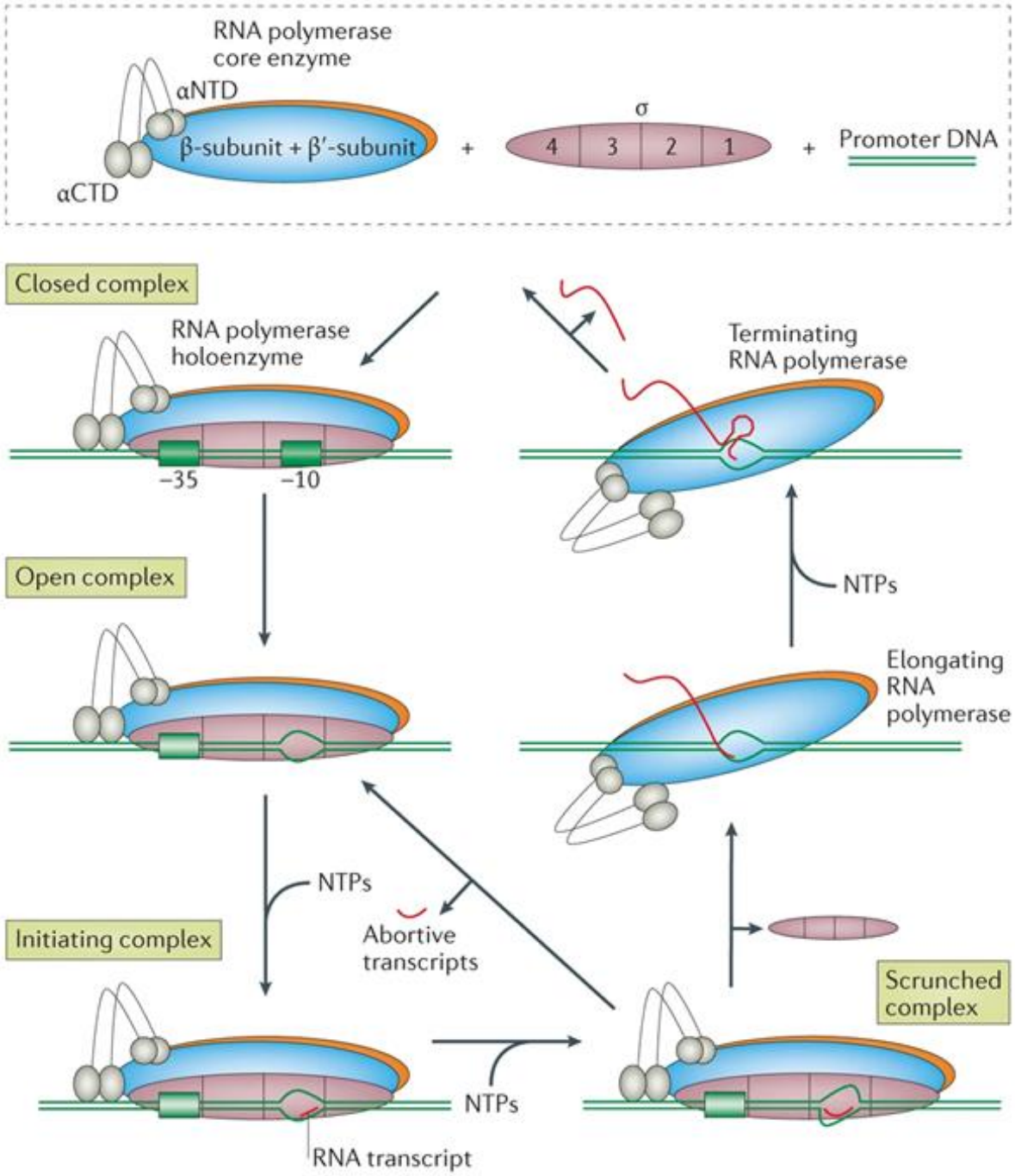

Figure 6. The transcription of bacterial genes (adapted from Browning and Busby 2016). NTPs, nucleoside triphosphates; α-CTD, the carboxyl terminal domain of the α subunit of RNA polymerase; α-NTD, the amino terminal domain of the α subunit of RNA polymerase; σ, sigma factor.

Many gene regulations by environmental factors occur at this transcription initiation step.

In order to control transcription, bacteria use DNA-binding transcriptional factors (activator

and repressor) for switching expression or repression of genes in response to external or internal stimuli. The transcription factors are categorized into local regulators, which activate a few genes in response to a specific signal, or global regulators, which activate many genes in response to complex signals that bacteria encounter in the environment (Babu et al., 2006). The latter plays a vital role for bacteria in adaptation to environmental changes. Notably, one global regulator that acts as a repressor to control transcription in response to complex signals is histone-like nucleoid structuring protein (H-NS).

H-NS was initially found along with HU protein as an effort to find histone-like protein in bacteria (Varshavsky et al., 1977), and extensive studies found that H-NS is a global transcriptional repressor widely distributed in Gram-negative bacteria (Singh et al., 2016). H-NS preferentially binds to AT-rich sequences for silencing target genes, mainly horizontally acquired foreign DNA with low GC content; hence it is also called "xenogeneic silencing" (Walthers et al., 2007). The virulence-related genes with the feature of foreign DNA are also silenced by H-NS in pathogenic bacteria, such as *Salmonella* (Navarre et al., 2006), *V. cholerae* (Ayala et al., 2015, 2017), EPEC (Bustamante et al., 2001), *Shigella* (Tobe et al., 1993).

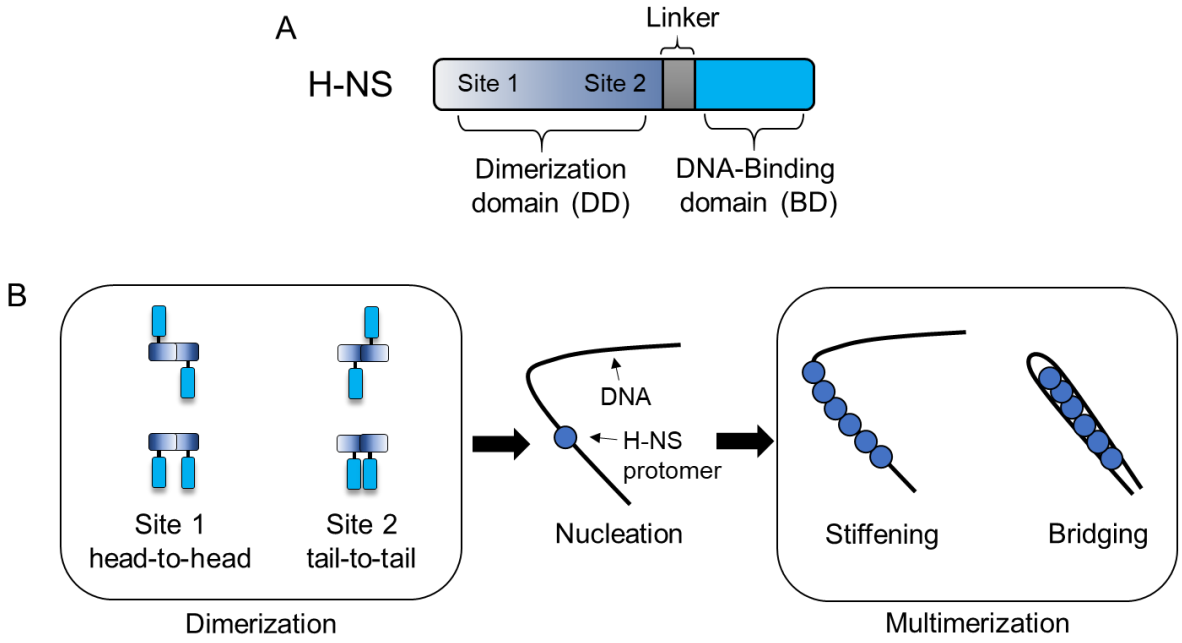

Figure 7. Schematic representation of H-NS: (**A**) its functional domain structures and (**B**) the proposed dimerization/multimerization conformations.

H-NS has three functional domains (**Fig. 7A**): the C-terminal domain with an AT-hook like motif that binds to the DNA minor groove (Gordon et al., 2011) and the N-terminal domain for dimerization and subsequently multimerization, which is facilitated by two different dimerization sites, site 1 (head-to-head dimer) and site 2 (tail-to-tail dimer) (Arold et al., 2010). These two domains are connected by a flexible linker, which promotes DNA binding of H-NS (Arold et al., 2010). The multimerization of H-NS underlies its silencing activity: from the individual binding of H-NS protomer to AT-rich sequence on the DNA (nucleation) to the rigid DNA filament formation by H-NS multimerization (DNA stiffening) and the DNA duplexes formation by DNA binding of H-NS (DNA bridging) (Liu et al., 2010) (**Fig. 7B**). In general, H-NS silences its target gene by interfering the transcriptional activity of RNA polymerase

(RNAP) in several ways (**Fig. 8**): (i) H-NS–DNA filament complex within promoter region block the RNAP-binding site (Amit et al., 2003; Chen et al., 2005); (ii) H-NS–DNA filament complexes serve as a roadblock and obstruct transcription elongation of RNAP (Dame et al., 2002); (iii) H-NS–DNA bridge complexes mediate DNA hairpin formation and trap RNAP in the hairpin loop (Dame et al., 2002).

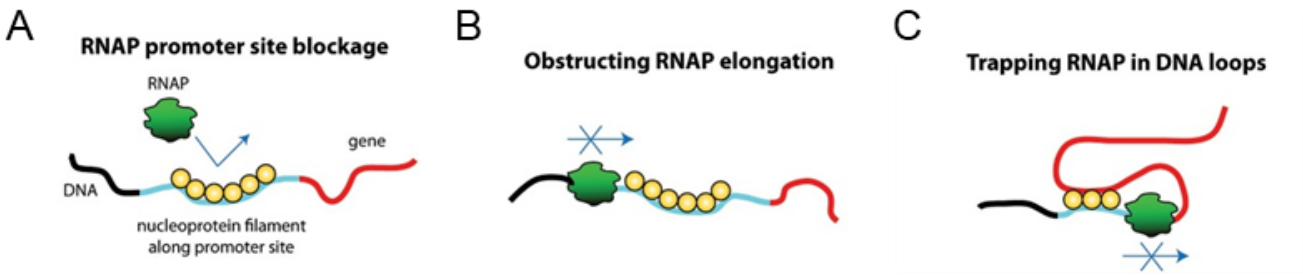

Figure 8. General mechanism of target gene silencing by H-NS (adapted from Lim et al., 2012).

Temperature and osmolarity are two driven factors that dictate the H-NS silencing activity through the H-NS dimerization domain. Hameed and colleagues have shown that at a body temperature of 37°C, dimerization site 2 of H-NS is unfolded and multimer formation of H-NS is broken, which results in the low silencing activity of H-NS at this condition (Hameed et al., 2019). Qin and colleagues have proposed that osmolarity through ionic strength of salts drives the switch of H-NS–DNA complexes between nucleation to DNA stiffening and bridging, and bridge disruption, in which the increase in ionic strength affects the electrostatic interaction and changes the H-NS protomer conformation (Qin et al., 2020). It is still unknown which formation, DNA stiffening or DNA bridging, can cause more robust silencing activity. One

study has reported that SsrB, the *Salmonella* T3SS-2 regulator, could outcompete the silencing by H-NS in nucleoprotein filament but not in bridged complexes (Walthers et al., 2011). Another study showed that bridged DNA–H-NS–DNA promotes Rho-dependent termination (Kotlajich et al., 2015). Although these studies suggest that DNA bridging of H-NS might show a more potent silencing activity, it should be noted that these studies are conducted *in vitro,* and its relevance *in vivo* remains unclear.

In *V. parahaemolyticus*, several studies reported that H-NS is involved in many gene regulations such as T3SS1 (Kodama et al., 2010), T3SS2 (Sun et al., 2014), T6SS1 (Salomon et al., 2014), T6SS2 (Sun et al., 2014), Biofilm (Enos-Berlage et al., 2005), polar flagella (Enos-Berlage et al., 2005) and lateral flagella (Wang et al., 2017), suggesting H-NS as a global regulator in this bacterium. Of interest, Sun and colleagues have shown that *hns* deletion upregulates the T3SS2 genes, *vtrA* and *vopB2* in *V. parahaemolyticus*. Furthermore, they have demonstrated that H-NS binds to the *vtrA* promoter region, and concluded that H-NS regulates T3SS2 through the repression of *vtrA*. However, that study did not examine other positive regulators of T3SS2, Vp-ToxR and VtrB, in the *hns*-deleted background. Moreover, the study was conducted in a single growth condition, and therefore did not explore whether the *vtrA* repression by H-NS varies in response to the environmental stimuli.

1.5 Overview of this study

The effort to understand the *V. parahaemolyticus* infections for almost 70 years has taught us how this pathogenic bacterium can cause disease by combining several factors to become a successful human pathogen. Given the similar mechanism between *V. parahaemolyticus* and *V. cholerae* to govern virulence genes expression, understanding the virulence regulation of *V. parahaemolyticus* may offer the possibility to explore an anti-virulence therapeutic strategy to control the diseases caused by these pathogenic bacteria without antibiotics for eradication, which may avoid the potential risk of the emergence of antibiotic-resistant bacteria that is a growing public health concern.

As described earlier, the *V. parahaemolyticus* T3SS2-related proteins are not produced under the non-permissive conditions that mimic the marine environment in which *V. parahaemolyticus* inhabits, but are expressed under the permissive condition that is similar to the host environment, an observation indicating that such physical changes trigger off the expression of virulence factors of *V. parahaemolyticus* in the host environment during infection. Given that the expression of virulence factors is a substantial metabolic burden for bacteria (Sturm et al., 2011), it is rational for *V. parahaemolyticus* to express its T3SS2-related proteins when and where they are needed and not when and where they are not needed. Due to the indispensable role of T3SS2 in enterotoxicity of *V. parahaemolyticus*, the temperature- and salinity-dependent T3SS2 regulation is probably critical for the virulence regulation of *V.*

parahaemolyticus in establishing its enteric infection, but its molecular mechanism has remained unclear. Thus, in this study I explored the question: how is T3SS2 expression regulated in a temperature and salinity-dependent manner?

To begin with, I sought to answer this question by first examining the status of T3SS2-related proteins and regulators at various temperature and salinity, and identified that transcriptional activation of *vtrB* is the checkpoint in temperature- and salinity-dependent T3SS2 regulation. The expression of two positive regulators of *vtrB*, VtrA and Vp-ToxR, was not affected by changes in temperature and salinity, suggesting that these environmental cues are not stimuli for two positive regulators' activity. Furthermore, I found that the *hns*-deleted strain abolishes the temperature- and salinity-dependent suppression of *vtrB* but not that of *vtrA* transcription. The discrepancy between my result and the previous report could be explained by extensive observation of this study on T3SS2 regulators' status at transcriptional and translational levels under various conditions. Moreover, the binding regions of VtrA and Vp-ToxR within the *vtrB* promoter were AT-rich regions overlapping with the binding sites of H-NS. Mutations at two critical residues for oligomerization of H-NS, leucine to proline at residue 30 (L30P) and isoleucine to cysteine at residue 70 (I70C), dampened the silencing activity of H-NS on VtrB protein production under the non-permissive conditions. Thus, these findings suggest that H-NS blocks the binding of VtrA and Vp-ToxR to *vtrB* promoter by its binding and multimerization forming stiffened filament and/or bridging DNA duplexes at non-

permissive conditions, which may underlie the temperature- and salinity-dependent regulation of T3SS2 in *V. parahaemolyticus.*

CHAPTER 2

METHODOLOGY

2.1 Bacterial strains, primers, plasmids, and growth conditions

Vibrio parahaemolyticus RIMD2210633 (a *tdh*- and T3SS2-positive clinical isolate, serotype O3:K6) (Makino et al., 2003) was used as the wild-type strain in this study. *E. coli* DH5α and SM10λ*pir* were used for DNA manipulation. Strains and plasmids are listed in Tables 1–4. The *V. parahaemolyticus* strains were grown in LB medium with modified NaCl concentrations (tryptone, 1%; yeast extract, 0.5%; NaCl, 0.1–0.5 M).

2.2 Mutant constructions

A four-primer PCR technique was used to engineer deletion mutants as described previously (Park et al., 2004). Briefly, the DNA fragment of the deletion target was cloned into the suicide vector, pYAK1, which contains R6K origin of replication and the *sacB* gene conferring sensitivity to sucrose. This deletion plasmid was introduced into *E. coli* SM10 λ*pir* and transferred into *V. parahaemolyticus* strains by conjugation. The mutant strain was selected from LB plates supplemented with 10% sucrose.

2.3 Protein sample preparation and analysis

V. parahaemolyticus strains were grown in LB medium with different osmolytes in

indicated concentrations at 30ºC or 37ºC to an OD600 of 1 or 1.8. The culture was centrifuged at 15,000 g for 5 min to separate pellets, which contain bacterial cells, and the supernatants, which contain secreted proteins. The pellets were solubilized in SDS-PAGE sample buffer, followed by sonication and denaturation at 95ºC for 5 min, and used as whole cell lysates. For the secreted proteins, the proteins were collected from the supernatant fraction by precipitation with ice-cold trichloroacetic acid at a final concentration of 10% (vol/vol) on ice for 120 min, followed by centrifugation at 25,000 g for 30 min. The resulting pellets were rinsed with cold acetone and solubilized in SDS-PAGE sample buffer, followed by denaturation at 95ºC for 5 min.

For western blot analysis, proteins were separated by SDS-PAGE and transferred to a polyvinylidene difluoride (PVDF) membrane by electroblotting. After transfer, the membranes were probed with the primary antibody against the protein of interest. Anti-VtrA, anti-VtrB, anti-VscJ2 and anti-VopD2 antibodies were in-house polyclonal antibodies generated by immunizing New Zealand White rabbits (Park et al., 2004; Kodama et al., 2010); Monoclonal antibodies against FLAG (clone M2, code: F3165, Sigma-aldrich) and HA (clone TANA2, code: M180-3, Medical & Biological Laboratories) were commercially available. The membranes were then probed with horseradish peroxidase-conjugated goat anti-rabbit antibody (code: 62-1820, Invitrogen) or horseradish peroxidase-conjugated rabbit anti-mouse antibody (code: 61-6520, Invitrogen). The blots were developed using an ECL Western blotting kit (GE

Healthcare). The whole-cell lysate proteins with CBB staining of each sample was used as a loading control for immunoblotting.

For mass spectrometry analysis, proteins were separated by SDS-PAGE, followed by CBB staining for 60 min. The stained gels were rinsed and soaked in destaining solution (7.5% Acetic acid, 5% Methanol). The protein band was sliced from the gel and was subjected to mass spectrometry analysis at the Central Instrument Laboratory, Research Institute for Microbial Diseases, Osaka University. Proteins were identified from mass spectrometry data by a database search using the Mascot software (Matrix Science)

2.4 RNA extraction, qRT-PCR, and RNA sequencing

V. parahaemolyticus cells were grown in LB containing 0.1 M or 0.3 M NaCl at 30ºC or 37°C until OD_{600} reaches 1. RNAprotect bacterial reagent (Qiagen) was added to the culture to stabilize the RNA, and total RNA was extracted using the RNeasy mini kit (Qiagen) with DNase I treatment according to the manufacturer's instructions. Purified RNA samples were analyzed by PCR to confirm the absence of DNA contaminant. The concentration of each sample was measured by Nanodrop ND-1000 (ThermoFisher).

For qRT-PCR, the purified RNA sample was diluted to 10 ng/μl with nuclease-free water. The reactions were performed using RNA-direct Realtime PCR Master Mix (Toyobo) in QuantStudio 5 real-time PCR system (ThermoFisher) according to the manufacturer's

instructions. The relative abundance of mRNA transcripts was calculated using the ΔΔCT method and normalized to a housekeeping gene, *recA.*

For RNA sequencing, RNA libraries were prepared for sequencing using the TruSeq Stranded Total RNA with RiboZeroPlus kit (Illumina, San Diego, CA, USA). Whole transcriptome sequencing was applied to RNA samples using the Illumina NovaSeq 6000 platform in a 151 bp single-end mode. Sequenced reads were mapped to the *V. parahemolyticus* reference genome sequence (GCF_000196095.1_ASM19609v1) using Bowtie2 ver. 2.4.4 (Langmead & Salzberg, 2012) and then counted using HTseq 0.11.1 (Anders et al., 2014). The number of counts per million was analyzed using iDEP.94 (Ge, 2021).

2.5 Transcriptional reporter assay

V. parahaemolyticus WT or an isogenic *toxR* mutant, harboring pHRP309-P_{ompU} plasmid, was grown in LB broth under permissive and non-permissive conditions until OD_{600} of around 1.8. The β-galactosidase activity of bacterial cell lysates was measured using Miller's method with the substrate **o**-nitrophenyl-β-D-galactopyranoside as described previously (Miller, 1972).

2.6 Protein purification

For ToxR derivatives, the N-terminal terminal region of ToxR ($ToxR^N$: aa 1–180) fused with leucine-zipper dimerizing domain (ZIP) or its monomeric mutant (ZIP^m) were cloned into the pET28a expression plasmid (Novagen), yielding pET28a-$toxR^N$-*ZIP* or pET28a- $toxR^N$-

ZIP^{m}. For H-NS and its truncated derivatives, *hns* (135 amino acids), its N-terminus (aa 1–90), and its C-terminus (aa 91–135) were cloned into the pET28a plasmid, yielding pET28a-*hns*^{FL}, pET28a or pET28a-*hns*^{N} and pET28a-*hns*^{C}. These plasmids were transformed into *E. coli* BL21(DE3) and the resulting strains were grown in LB medium at 37°C to an OD_{600} of around 0.6. Then, protein expression was induced by adding 1 mM isopropyl-1-thio-β-D-galactopyranoside, followed by further incubation at 20°C overnight. Bacterial cells were harvested by centrifugation at 10,000 *g* for 5 min, and were lysed in CelLytic B cell lysis reagent (Sigma-Aldrich) containing protease inhibitor cocktail (P8849, Sigma-Aldrich), 40 units/ml benzonase (Sigma-Aldrich), and 0.2 mg/ml lysozyme (Sigma-Aldrich), and were sonicated for 15 min. The cell lysates were centrifuged at 20,000 *g* for 45 min, and the resulting supernatants including solubilized proteins were filtrated through 0.22-μm filter to remove insolubilized proteins and unbroken cells. Each 6×histidine-tagged protein was purified using Ni-NTA His·Bind beads (Novagen) according to the manufacturer's instructions. The 6×Histidine-tagged recombinant VtrA^{N}-GCN4-ZIP or VtrA^{N}-GCN4-ZIP^{m} protein was purified as previously described (R. Okada et al., 2017). The purified protein was quantified using Nanodrop ND-1000.

2.7 Electrophoretic mobility shift assay (EMSA)

The DNA probe corresponding to *vtrB* promoter (P_{vtrB}; 284-bp upstream region of *vtrB*) was amplified by PCR using pro-vtrB-F and pro-vtrB-R primers. The PCR product was then purified using QIAquick PCR purification kit (Qiagen). For EMSA, DNA probe was incubated with various concentration of purified recombinant proteins in reaction buffer [(10 mM Tris-HCl (pH7.4), 1 mM Na_2EDTA, 50 mM KCl, 5% Glycerol, 0.05% Nonidet P-40 and 100 ng/mL bovine serum albumin] at room temperature for 30 min. Reaction mixtures were then resolved on composite gels (3% polyacrylamide and 0.5% agarose) in TGE buffer (25 mM Tris, 190 mM glycine and 1 mM EDTA) at 150 V for 1-1.5 h at 4°C. The gels were then stained with ethidium bromide for 10–15 minutes, and DNA was visualized using UV transilluminator.

2.8 DNase footprinting assay

A 6-carboxyfluorescein (6-FAM) labeled *vtrB* promoter region (434-bp upstream *vtrB*) was amplified by PCR using 5-FAM-pro-vtrB-F primer, which is labeled with 6-FAM, and pro-vtrB-R primer pairs. The PCR product was then purified using QIAquick PCR purification kit (Qiagen). 6-FAM labeled *vtrB* promoter region was incubated with purified recombinant proteins in EMSA reaction buffer plus 5 mM $CaCl_2$, 3 mM $MgCl_2$ at room temperature for 30 min. DNase I (0.027 U) was added to the mixtures, mixed, and incubated for 3 min at room temperature. To stop DNase I activity, 5 mM EDTA was added to reaction mixtures, followed

by immediate incubation at 95°C for 5 min. After cooling down on ice, DNA was purified using PCR purification kit (Qiagen), and then was solubilized in HiDi formamide (ThermoFisher). GeneScan 500 LIZ (ThermoFisher) was added as an internal standard before being subjected to capillary electrophoresis on Applied Biosystem 3130 Genetic Analyzer. The protected region from DNase I digestion was identified by observing the region with decreased fluorescence output in chromatogram data. The position of the protected region was determined based on the internal standard.

Table 1. *V. parahaemolyticus* strains used in this study.

Strains	Genotypes/descriptions	References
RIMD2210633	A *tdh*- and T3SS2-positive clinical isolate, wild type	Laboratory collection
Δ*hns*	RIMD2210633 *hns* (*vp1133*)	(Kodama et al., 2010)
Δ*vtrA*	RIMD2210633 *vtrA* (*vpa1332*)	(Kodama et al., 2010)
Δ*vtrB*	RIMD2210633 *vtrB* (*vpa1348*)	(Kodama et al., 2010)
Δ*toxR*	RIMD2210633 *toxR* (*vp0820*)	(Okada et al., 2017)
HNS-3F	RIMD2210633 *hns*::*hns-3xFLAG*	This study
Δ*hns* Δ*vtrA*	RIMD2210633 *hns vtrA*	This study
Δ*vtrA* Δ*toxR*	RIMD2210633 *hns toxR*	This study

Table 2. *E. coli* strains used in this study.

Strains	Genotypes/descriptions	References
DH5α	F^- Φ80Δ*lacZ*M15 Δ(*lacZYA argF*)U169 *deoP recA1 endA1 hsdR17*(rK^- mK^-)	Laboratory collection
SM10λpir	*thi thr leu tonA lacY supE recA*::RP4-2-Tc::Mu λ*pir* R6K	Laboratory collection
BL21(DE3)	F^- *omp*T, $hsdS_B$ (r_B^-, m_B^-), *dcm*, *gal*, λ(DE3)	Laboratory collection
MC4100	F^- *raD139* Δ(*argF-lac*) *U169 rpsL150* (Str^r) *relA1 flbB5301 deoC1 ptsF25 rbsR*	Laboratory collection

Table 3. Plasmids used in this study.

Plasmids	Description	References
pBAD18cm	P_{BAD} promoter, pBR322 *ori*, Cm^R	Laboratory collection
pBAD-*vtrB*	pBAD18Cm containing *vtrB* gene	This study
pBAD-*HA*-*vtrA*	pBAD18Cm containing *vtrA* gene with N-terminal HA epitope tag	(Okada et al., 2017)
pBAD-*HA*-*Vp*-*toxR*	pBAD18Cm containing *V. pahrasmolyticus toxR* gene with N-terminal HA epitope tag	(Okada et al., 2017)
pHRP309	*lacZ* transcriptional fusion vector, Gm^R	Laboratory collection
pHRP309-P_{ompU}	pHRP309 containing ompU_{vc} promoter region	(Okada et al., 2017)
pSA19CP	Complementation vector for *V. parahaemolyticus*, Cm^R	Laboratory collection

pSA19-*Vphns-3×FLAG*	pSA19CP containing *V. parahaemolyticus hns* gene with 500 bp upstream of *Vphns* and C-terminal 3×FLAG tag	This study
pSA19-*Echns-3×FLAG*	pSA19CP containing *E. coli hns* gene with 500 bp upstream of *Vphns* and C-terminal 3×FLAG tag	This study
pSA19-*hns*-L30P-*3×FLAG*	pSA19-*Vphns-3×FLAG* with L30P mutation	This study
pSA19-*hns*-I70C-*3×FLAG*	pSA19-*Vphns-3×FLAG* with I70C mutation	This study
pSA19-*hns*Δ*N-3×FLAG*	pSA19CP containing *V. parahaemolyticus hns* (91–135) with C-terminal 3×FLAG tag	This study
pSA19-*hns*-P117A-*3×FLAG*	pSA19-*Vphns-3×FLAG* with P117A mutation	This study
pSA19-*hns*Δ*C-3×FLAG*	pSA19CP containing *V. parahaemolyticus hns* (1–90) with C-terminal 3×FLAG tag	This study
pET28a	Expression vector for *E. coli*, Km^R	Laboratory collection
pET28a-ZIP	pET28a containing ZIP domain from GCN4 between *SalI* and *XhoI* sites	(Okada et al., 2017)
pET28a-ZIP^m	pET28a containing monomeric ZIP domain from GCN4 between *SalI* and *XhoI* sites	(Okada et al., 2017)
pET28a-$vtrA^N$-*ZIP*	pET28a-ZIP containing *vtrA* (1–133)	(Okada et al., 2017)
pET28a-$vtrA^N$-ZIP^m	pET28a-ZIP^m containing *vtrA* (1–133)	(Okada et al., 2017)
pET28a-*Vp-toxR*^{N}-*ZIP*	pET28a-ZIP containing *V. parahaemolyticus toxR* (1–180)	This study
pET28a-$toxR^N$-ZIP^m	pET28a-ZIP^m containing *V. parahaemolyticus toxR* (1–180)	This study
pET28a-hns^{FL}	pET28a containing *V. parahaemolyticus hns*	This study
pET28a-hns^N	pET28a containing *V. parahaemolyticus hns* (1–90)	This study
pET28a-hns^C	pET28a containing *V. parahaemolyticus hns* (91–135)	This study
pET28a-*hns* L30P	pET28a-hns^{FL} with L30P mutation	This study
pET28a-*hns* I70C	pET28a-hns^{FL} with I70C mutation	This study
pYAK1	*ori*R6K, suicide vector for gene replacement, Cm^R	(Kodama et al., 2002)
pYAK1-inHNS-3F	A derivative of pYAK1 for integration of *hns-3×FLAG* into the *hns* locus	This study

Table 4. Primers used in this study

Primer	Sequence (5' to 3')	Description
VtrB A	AGGTTTAATGGTGGCGGAGG	For qRT-PCR
VtrB B	AGTACCGCAAGCAACATCCA	
VopD2 A	CTGTGTCACTGGCGGATGAT	
VopD2 B	GGCCACACGCATGTTTGAAT	
VscJ2 A	TCTACCAGCACGCCATAGC	
VscJ2 B	CAGGTTGCCGTGATTCAGG	
RecA A	GCTAGTAGAAAAAGCGGGTG	
RecA B	GCAGGTGCTTCTGGTTGAG	
SD-VtrB-F	GGGGCTAGCAACTGTGAAAAGGGCTCAGCGATG	For construction of pBAD-*vtrB*
VtrB-R	GGGAAGCTTTTATTTAAGCAACAAAATCATCGCCGTACTGG	
pro-vtrB-F	AGGGGCTATGCCCCTTTTATTTTTAATTCTC	For preparation of *vtrB* promoter probe
pro-vtrB-R	CGCTGAGCCCTTTTCACAGTTTTTCTTC	
BamHI-ups500-HNS-F	GGGGATCCTGAGTATTGTGCAACTGAAATCACG	For construction of pSA19-*Vphns-3×FLAG* (P_{hns})
SalI-HNS-R	GGGTCGACTTAGATTAGGAAATCGTCTAGTGATTTACCTGC	
BamHI-HNS-F	GGGGATCCATGTCAGAGCTGACTAAAACACTTCTAAATATCC	For construction of pET28a-hns^{FL}
XhoI-HNS-R	GCGCTCGAGTTAGATTAGGAAATCGTCTAGTGATTTACC	
L30P-HNS-F	CAATTGGAAGAAGCTCCTGATAAACTAACTACTGTTGTTG	For single amino acid mutation of H-NS, L30P
L30P-HNS-R	CAACAACAGTAGTTAGTTTATCAGGAGCTTCTTCCAATTG	
I70C-HNS-F	CTCAAGACGGTTGTGACGTTGAAGCACTAATTAGC	For single amino acid mutation of H-NS, I70C
I70C-HNS-R	GCTAATTAGTGCTTCAACGTCACAACCGTCTTGAG	

BamHI-ΔN-HNS-F	GGGGATCCCGCGCTCCTCGCCCAGCTAAGTACAAGTAC	For truncation of H-NS DNA-binding domain (91-135)
P117A-HNS-F	GCCAAGGTCGTACAGCTTCTGCAATTCAAGAGC	For single amino acid mutation of H-NS, P117A
P117A-HNS-R	GCTCTTGAATTGCAGAAGCTGTACGACCTTGGC	
XhoI-ΔC-HNS-R	GCGCTCGAGTTACTTAGATTTTGCTTTAGTCTTAGTTTCGCC	For truncation of H-NS dimerization domain (1-90)
BamHI-ToxR-F	GGGGATCCATGACTAACATCGGCACCAAATTTCTACTTG	For construction of pET28a-*Vp-toxR^{N}-ZIP*/*ZIP^{m}*
SalI-ToxR(180)-R	GGGTCGACGCGTGGAATCCAAGGATTCACAGC	
EcHNS-F1	AAAATGCCAAACACGTTAACCTATTAATAGGAATCGTTATGAGCGAAGCACTTAAAATTCTGAACAAC	For construction of pSA19-*Echns-3×FLAG*
EcHNS-R1	GTTGTTCAGAATTTTAAGTGCTTCGCTCATAACGATTCCTATTAATAGGTTAACGTGTTTGGCATTTT	
VpHNS-EcHNS-Dbd-3F(37)-R	CATGATCTTTATAATCACCGTCATGGTCTTTGTAGTCTTGCTTGATCAGGAAATCGTCGAGGG	
3xFLAG-SalI-R	GGGTCGACCTACTTGTCATCGTCATCCTTGTAGTCGATGTCATGATCTTTATAATCACCGTCATGGTCTTTGTAGTC	
5-FAM VtrB-F	AGCAAGGGCAAAATGGTGAAAATAG	For preparation of 5’-FAM labeled *vtrB* promoter probe
BamHI- inVP1133-F	GGCGGATCCCACATCAAACTAAATTAAACTAATAAATAATCGCCAACC	For construction of pYAK1-inHNS-3F
inVP1133-1R	CAGCTCTGACATAACGATTCCTATTAATAGGTTAACGTGTTTGGC	
inVP1133-2F	GCCAAACACGTTAACCTATTAATAGGAATCGTTATGTCAGAGCTG	
inVP1133-2R	GGGAGCCTTTTTAAACAAGAACGACTACTTGTCATCGTCATCCTT	
inVP1133-3F	AAGGATGACGATGACAAGTAGTCGTTCTTGTTTAAAAAGGCTCCC	
inVP1133-3F	GGGCATGCTTGTCTGCTGTTCTTCATGACATGG	

CHAPTER 3

RESULTS

3.1 VtrB production is crucial for the temperature- and salinity-dependent regulation of T3SS2

Gotoh et al. have reported that T3SS2-related proteins are expressed at a body temperature (37°C) and low salinity (0.1 M NaCl) but not at 25–30°C and high salinity (above 0.3 M NaCl)(Gotoh et al., 2010). First, to revisit this temperature- and salinity-dependent regulation of T3SS2, I reexamined the expression of T3SS2-related proteins, VscJ2 and VopD2, which are a T3SS apparatus protein (an inner membrane ring protein comprising the basal body of T3SS2) and a T3SS2-secreted protein (translocator comprising the translocon of T3SS2), respectively, in *V. parahaemolyticus* strain RIMD2210633 (hereinafter referred to as WT) grown in LB medium with various NaCl concentrations at 25, 30 and 37°C, by immunoblot analysis. Secretion of VopD2 into the culture supernatant was also monitored as an indicator of the secretion activity of T3SS2. Consistent with the previous report, the protein production of VscJ2 and VopD2 was observed at 37°C and 0.1 M NaCl (**Fig. 9A**). Even at 37°C, both proteins were not produced at higher salinity (0.3 and 0.5 M NaCl). Similarly, even at low salinity of 0.1 M NaCl, the expression of both proteins was not observed at a lower temperature (25 and 30°C). Similar results were also observed in VopD2 secretion. Thus, these results reconfirmed that T3SS2-related protein expression is temperature- and salinity-dependent, with expression

at 37°C and 0.1 M NaCl (the permissive condition), but not at lower temperature or higher salinity (the non-permissive conditions).

Given that T3SS2 gene expression is governed by the VtrA-VtrB regulatory cascade (Kodama et al., 2010), I next examined the expression of VtrA and VtrB at the permissive and non-permissive conditions (lower temperature or high salinity). The expression of VtrA was observed in all conditions tested, whereas the expression of VtrB was observed at the permissive condition but not at the non-permissive condition (**Fig. 9A**). To examine whether T3SS2-related gene transcripts also vary with changes in temperature and salinity, I analyzed the transcriptome of *V. parahaemolyticus* WT grown under the permissive condition and two non-permissive conditions (30°C, 0.1 M NaCl and 37°C, 0.3 M NaCl) using RNA-seq. In this transcriptome-wide analysis, *vtrA* transcript level was comparable in all three conditions, whereas *vtrB* and all T3SS2-related genes were not expressed at non-permissive conditions (**Fig. 9B** and **Table 5**). This transcriptome profiling was validated by qRT-PCR, in which *vtrB*, *vscJ2,* and *vopD2* were upregulated under the permissive condition but were downregulated under the non-permissive conditions (**Fig. 9C**), thus indicating the repression of those genes at the transcriptional level under the non-permissive conditions. Given the central regulatory role of VtrB in T3SS2 gene expression, I next examined whether VtrB production determines the T3SS2 gene expression under the non-permissive conditions. To this end, VtrB was expressed in the *vtrB*-deleted mutant of *V. parahaemolyticus* (Δ*vtrB*) under the control of the arabinose-

inducible P_{BAD} promoter (Guzman et al., 1995). The induction of VtrB expression under the non-permissive conditions produced the expression of VscJ2 and VopD2, together with the secretion of VopD2 (**Fig. 9D**). Thus, these results indicate that the *vtrB* transcriptional status affects the subsequent T3SS2 gene expression under the non-permissive conditions.

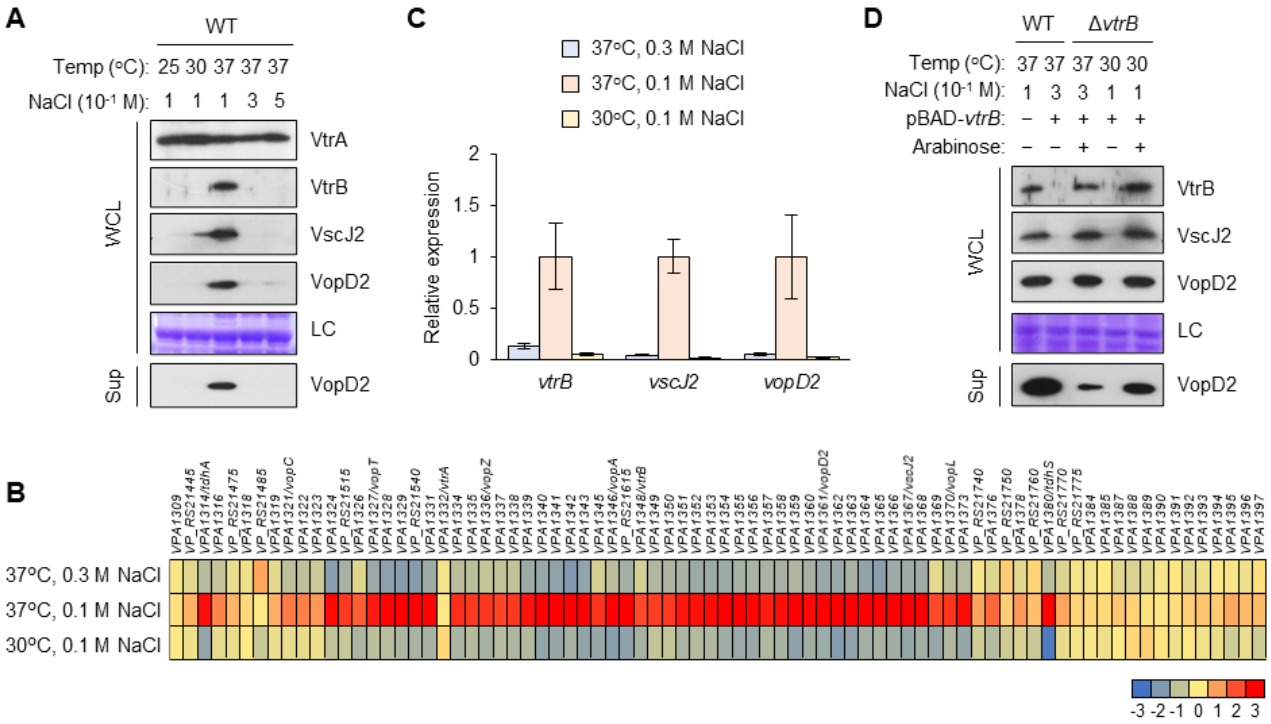

Figure 9. VtrB is produced at a certain temperature and salinity.

(**A**) Production of T3SS2-related proteins and VtrB but not VtrA varied with changes in temperature and salinity. Bacterial whole-cell lysates (WCL) and the culture supernatants (Sup) from *V. parahaemolyticus* WT grown at indicated temperature and concentrations of NaCl were analyzed by immunoblotting for VtrA, VtrB, and T3SS2-related proteins (VscJ2 and VopD2) as indicated. Whole-cell lysate protein is used as a Loading control (LC). (**B**) Heat map of transcriptome representing the log2 fold change values of Vp-PAI genes. Total RNA was extracted from *V. parahaemolyticus* WT grown at indicated temperature and concentrations of NaCl, which was subjected to RNA-Seq. Up-regulation and down-regulation are indicated in red and blue, respectively. (**C**) Relative expression of *vtrB, vscJ2,* and *vopD2* with housekeeping gene *recA* in *V. parahaemolyticus* WT grown at indicated temperature and concentrations of NaCl were analyzed by qRT-PCR. The values are the means with error bars representing the standard deviations (SD) for three independent experiments. (**D**) Expression of VtrB under the control of P_{BAD} promoter produced the T3SS2 expression at the non-

permissive conditions. *V. parahaemolyticus* WT or Δ*vtrB* harboring pBAD-*vtrB* was grown at indicated temperature and concentrations of NaCl. P_{BAD}-driven expression was induced by the addition of arabinose at the final concentration of 0.01%. Bacterial whole-cell lysates (WCL) and the culture supernatants (Sup) were analyzed by immunoblotting for indicated antibodies. For P_{BAD}-driven expression of VtrB, 10-fold diluted samples were applied to observe VtrB production. A cell lysate protein visualized with CBB staining is used as a Loading control (LC).

Table 5. Upregulated and downregulated genes under permissive compared to non-permissive conditions in WT from RNA-seq analysis.

Locus	Gene ID	Protein	log_2 (normalization by mean)		
			30°C 0.1 M[a]	**37°C 0.1 M[a]**	**37°C 0.3 M[a]**
VP_RS00280	VP0053	hypothetical protein	0.32	-1.59	1.28
VP_RS00315	VP0060	multidrug transporter subunit MdtJ	0.87	2.10	-2.97
VP_RS00320	VP0061	multidrug transporter	0.72	2.15	-2.87
VP_RS00335	VP0064	GntP family permease	-1.20	-1.54	2.74
VP_RS01425	VP0291	uroporphyrinogen-III C-methyltransferase	-1.68	-2.19	3.87
VP_RS01430	VP0292	sulfate adenylyltransferase subunit CysD	-0.88	-1.94	2.82
VP_RS01435	VP0293	sulfate adenylyltransferase subunit CysN	-0.57	-2.02	2.60
VP_RS01440	VP0295	SLC13 family permease	-0.87	-1.68	2.54
VP_RS02510	VP0526	Na/Pi cotransporter family protein	0.14	1.50	-1.65
VP_RS03415	VP0712	hypothetical protein	0.87	-4.07	3.20
VP_RS03880	VP0790	flagellin	0.87	-1.84	0.97
VP_RS03885	VP0791	flagellin	0.76	-1.64	0.88
VP_RS04920	VP1008	porin	0.43	-2.16	1.73
VP_RS05370	VP1103	alanine dehydrogenase	0.65	1.70	-2.35
VP_RS05620	VP1156	TIGR02647 family protein	0.35	-1.57	1.21

VP_RS07020	VP1447	dimethyl sulfoxide reductase subunit A	-2.14	-1.76	3.91
VP_RS07025	VP1448	dimethylsulfoxide reductase subunit B	-0.95	-1.66	2.60
VP_RS08485	VP1764	EamA family transporter	-0.94	-1.98	2.93
VP_RS08500	VP1767	Ig-like domain-containing protein	0.01	2.97	-2.97
VP_RS09780	VP2013	polysulfide reductase NrfD	-2.60	-1.55	4.15
VP_RS10965	VP2258	flagellin	0.90	-1.55	0.65
VP_RS10970	VP2259	flagellin	0.86	-2.05	1.19
VP_RS10975	VP2261	flagellin	1.02	-1.62	0.60
VP_RS11590	VP2388	glycerol-3-phosphate dehydrogenase	0.10	-1.60	1.50
VP_RS11875	VP2448	U32 family peptidase	-1.54	-1.54	3.08
VP_RS13365	VP2720	phosphoadenylyl-sulfate reductase	-0.13	-1.71	1.84
VP_RS13370	VP2721	assimilatory sulfite reductase (NADPH) hemoprotein subunit	-0.33	-1.91	2.24
VP_RS13375	VP2722	assimilatory sulfite reductase (NADPH) flavoprotein subunit	-0.68	-2.09	2.77
VP_RS13590	VP2768	bacterioferritin	0.26	1.58	-1.84
VP_RS13710	VP2794	DUF1338 domain-containing protein	1.11	1.61	-2.72
VP_RS13980	VP2840	fumarate reductase (quinol) flavoprotein subunit	-0.95	-1.80	2.75
VP_RS13985	VP2841	succinate dehydrogenase/fumarate reductase iron-sulfur subunit	-1.06	-1.51	2.58
VP_RS14020	VP2849	MgtC/SapB family protein	2.38	1.99	-4.37
VP_RS15810	VPA0117	glycerate kinase	0.68	1.53	-2.21
VP_RS15860	VPA0127	NapC/NirT family cytochrome c	-2.33	-1.52	3.86
VP_RS16095	VPA0168	multidrug efflux MFS transporter EmrD	0.89	1.51	-2.40
VP_RS16380	VPA0229	PTS ascorbate transporter subunit IIC	2.17	-5.18	3.01

VP_RS16385	VPA0230	PTS sugar transporter subunit IIB	2.40	-5.40	3.01
VP_RS16390	VPA0231	PTS sugar transporter subunit IIA	2.54	-4.96	2.42
VP_RS16640	VPA0286	co-chaperone GroES	-1.81	1.81	0.00
VP_RS16645	VPA0287	chaperonin GroEL	-1.96	1.82	0.14
VP_RS16700	VPA0297	PTS fructose transporter subunit IIC	3.25	-3.20	-0.05
VP_RS16705	VPA0298	PTS sugar transporter subunit IIA	3.63	-3.75	0.13
VP_RS17040	VPA0375	adenylosuccinate synthase	1.84	-2.85	1.01
VP_RS17265	VPA0424	biopolymer transporter ExbD	0.74	1.58	-2.32
VP_RS17270	VPA0425	MotA/TolQ/ExbB proton channel family protein	0.96	1.84	-2.80
VP_RS17275	VPA0426	energy transducer TonB	1.01	2.15	-3.16
VP_RS17280	VPA0427	heme anaerobic degradation radical SAM methyltransferase ChuW/HutW	1.59	2.15	-3.74
VP_RS17945	#N/A	hypothetical protein	0.09	2.34	-2.43
VP_RS17950	#N/A	hypothetical protein	0.42	2.12	-2.53
VP_RS18050	VPA0592	arginase family protein	1.89	1.88	-3.78
VP_RS18055	VPA0593	IclR family transcriptional regulator	2.04	1.81	-3.85
VP_RS18570	VPA0706	anaerobic C4-dicarboxylate transporter DcuC	-2.52	-1.60	4.13
VP_RS18890	VPA0775	PaaI family thioesterase	0.03	-1.50	1.47
VP_RS19240	VPA0851	formate transporter FocA	-1.44	-1.52	2.97
VP_RS20365	VPA1083	ribokinase	-1.32	-1.74	3.06
VP_RS20370	VPA1084	ribose ABC transporter substrate-binding protein RbsB	-0.54	-2.86	3.40
VP_RS20375	VPA1085	ribose ABC transporter permease	-1.04	-1.89	2.92
VP_RS20380	VPA1086	ribose ABC transporter ATP-binding protein RbsA	-0.76	-1.72	2.48
VP_RS21320	VPA1285	hypothetical protein	1.13	1.52	-2.64
VP_RS21350	#N/A	hypothetical protein	0.48	1.83	-2.30

VP_RS21465	VPA1314	thermostable direct hemolysin TDH	-1.14	2.84	-1.70
VP_RS21510	VPA1324	EAL domain-containing protein	-1.89	2.90	-1.01
VP_RS21515	#N/A	IS4 family transposase	-1.41	2.29	-0.87
VP_RS21520	VPA1326	hypothetical protein	-0.49	1.82	-1.33
VP_RS21525	VPA1327	T3SS effector ADP-ribosyltransferase toxin VopT	-1.60	2.68	-1.08
VP_RS21530	VPA1328	hypothetical protein	-1.83	2.96	-1.13
VP_RS21535	VPA1329	conjugal transfer protein TraA	-1.91	3.24	-1.33
VP_RS21540	#N/A	DUF4116 domain-containing protein	-1.94	3.34	-1.40
VP_RS21545	VPA1331	VPA1331 family putative T3SS effector	-1.57	2.98	-1.41
VP_RS21555	VPA1334	hypothetical protein	-1.09	2.42	-1.33
VP_RS21560	VPA1335	flagellar biosynthetic protein FliQ	-1.11	2.28	-1.17
VP_RS21565	VPA1336	type III secretion system effector VopZ	-0.92	2.32	-1.39
VP_RS21570	VPA1337	VPA1337 family putative T3SS effector	-0.98	2.14	-1.16
VP_RS21575	VPA1338	type III secretion system ATPase	-0.97	2.28	-1.31
VP_RS21580	VPA1339	secretin	-1.57	2.78	-1.21
VP_RS21585	VPA1340	VPA1340 family putative T3SS effector	-1.68	3.41	-1.73
VP_RS21590	VPA1341	hypothetical protein	-1.78	3.42	-1.65
VP_RS21595	VPA1342	EscR/YscR/HrcR family type III secretion system export apparatus protein	-2.03	3.43	-1.39
VP_RS21600	VPA1343	hypothetical protein	-1.76	3.50	-1.74
VP_RS21605	VPA1345	hypothetical protein	-0.69	2.34	-1.65
VP_RS21610	VPA1346	type III secretion system YopJ family effector VopA	-1.12	2.99	-1.87
VP_RS21615	#N/A	hypothetical protein	-1.46	3.25	-1.79
VP_RS21620	VPA1348	winged helix-turn-helix domain-containing protein	-0.69	2.08	-1.39

VP_RS21625	VPA1349	FliM/FliN family flagellar motor switch protein	-1.27	2.22	-0.95
VP_RS21630	VPA1350	VPA1350 family putative T3SS effector	-1.33	2.29	-0.96
VP_RS21635	VPA1351	VPA1351 family putative T3SS effector	-1.39	2.74	-1.35
VP_RS21640	VPA1352	VPA1352 family putative T3SS effector	-1.60	2.80	-1.21
VP_RS21645	VPA1353	OmpA family protein	-1.59	2.85	-1.26
VP_RS21650	VPA1354	EscU/YscU/HrcU family type III secretion system export apparatus switch protein	-1.57	3.08	-1.51
VP_RS21655	VPA1355	FHIPEP family type III secretion protein	-1.41	3.00	-1.59
VP_RS21660	VPA1356	hypothetical protein	-1.37	2.99	-1.62
VP_RS21665	VPA1357	hypothetical protein	-1.38	2.63	-1.25
VP_RS21670	VPA1358	dimethyladenosine transferase	-1.42	2.82	-1.40
VP_RS21675	VPA1359	hypothetical protein	-1.27	3.06	-1.79
VP_RS21680	VPA1360	hypothetical protein	-1.42	2.92	-1.50
VP_RS21685	VPA1361	hypothetical protein	-1.63	3.24	-1.61
VP_RS21690	VPA1362	hypothetical protein	-1.62	3.54	-1.92
VP_RS21695	VPA1363	molecular chaperone	-1.37	3.14	-1.77
VP_RS21700	VPA1364	hypothetical protein	-1.77	3.25	-1.48
VP_RS21705	VPA1365	hypothetical protein	-1.86	3.23	-1.37
VP_RS21710	VPA1366	hypothetical protein	-1.57	3.08	-1.51
VP_RS21715	VPA1367	type III secretion protein	-1.56	3.25	-1.69
VP_RS21720	VPA1368	hypothetical protein	-1.53	3.02	-1.49
VP_RS21725	VPA1369	hypothetical protein	-0.42	2.07	-1.64
VP_RS21730	VPA1370	type III secretion system effector VopL	-1.09	2.33	-1.24
VP_RS21735	VPA1373	hypothetical protein	-1.18	2.85	-1.67
VP_RS21745	VPA1376	accessory colonization factor AcfD	-0.52	1.70	-1.17
VP_RS21765	VPA1380	type III secretion system effector OspB	-1.12	3.92	-2.79

VP_RS21955	VPA1420	PTS sugar transporter subunit IIA	1.23	-2.04	0.81
VP_RS21960	VPA1421	PTS fructose transporter subunit IIB	0.56	-1.72	1.16
VP_RS21965	VPA1422	PTS sugar transporter subunit IIA	0.32	-1.78	1.46
VP_RS21970	VPA1423	helix-turn-helix transcriptional regulator	2.29	-4.39	2.10
VP_RS21975	VPA1424	PTS sugar transporter subunit IIA	2.61	-5.70	3.09
VP_RS21980	VPA1425	mannose-6-phosphate isomerase, class I	1.74	-2.93	1.19
VP_RS22100	VPA1449	methyl-accepting chemotaxis protein	0.99	-1.68	0.69
VP_RS22130	VPA1456	BatD family protein	-1.22	1.51	-0.30
VP_RS23095	VPA1658	hypothetical protein	1.27	1.67	-2.94
VP_RS23645	#N/A	hypothetical protein	2.04	1.84	-3.88

[a]Concentration of NaCl used in the experiment.

The cut off is -1.5 < X > 1.5 at the permissive condition.

3.2 ToxR is active under non-permissive conditions

Given the consistent depletion of *vtrB* transcripts under non-permissive conditions, I speculated that factors for transcriptional activation of *vtrB* might be involved in the repression of *vtrB* under the non-permissive conditions. Indeed, VtrA was consistently expressed under the non-permissive conditions, while another transcriptional regulator Vp-ToxR is also involved in transcriptional activation of *vtrB* (Hubbard et al., 2016). Therefore, I examined whether ToxR is affected under the non-permissive conditions. In the earlier RNA-seq, *Vp-toxR* was consistently expressed as shown by $\log_2$ value under permissive (11.297) and non-

permissive conditions (11.981 at 37ºC, 0.3 M NaCl and 11.077 at 30ºC, 0.1 M NaCl). Then, I sought to examine the transcriptional activity of Vp-ToxR under the non-permissive conditions. Vp-ToxR activates gene expression of outer membrane porin U (OmpU), an abundant protein in *Vibrio* and important for survival under stress conditions such as acid, bile salts and sodium dodecyl sulfate stresses (Whitaker et al., 2012). To examine the *ompU* transcription of *V. parahaemolyticus* by Vp-ToxR, I employed the pHRP309 plasmid-based (Parales & Harwood, 1993) *lacZ* transcriptional reporter to monitor transcriptional activation of *ompU*. I constructed a pHRP309-P*ompU* which contains 300-bp upstream promoter region of *ompU* (P_{ompU}), and introduced the plasmid to *V. parahaemolyticus* WT and a *Vp-toxR*-deleted mutant (Δ*Vp-toxR*). Those strains were grown under the permissive and non-permissive conditions, and *ompU* transcription was evaluated by measuring the β-galactosidase activity. The P_{ompU}-*lacZ* expression was observed in *V. parahaemolyticus* WT but not in Δ*Vp-toxR*, indicating that *ompU* of *V. parahaemolyticus* is regulated by Vp-ToxR (**Fig. 10A**). The P_{ompU}-*lacZ* expression in *V. parahaemolyticus* was consistent under the permissive and the non-permissive conditions. This observation was supported by the earlier RNA-seq, in which *ompU* transcripts were comparable under the permissive (log_2 is 16.897) and the non-permissive conditions (log_2 is 18.097 at 37ºC, 0.3 M NaCl and 17.413 at 30ºC, 0.1 M NaCl). Furthermore, I observed an abundant protein with a molecular weight of around 40 kDa on the CBB-stained SDS-PAGE gels separating the whole cell lysates of *V. parahaemolyticus* that is expressed in a Vp-ToxR

dependent manner (**Fig. 10B**). Expectedly, this protein was identified as OmpU by liquid chromatography-tandem mass spectrometry. These results indicate that Vp-ToxR constitutively activates the transcription of OmpU expression even under the non-permissive conditions.

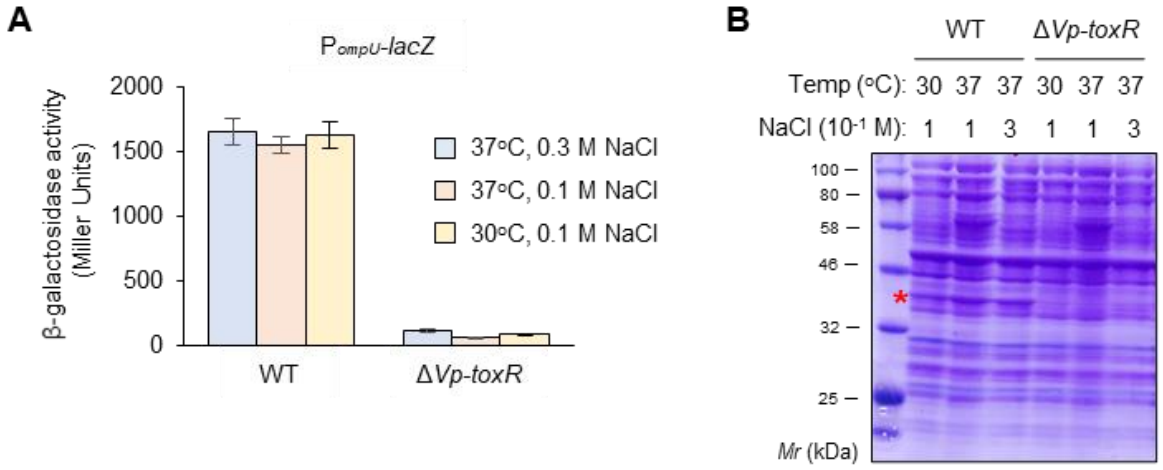

Figure 10. ToxR is in a steady-state under the permissive and non-permissive conditions. (**A**) β-galactosidase activity from P$_{ompU}$-*lacZ* transcriptional reporter of *V. parahaemolyticus* WT and Δ*Vp-toxR* has grown at indicated temperature and concentrations of NaCl. The value represents means ± SD for three independent experiments. (**B**) SDS-PAGE profile of the whole-cell lysates from *V. parahaemolyticus* WT and Δ*Vp-toxR* grown at indicated temperature and concentrations of NaCl. Proteins were visualized by CBB-staining. The location of OmpU is indicated by the asterisk.

3.3 A xenogeneic silencer H-NS is involved in the repression of *vtrB* under the non-permissive conditions

Since *vtrB* transcription was repressed under non-permissive conditions even though the two upstream regulators were in the steady-state, I hypothesized that another factor(s) might function in a repressive manner on *vtrB* transcription. Given the AT-rich feature of the *vtrB* promoter, including T-rich repetitive elements (TRE), which are necessary for *vtrB*

transcriptional activation (Okada et al., 2017), I speculated that H-NS might be involved in the repression of *vtrB* transcription; H-NS is a global transcriptional repressor of Gram-negative bacteria that preferentially binds to AT-rich sequences for silencing its target genes (Gordon et al., 2011). To examine the hypothesis, a mutant strain of *V. parahaemolyticus* in which the gene encoding H-NS is deleted (Δ*hns*) (Kodama et al., 2010) was grown under the permissive and non-permissive conditions, and the production of VtrA, VtrB and the T3SS-related proteins were determined (**Fig. 11A**). Intriguingly, the production of VtrB, VscJ2 and VopD2 were observed in the Δ*hns* mutant grown under the non-permissive conditions, which were comparable to those in WT and Δ*hns* grown under the permissive condition. Moreover, VopD2 secretion from Δ*hns* was also observed under the non-permissive conditions. The complementation of the *hns* gene into Δ*hns* restored the negligible production of VtrB and the T3SS2-related proteins (**Fig. 11B**). These results indicate that H-NS has an inhibitory effect on VtrB production under non-permissive conditions. Next, to verify whether the changes in VtrB and the T3SS2-related proteins are due to the amount of H-NS, I examined the production level of H-NS under the permissive and non-permissive conditions. To this end, a strain chromosomally expressing C-terminal 3×FLAG-tagged H-NS (H-NS3xFLAG) was constructed to monitor H-NS production. I observed that H-NS-3×FLAG production was consistent regardless of the conditions (**Fig. 11C**), indicating that the production of VtrB and the T3SS2-related proteins are independent of H-NS protein levels.

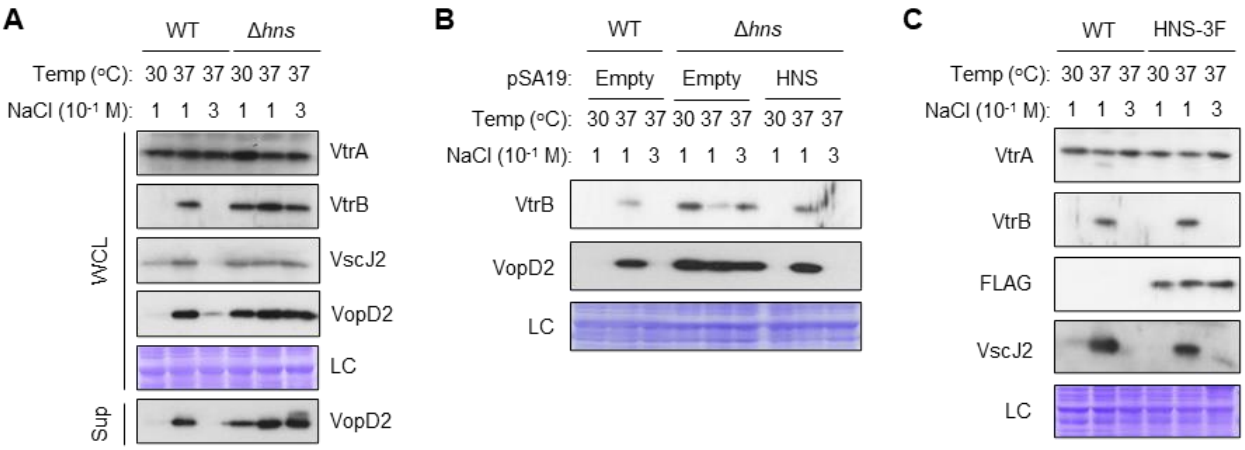

Figure 11. H-NS is required for the repression of VtrB production under non-permissive conditions.

(**A**) The T3SS2 repression under the non-permissive conditions was broken in the *hns* deletion mutant of *V. parahaemolyticus*. Bacterial whole-cell lysates (WCL) and the culture supernatants (Sup) from *V. parahaemolyticus* strains WT and Δ*hns* grown at indicated temperature and concentrations of NaCl were analyzed by immunoblotting for indicated antibodies. LC, loading control. (**B**) The complementation of H-NS restored the repressive effect on the VtrB production. *V. parahaemolyticus* WT and Δ*hn*s harboring pSA19 empty vector, and Δ*hns* harboring pSA19-*hns* with the endogenous promoter were grown at indicated temperature and concentrations of NaCl, and the production of VtrB and VopD2 were analyzed by immunoblotting. LC, loading control. (**C**) H-NS production did not vary with the permissive and non-permissive conditions. *V. parahaemolyticus* strains WT and Δ*hns*::*hns-3×FLAG* (HNS-3F) were grown at indicated temperature and concentrations of NaCl, and bacterial whole-cell lysates were analyzed by immunoblotting for indicated antibodies. LC, loading control.

Next, I performed RNA-seq based comparative transcriptomic analysis between *V. parahaemolyticus* strains WT and Δ*hns* under the permissive and non-permissive conditions (**Fig. 12A**). The result showed that 46 genes were downregulated and 268 genes were upregulated in Δ*hns* compared to WT under non-permissive conditions (**Table 6**). Consistent

with the protein production, *vtrB* and T3SS2 gene transcripts were increased in Δ*hns* at the non-permissive conditions compared to the WT. Besides the T3SS2 gene cluster, the genes for T3SS1, type VI secretion system 1 and 2 (T6SS1/2) and lateral flagella were upregulated, and the genes for polar flagella were downregulated (**Fig. 12A** and **Table 6**), which is consistent with the properties of mutant strains that have been reported previously (Enos-Berlage et al., 2005; Kodama et al., 2010; Salomon et al., 2014; Sun et al., 2014; Wang et al., 2017), thus supporting the validity of my comparative transcriptomic analysis. Moreover, most of the promoter regions of this upregulated gene cluster contained AT-rich sequences (**Fig. 12B**).

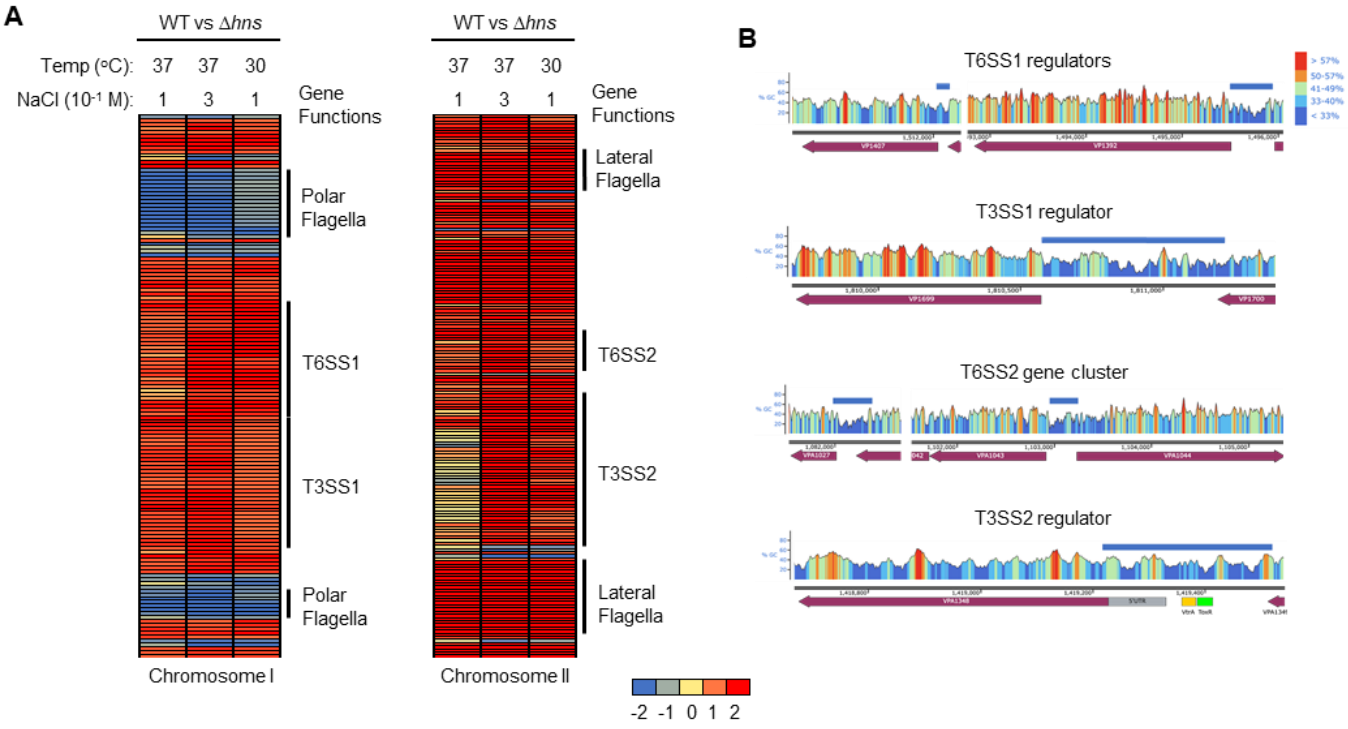

Figure 12. Comparative transcriptomic analysis between WT and Δ*hns*.

(**A**) Heat map of the comparative transcriptome of WT and Δ*hns* representing the log2 fold change values of up- and down-regulated genes on chromosome I (left) and chromosome II (right) under the permissive and non-permissive conditions. (**B**) The GC-content compositions of several promoters were upregulated in Δ*hns* as visualized by Snapgene Viewer.

Table 6. Upregulated and downregulated genes in Δ*hns* strains when compared to WT under permissive and non-permissive conditions from RNA-seq analysis

Locus	Gene ID	Protein	log_2 (normalization by each condition)		
			37ºC 0.1 M[a]	37ºC 0.3 M[a]	30ºC 0.1 M[a]
VP_RS00275	VP0051	SPOR domain-containing protein	-1.29	-1.57	-1.03
VP_RS00435	VP0084	hemerythrin domain-containing protein	1.21	1.19	1.04
VP_RS00445	VP0086	hypothetical protein	1.17	1.79	1.31
VP_RS01805	VP0375	DUF4382 domain-containing protein	0.78	2.04	1.10
VP_RS01810	VP0376	EAL domain-containing protein	1.08	1.04	1.60
VP_RS01815	VP0377	helix-turn-helix transcriptional regulator	1.73	1.85	2.24
VP_RS01850	VP0384	hypothetical protein	3.24	3.22	3.11
VP_RS02255	VP0472	hypothetical protein	1.94	2.45	2.04
VP_RS02260	VP0473	hypothetical protein	1.59	2.00	1.48
VP_RS02265	VP0474	TSUP family transporter	1.09	1.61	1.21
VP_RS02395	VP0502	DUF3545 family protein	0.03	-1.59	-1.28
VP_RS02645	VP0556	ribosome-associated translation inhibitor RaiA	0.28	-2.04	-1.03
VP_RS03055	VP0636	porin family protein	1.96	2.35	2.01
VP_RS03770	VP0766	hypothetical protein	2.10	2.01	1.21
VP_RS03780	VP0767	flagellar assembly protein T N-terminal domain-containing protein	-1.68	-1.39	-1.09
VP_RS03785	VP0768	membrane protein	-2.54	-2.34	-1.20
VP_RS03790	VP0769	flagellar assembly lipoprotein FlgP	-2.53	-2.25	-1.30
VP_RS03820	VP0775	flagellar basal body rod protein FlgB	-2.06	-1.57	-1.01
VP_RS03825	VP0776	flagellar basal body rod protein FlgC	-2.11	-1.65	-1.02
VP_RS03830	VP0777	flagellar hook assembly protein FlgD	-2.24	-1.78	-1.07
VP_RS03835	VP0778	flagellar hook protein FlgE	-2.17	-1.79	-1.02

VP_RS03840	VP0780	flagellar basal body rod protein FlgF	-3.04	-2.86	-1.17
VP_RS03845	VP0781	flagellar basal-body rod protein FlgG	-2.41	-2.51	-1.16
VP_RS03850	VP0782	flagellar basal body L-ring protein FlgH	-2.25	-2.07	-1.06
VP_RS03855	VP0783	flagellar basal body P-ring protein FlgI	-2.43	-2.38	-1.17
VP_RS03860	VP0784	flagellar assembly peptidoglycan hydrolase FlgJ	-2.29	-2.68	-1.19
VP_RS03865	VP0785	flagellar hook-associated protein FlgK	-2.77	-2.72	-1.24
VP_RS03870	VP0786	flagellar hook-associated protein FlgL	-2.33	-2.44	-1.31
VP_RS03875	VP0788	flagellin	-2.64	-2.61	-1.33
VP_RS03880	VP0790	flagellin	-2.44	-3.13	-2.89
VP_RS03885	VP0791	flagellin	-0.85	-1.71	-1.98
VP_RS04395	VP0902	HlyC/CorC family transporter	0.21	-1.29	-1.07
VP_RS04645	VP0948	hypothetical protein	1.30	1.25	1.77
VP_RS04865	VP0996	flagellar sheath protein A	-2.38	-2.39	-1.36
VP_RS04995	VP1023	glucose-1-phosphate adenylyltransferase	-0.69	-1.42	-1.21
VP_RS05000	VP1024	glycogen synthase GlgA	-0.72	-1.21	-1.06
VP_RS05510	VP1133	DNA-binding protein H-NS	-4.35	-3.92	-4.77
VP_RS05930	VP1221	cytochrome subunit of sulfide dehydrogenase	1.48	1.29	1.64
VP_RS06400	VP1318	hypothetical protein	1.19	1.11	1.44
VP_RS06405	VP1319	polysaccharide pyruvyl transferase family protein	1.50	1.65	1.87
VP_RS06410	VP1320	2-C-methyl-D-erythritol 4-phosphate cytidylyltransferase	1.54	1.41	1.87
VP_RS06415	VP1321	NAD-dependent epimerase/dehydratase family protein	1.31	1.37	1.82
VP_RS06420	VP1322	LicD family protein	1.20	1.23	1.21
VP_RS06435	VP1325	hypothetical protein	1.80	1.89	1.37
VP_RS06440	VP1326	peptidase S41	2.07	1.88	1.44

VP_RS06595	VP1357	hypothetical protein	0.99	1.06	1.15
VP_RS06735	VP1385	peptidoglycan DD-metalloendopeptidase family protein	1.75	2.25	1.67
VP_RS06740	VP1387	tandem large repeat	0.78	1.65	1.46
VP_RS06760	VP1391	sigma-54-dependent Fis family transcriptional regulator	1.56	2.70	2.71
VP_RS06765	VP1392	type VI secretion system ATPase TssH	2.13	2.99	2.89
VP_RS06770	VP1393	Hcp family type VI secretion system effector	1.47	1.80	3.57
VP_RS06775	VP1394	type VI secretion system tip protein VgrG	1.25	1.73	2.32
VP_RS06780	VP1395	hypothetical protein	1.03	1.75	1.96
VP_RS06785	#N/A	hypothetical protein	1.11	1.50	1.95
VP_RS06790	VP1398	DUF2169 domain-containing protein	1.19	1.50	1.91
VP_RS06795	VP1399	hypothetical protein	1.11	1.49	1.90
VP_RS06800	VP1400	protein kinase family protein	1.32	3.36	2.77
VP_RS06805	VP1401	type VI secretion system protein TssA	1.36	3.06	2.80
VP_RS06810	VP1402	type VI secretion system contractile sheath small subunit	1.25	2.78	2.77
VP_RS06815	VP1403	type VI secretion system contractile sheath large subunit	1.28	2.93	2.75
VP_RS06820	VP1404	type VI secretion system baseplate subunit TssE	0.89	2.26	2.54
VP_RS06825	VP1405	type VI secretion system baseplate subunit TssF	1.08	2.36	2.61
VP_RS06830	VP1406	type VI secretion system baseplate subunit TssG	0.52	1.87	2.19
VP_RS06835	VP1407	Lrp/AsnC family transcriptional regulator	1.43	1.80	1.43
VP_RS06840	VP1408	type VI secretion system membrane subunit TssM	1.15	1.98	1.47

VP_RS06845	VP1409	type VI secretion system ImpA family N-terminal domain-containing protein	1.32	2.06	1.58
VP_RS06850	VP1410	hypothetical protein	1.51	3.42	2.63
VP_RS06855	VP1411	FHA domain-containing protein	1.49	3.23	2.47
VP_RS06860	VP1412	type VI secretion system lipoprotein TssJ	0.82	3.13	2.50
VP_RS06865	VP1413	type VI secretion system baseplate subunit TssK	1.32	3.17	2.50
VP_RS06870	VP1414	DotU family type IV/VI secretion system protein	0.92	2.84	2.61
VP_RS06875	VP1415	DUF4150 domain-containing protein	0.21	1.43	1.41
VP_RS06880	VP1416	hypothetical protein	0.47	1.47	1.33
VP_RS06885	VP1417	hypothetical protein	0.64	1.60	1.33
VP_RS06890	VP1418	hypothetical protein	1.77	2.53	2.08
VP_RS06895	VP1419	hypothetical protein	1.89	3.03	2.19
VP_RS06900	VP1420	hypothetical protein	1.47	2.48	1.75
VP_RS06905	VP1421	hypothetical protein	1.14	2.21	1.67
VP_RS07975	VP1656	type III secretion system translocon subunit VopD	1.91	1.89	1.27
VP_RS07980	VP1657	type III secretion system translocon subunit VopB	1.88	1.89	1.25
VP_RS07985	VP1658	SycD/LcrH family type III secretion system chaperone VcrH	1.92	1.88	1.27
VP_RS07990	VP1659	type III secretion system needle tip protein VcrV	1.65	1.72	1.14
VP_RS07995	VP1660	LcrG family type III secretion system chaperone VcrG	1.54	1.67	1.08
VP_RS08000	VP1661	LcrR family type III secretion system chaperone VcrR	1.25	1.48	1.14
VP_RS08005	VP1662	SctV family type III secretion system export apparatus subunit VcrD	1.13	1.52	1.05
VP_RS08010	VP1663	type III secretion system chaperone VscY	1.10	1.68	1.02

VP_RS08015	VP1664	type III secretion system protein VscX	1.43	1.53	1.11
VP_RS08020	VP1665	type III secretion chaperone SycN	1.55	1.72	1.11
VP_RS08025	VP1666	TyeA family type III secretion system gatekeeper subunit	1.58	1.86	1.10
VP_RS08030	VP1667	SctW family type III secretion system gatekeeper subunit VopN	1.66	1.93	1.06
VP_RS08040	VP1669	type III secretion system central stalk protein VscO	1.22	1.91	1.00
VP_RS08045	VP1670	type III secretion system needle length determinant VscP	1.42	1.82	1.11
VP_RS08050	VP1671	SctQ family type III secretion system cytoplasmic ring protein VscQ	1.32	1.72	1.07
VP_RS08055	VP1672	SctR family type III secretion system export apparatus subunit VscR	1.27	1.56	1.04
VP_RS08060	VP1673	SctS family type III secretion system export apparatus subunit VscS	1.12	1.39	1.04
VP_RS08065	VP1674	SctT family type III secretion system export apparatus subunit VscT	1.13	1.60	1.16
VP_RS08070	VP1675	SctU family type III secretion system export apparatus subunit VscU	1.01	1.25	1.02
VP_RS08095	VP1680	type III secretion system effector VopQ	1.91	1.97	1.37
VP_RS08100	VP1682	CesT family type III secretion system chaperone VecA	1.81	2.08	1.20
VP_RS08105	VP1683	type III secretion system effector VopR	1.69	1.99	1.21
VP_RS08110	VP1684	type III secretion system chaperone	1.62	1.96	1.28
VP_RS08115	VP1686	T3SS effector adenosine monophosphate-protein transferase VopS	2.12	2.05	1.42

VP_RS08120	VP1687	CesT family type III secretion system chaperone	2.13	2.10	1.46
VP_RS08125	VP1688	SctL family type III secretion system stator protein VscL	1.32	1.83	1.08
VP_RS08130	VP1689	SctK family type III secretion system sorting platform protein VscK	1.35	1.84	1.07
VP_RS08135	VP1690	SctJ family type III secretion inner membrane ring lipoprotein Vsc	1.41	1.83	1.06
VP_RS08140	VP1691	SctI family type III secretion system inner rod subunit VscI	1.42	1.69	1.11
VP_RS08145	VP1692	YopR family T3SS polymerization control protein VscH	1.41	1.80	1.02
VP_RS08165	VP1695	SctD family type III secretion system inner membrane ring subunit VscD	1.22	1.79	1.03
VP_RS08175	VP1697	YscB family type III secretion system chaperone VscB	1.21	1.72	1.11
VP_RS08185	VP1699	type III secretion system transcriptional regulator ExsA	1.58	2.31	1.52
VP_RS08190	VP1700	YscW family type III secretion system pilotin	1.62	1.91	1.29
VP_RS09180	VP1888	hypothetical protein	1.20	1.83	1.39
VP_RS09185	VP1889	cold-shock protein	0.60	2.20	1.34
VP_RS09740	VP2004	hypothetical protein	2.23	1.87	2.03
VP_RS09815	VP2020	glycosyltransferase family 39 protein	1.25	1.58	1.79
VP_RS09820	VP2021	VTT domain-containing protein	1.17	1.72	1.72
VP_RS09825	VP2022	glycosyltransferase family 2 protein	1.34	1.81	1.66
VP_RS09830	VP2023	NAD-dependent epimerase	1.38	2.06	1.49
VP_RS10270	VP2111	OmpA family protein	-1.25	-1.46	-1.01
VP_RS10300	VP2119	hypothetical protein	-1.15	-2.27	-1.77
VP_RS10305	VP2120	SDR family oxidoreductase	-0.25	-1.12	-1.85
VP_RS10505	VP2162	hypothetical protein	-1.19	-1.48	-1.40
VP_RS10945	VP2254	flagellar export chaperone FliS	-1.58	-2.22	-1.47

VP_RS10950	VP2255	flagellar protein FliT	-1.50	-2.17	-1.18
VP_RS10955	VP2256	flagellar filament capping protein FliD	-1.96	-2.04	-1.19
VP_RS10960	VP2257	flagellar protein FlaG	-2.10	-2.31	-1.73
VP_RS10965	VP2258	flagellin	-2.31	-3.06	-2.74
VP_RS10970	VP2259	flagellin	-2.01	-3.68	-2.96
VP_RS10975	VP2261	flagellin	-1.48	-2.96	-2.19
VP_RS12200	VP2516	transcriptional regulator OpaR	-0.71	-1.49	-1.17
VP_RS12915	VP2634	6-phospho-beta-glucosidase	1.36	1.12	1.82
VP_RS12920	VP2635	PTS lactose/cellobiose transporter subunit IIA	1.35	1.25	1.66
VP_RS12925	VP2636	PTS sugar transporter subunit IIC	1.67	1.38	1.42
VP_RS12930	VP2637	PTS sugar transporter subunit IIB	1.54	1.79	2.18
VP_RS12935	VP2638	chitin oligosaccharide deacetylase	1.50	1.14	1.02
VP_RS13775	VP2811	sel1 repeat family protein	-1.46	-1.88	-1.71
VP_RS13920	VP2827	methyl-accepting chemotaxis protein	-0.87	-2.17	-1.92
VP_RS14340	VP2907	hypothetical protein	1.26	1.66	1.42
VP_RS14345	VP2908	hypothetical protein	1.22	1.53	1.40
VP_RS14350	VP2909	site-specific integrase	1.19	1.57	1.48
VP_RS15570	VPA0068	GGDEF domain-containing protein	1.03	1.71	1.14
VP_RS15735	VPA0101	hypothetical protein	1.50	2.01	1.02
VP_RS15740	VPA0102	alpha-glucosidase	1.54	2.19	1.60
VP_RS16330	VPA0219	hypothetical protein	1.70	2.14	1.82
VP_RS16335	VPA0220	YtfJ family protein	2.25	3.29	2.56
VP_RS16340	VPA0221	carbonic anhydrase family protein	2.53	3.30	2.74
VP_RS16345	VPA0222	porin	2.69	3.71	2.81
VP_RS16350	VPA0223	efflux RND transporter periplasmic adaptor subunit	1.49	1.78	1.70
VP_RS16355	VPA0224	MacB family efflux pump subunit	1.22	1.36	1.61
VP_RS16360	VPA0225	efflux transporter outer membrane subunit	1.27	1.51	1.56
VP_RS16520	VPA0260	lytic transglycosylase domain-containing protein	0.44	1.04	2.01
VP_RS16525	VPA0261	flagellar export chaperone FlgN	0.84	1.15	2.16

VP_RS16540	VPA0264	flagellar basal body rod protein FlgB	3.20	3.86	4.22
VP_RS16545	VPA0265	flagellar basal body rod protein FlgC	3.57	4.48	4.02
VP_RS16550	VPA0266	flagellar hook assembly protein FlgD	3.41	3.67	4.43
VP_RS16555	VPA0267	flagellar basal body protein FlgE	3.24	3.80	4.51
VP_RS16560	VPA0268	flagellar basal body rod protein FlgF	3.04	3.71	4.43
VP_RS16565	VPA0269	flagellar basal-body rod protein FlgG	3.00	3.58	4.40
VP_RS16570	VPA0270	flagellar basal body L-ring protein FlgH	2.97	3.71	3.75
VP_RS16575	VPA0271	flagellar basal body P-ring protein FlgI	2.46	3.04	3.95
VP_RS16580	VPA0272	rod-binding protein	2.41	2.94	3.55
VP_RS16585	VPA0273	flagellar hook-associated protein FlgK	3.00	3.20	4.17
VP_RS16590	VPA0274	flagellar hook-associated protein FlgL	2.47	3.04	3.49
VP_RS16595	VPA0275	flagellin	1.56	2.29	2.40
VP_RS16700	VPA0297	PTS fructose transporter subunit IIC	0.58	1.13	-2.06
VP_RS16905	VPA0347	hypothetical protein	1.95	2.37	1.93
VP_RS16910	VPA0348	hypothetical protein	1.73	2.51	1.87
VP_RS17040	VPA0375	adenylosuccinate synthase	-0.18	-2.22	-2.67
VP_RS17390	VPA0450	VPA0450 family T3SS effector inositol phosphatase	2.00	2.38	1.39
VP_RS17395	VPA0451	Ati1 family type III secretion system chaperone	1.94	2.32	1.31
VP_RS17480	VPA0469	hypothetical protein	2.26	2.41	2.50
VP_RS17485	VPA0470	efflux RND transporter periplasmic adaptor subunit VmeP	1.99	2.20	2.68
VP_RS17490	VPA0471	efflux RND transporter permease subunit VmeQ	1.59	1.91	2.04
VP_RS17495	VPA0472	outer membrane protein transport protein	1.82	1.87	2.21

VP_RS17500	VPA0473	hypothetical protein	0.66	1.14	1.49
VP_RS17585	VPA0491	methyl-accepting chemotaxis protein	1.68	3.66	2.00
VP_RS17840	VPA0548	OmpA family protein	-1.73	-1.87	-1.63
VP_RS18080	VPA0600	arylsulfatase	1.47	1.08	1.46
VP_RS18085	VPA0601	anaerobic sulfatase maturase	1.68	1.09	1.53
VP_RS18550	VPA0701	OFA family MFS transporter	-0.02	2.45	1.04
VP_RS18605	VPA0713	EAL domain-containing protein	2.04	2.27	2.94
VP_RS18610	VPA0714	collagenase	2.03	3.59	3.27
VP_RS18615	VPA0715	M6 family metalloprotease domain-containing protein	2.36	3.33	4.66
VP_RS18620	VPA0716	helix-turn-helix domain-containing protein	1.11	1.46	2.29
VP_RS18625	VPA0717	LysR family transcriptional regulator	1.91	2.38	2.37
VP_RS18630	VPA0718	prepilin peptidase	2.33	2.62	2.68
VP_RS18635	VPA0719	Flp family type IVb pilin	3.61	5.21	5.67
VP_RS18640	VPA0720	hypothetical protein	2.92	4.91	5.39
VP_RS18645	VPA0721	pilus assembly protein N-terminal domain-containing protein	2.83	4.07	4.90
VP_RS18650	VPA0722	hypothetical protein	2.64	4.08	4.83
VP_RS18655	VPA0723	AAA family ATPase	2.94	3.81	5.08
VP_RS18660	VPA0724	CpaF family protein	2.64	3.44	4.81
VP_RS18665	VPA0725	type II secretion system F family protein	3.00	3.35	4.27
VP_RS18670	VPA0726	type II secretion system F family protein	2.72	3.70	4.63
VP_RS18675	VPA0727	tetratricopeptide repeat protein	2.62	3.51	4.82
VP_RS18680	VPA0728	pilus assembly protein	2.23	2.81	3.94
VP_RS18685	VPA0729	pilus assembly protein TadF	2.44	3.05	4.13
VP_RS18690	VPA0730	VWA domain-containing protein	1.94	2.61	3.55
VP_RS18695	VPA0731	OmpA family protein	2.04	2.55	3.48
VP_RS18700	VPA0732	hypothetical protein	2.07	2.87	3.68
VP_RS18740	VPA0740	LysR family transcriptional regulator	0.18	1.10	1.38
VP_RS19535	#N/A	hypothetical protein	1.47	1.17	1.45
VP_RS19540	VPA0913	hypothetical protein	1.79	2.19	2.05

VP_RS19545	VPA0912	LysR family transcriptional regulator	1.47	1.44	1.40
VP_RS19740	VPA0954	TolC family outer membrane protein	1.30	2.02	1.32
VP_RS19910	VPA0991	cadherin-like domain-containing protein	1.42	1.19	1.68
VP_RS19930	VPA0993	cadherin-like domain-containing protein	1.53	1.87	1.59
VP_RS19935	VPA0994	DsbA family protein	1.48	2.10	1.77
VP_RS20085	VPA1024	hypothetical protein	2.31	2.09	2.50
VP_RS20090	VPA1025	PAAR domain-containing protein	2.44	2.20	2.77
VP_RS20095	VPA1026	type VI secretion system tip protein VgrG	2.69	2.63	2.87
VP_RS20100	VPA1027	type VI secretion system tube protein Hcp	3.50	3.98	3.70
VP_RS20130	VPA1033	type VI secretion system contractile sheath large subunit	0.41	1.62	1.10
VP_RS20135	VPA1034	type VI secretion system contractile sheath large subunit	1.42	1.95	1.19
VP_RS20140	VPA1035	type VI secretion system contractile sheath small subunit	1.28	1.96	1.19
VP_RS20145	VPA1036	type VI secretion system protein TssA	0.99	2.00	1.28
VP_RS20150	VPA1037	serine/threonine-protein phosphatase	0.99	1.97	1.39
VP_RS20155	VPA1038	type VI secretion system-associated protein TagF	0.88	2.39	1.23
VP_RS20160	VPA1039	type VI secretion system membrane subunit TssM	1.08	2.04	1.31
VP_RS20165	VPA1040	type VI secretion system protein TssL	1.25	2.74	1.05
VP_RS20185	VPA1044	serine/threonine protein kinase	1.76	2.93	1.10
VP_RS20400	VPA1091	murein L,D-transpeptidase catalytic domain family protein	1.34	2.81	1.66
VP_RS20605	VPA1135	sugar O-acetyltransferase	-0.28	-1.01	-1.01
VP_RS20940	VPA1204	acetyl-CoA C-acetyltransferase	2.01	1.84	2.11
VP_RS20945	VPA1205	SDR family oxidoreductase	2.07	2.18	1.98

VP_RS21370	VPA1294	SPOR domain-containing protein	1.37	2.06	2.75
VP_RS21375	VPA1295	hypothetical protein	0.84	1.28	2.81
VP_RS21460	#N/A	hypothetical protein	1.55	1.47	1.60
VP_RS21465	VPA1314	thermostable direct hemolysin TDH	0.49	3.07	1.80
VP_RS21470	VPA1316	IS5 family transposase	1.22	2.42	2.41
VP_RS21475	#N/A	DDE-type integrase/transposase/recombinase	0.67	1.55	1.34
VP_RS21495	VPA1321	T3SS2 effector GTPase-activating deamidase VopC	1.58	2.92	2.70
VP_RS21500	VPA1322	hypothetical protein	1.58	2.88	2.67
VP_RS21505	VPA1323	hypothetical protein	1.84	2.70	2.79
VP_RS21510	VPA1324	EAL domain-containing protein	0.17	3.12	2.01
VP_RS21515	#N/A	IS4 family transposase	0.38	2.66	2.05
VP_RS21520	VPA1326	hypothetical protein	1.44	3.17	2.54
VP_RS21525	VPA1327	T3SS effector ADP-ribosyltransferase toxin VopT	1.97	3.80	3.65
VP_RS21530	VPA1328	hypothetical protein	1.72	3.73	3.49
VP_RS21535	VPA1329	conjugal transfer protein TraA	1.29	3.57	3.25
VP_RS21540	#N/A	DUF4116 domain-containing protein	-0.01	2.80	2.25
VP_RS21545	VPA1331	VPA1331 family putative T3SS effector	-0.01	2.63	1.84
VP_RS21555	VPA1334	hypothetical protein	-0.33	2.73	1.49
VP_RS21560	VPA1335	flagellar biosynthetic protein FliQ	-0.32	2.46	1.39
VP_RS21585	VPA1340	VPA1340 family putative T3SS effector	-1.05	3.45	1.22
VP_RS21590	VPA1341	hypothetical protein	-1.36	3.38	1.07
VP_RS21605	VPA1345	hypothetical protein	0.86	3.53	2.24
VP_RS21610	VPA1346	type III secretion system YopJ family effector VopA	0.63	3.90	2.71
VP_RS21615	#N/A	hypothetical protein	0.59	4.03	2.98
VP_RS21620	VPA1348	winged helix-turn-helix domain-containing protein	0.34	2.67	1.54
VP_RS21625	VPA1349	FliM/FliN family flagellar motor switch protein	-0.12	2.83	1.57

VP_RS21630	VPA1350	VPA1350 family putative T3SS effector	-0.12	2.90	1.59
VP_RS21635	VPA1351	VPA1351 family putative T3SS effector	-0.31	3.04	1.57
VP_RS21640	VPA1352	VPA1352 family putative T3SS effector	-0.33	2.96	1.67
VP_RS21645	VPA1353	OmpA family protein	-0.34	3.06	1.66
VP_RS21650	VPA1354	EscU/YscU/HrcU family type III secretion system export apparatus switch protein	-0.67	2.94	1.62
VP_RS21655	VPA1355	FHIPEP family type III secretion protein	-0.97	2.89	1.09
VP_RS21660	VPA1356	hypothetical protein	-1.01	2.86	1.08
VP_RS21665	VPA1357	hypothetical protein	0.68	2.93	2.27
VP_RS21670	VPA1358	dimethyladenosine transferase	0.41	2.94	2.34
VP_RS21675	VPA1359	hypothetical protein	0.20	3.16	2.26
VP_RS21680	VPA1360	hypothetical protein	0.09	3.01	2.17
VP_RS21685	VPA1361	hypothetical protein	0.18	3.41	1.99
VP_RS21690	VPA1362	hypothetical protein	0.17	3.66	1.84
VP_RS21695	VPA1363	molecular chaperone	-0.13	3.10	1.96
VP_RS21700	VPA1364	hypothetical protein	-0.26	3.10	1.65
VP_RS21705	VPA1365	hypothetical protein	-0.32	3.11	1.16
VP_RS21710	VPA1366	hypothetical protein	-0.23	3.13	1.03
VP_RS21715	VPA1367	type III secretion protein	-0.25	3.37	1.10
VP_RS21720	VPA1368	hypothetical protein	0.00	3.13	1.22
VP_RS21725	VPA1369	hypothetical protein	1.11	2.19	1.08
VP_RS21735	VPA1373	hypothetical protein	0.33	2.45	2.34
VP_RS21740	#N/A	transposase	0.41	1.26	1.03
VP_RS21755	VPA1378	thermostable direct hemolysin TDH	0.65	1.69	1.10
VP_RS21760	#N/A	IS4 family transposase	1.15	1.58	1.26
VP_RS21765	VPA1380	type III secretion system effector OspB	-0.17	3.44	1.66
VP_RS21770	#N/A	IS200/IS605 family transposase	0.99	1.59	1.93
VP_RS21865	VPA1402	maltose/maltodextrin ABC transporter ATP-binding protein MalK	-0.22	-1.29	-1.43

VP_RS21870	VPA1403	undecaprenyl-phosphate glucose phosphotransferase	-0.89	-2.03	-1.08
VP_RS22065	VPA1442	DUF11 domain-containing protein	1.51	1.57	1.05
VP_RS22100	VPA1449	methyl-accepting chemotaxis protein	-0.89	-2.36	-2.11
VP_RS22300	VPA1492	methyl-accepting chemotaxis protein	0.17	1.13	1.32
VP_RS22485	VPA1532	flagellar export protein FliJ	2.73	3.47	3.43
VP_RS22490	VPA1533	flagellar protein export ATPase FliI	2.75	3.35	3.37
VP_RS22495	VPA1534	flagellar assembly protein H	3.08	3.43	3.51
VP_RS22500	VPA1535	flagellar motor switch protein FliG	2.97	3.59	3.52
VP_RS22505	VPA1536	flagellar M-ring protein FliF	3.36	3.76	3.73
VP_RS22510	VPA1537	flagellar hook-basal body complex protein FliE	3.35	3.75	3.95
VP_RS22515	VPA1538	sigma-54-dependent Fis family transcriptional regulator	3.43	3.84	3.94
VP_RS22520	VPA1539	OmpA family protein	3.93	4.66	4.49
VP_RS22525	VPA1540	flagellar motor switch protein FliM	4.01	4.37	4.29
VP_RS22530	VPA1541	flagellar motor switch protein FliN	3.82	4.42	4.01
VP_RS22535	VPA1542	flagellar type III secretion system pore protein FliP	3.61	3.98	3.95
VP_RS22540	VPA1543	flagellar biosynthesis protein FliQ	3.34	3.63	3.71
VP_RS22545	VPA1544	flagellar biosynthetic protein FliR	3.54	3.69	3.81
VP_RS22550	VPA1545	flagellar type III secretion system protein FlhB	3.23	3.10	3.70
VP_RS22555	VPA1546	flagellar biosynthesis protein FlhA	2.91	2.56	3.01
VP_RS22565	VPA1548	lateral flagellin LafA	3.40	2.78	4.76
VP_RS22575	VPA1550	flagellar filament capping protein FliD	3.73	3.82	4.52
VP_RS22580	VPA1551	flagellar export chaperone FliS	3.34	3.58	4.28
VP_RS22585	VPA1552	hypothetical protein	3.13	3.51	3.97
VP_RS22590	VPA1553	flagellar hook-length control protein FliK	3.46	3.60	4.82
VP_RS22595	VPA1554	flagellar basal body-associated FliL family protein	3.18	3.88	3.98

VP_RS22600	VPA1555	lateral flagellar system RNA polymerase sigma factor LafS	3.13	3.42	4.23
VP_RS22605	VPA1556	flagellar motor stator protein MotA	3.01	3.34	4.11
VP_RS22610	VPA1557	OmpA family protein	2.49	2.94	3.48
VP_RS22615	VPA1558	hypothetical protein	1.34	1.42	2.35
VP_RS22895	VPA1616	alpha-amylase	-0.44	-1.60	-1.07
VP_RS22965	VPA1632	pyridoxal kinase PdxY	1.56	2.05	1.45
VP_RS22970	VPA1633	AbrB/MazE/SpoVT family DNA-binding domain-containing protein	3.61	3.20	3.80
VP_RS22975	VPA1634	putrescine-ornithine antiporter	4.41	5.80	4.74
VP_RS22980	VPA1635	ornithine decarboxylase SpeF	4.51	6.53	4.73
VP_RS22985	VPA1636	helix-turn-helix domain-containing protein	3.03	3.36	2.93

[a]Concentration of NaCl used in the experiment.
The cut off is -1.5 < X > 1.5 at the non-permissive conditions.

3.4 H-NS binds to the promoter region of *vtrB*, which overlaps with the binding sites of VtrA and Vp-ToxR

Given the DNA-binding feature of H-NS, I next examined whether H-NS binds to the promoter region of *vtrB* using EMSA (**Fig. 13A**). The DNA probe corresponding to the *vtrB* promoter was incubated with purified H-NS protein and was separated in the composite gels. The shift of the DNA probe was observed starting at a DNA/protein molar ratio of 1:2. H-NS has a dimerization domain at the N-terminus and a DNA-binding domain at the C-terminus. I also purified two truncated proteins of H-NS: the N-terminus (aa 1–90) and the C-terminus (aa 91–135). These proteins were also subjected to EMSA with the *vtrB* promoter probe, but no shift of the DNA probe was observed even at a DNA/protein molar ratio of 1:14. These results

indicate that H-NS is capable of binding to the *vtrB* promoter, which requires both the N-terminal dimerization domain and the C-terminal DNA-binding domain of H-NS. Furthermore, I determined the binding region of H-NS in the *vtrB* promoter using DNase footprinting assay, in which showed that H-NS is bound to a broad region within the *vtrB* promoter (**Fig. 13B**).

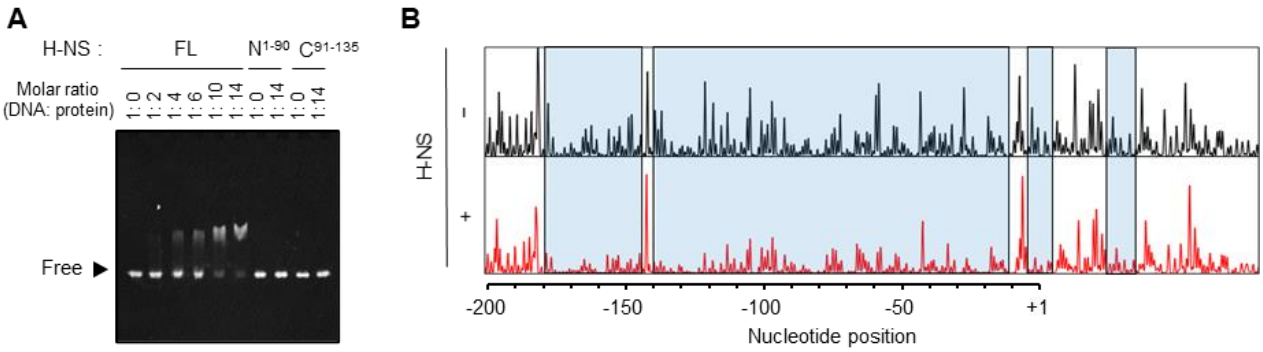

Figure 13. H-NS binds to AT-rich regions within the *vtrB* promoter.

(**A**) Electrophoretic mobility shift assays (EMSA) using the *vtrB* promoter probe with purified full-length protein of HNS (FL) and its truncated variants of the N-terminus (N^{1-90}) and C-terminus (C^{91-135}). The DNA probe corresponding to the *vtrB* promoter (Pro*vtrB*: 50 nM) was incubated with indicated concentrations of each purified protein. The mixtures were then separated in Polyacrylamide/agarose composite gels, followed by staining with ethidium bromide (EtBr). The probe was visualized on a UV trans-illuminator. (**B**) DNase footprinting by H-NS on the *vtrB* promoter. The 6-FAM labeled promoter region of *vtrB* (50 nM) with either BSA (−) or 700 nM H-NS (+) was incubated with DNase I, and was then subjected to the capillary electrophoresis. The region protected by H-NS is indicated by blue shading.

To compare the binding region of H-NS with those of regulators VtrA and Vp-ToxR, I sought to determine the binding sites of VtrA and Vp-ToxR within the *vtrB* promoter. However, due to the insoluble nature of membrane proteins, full-length proteins of both could not be available. Instead, I constructed the chimeric proteins of N-terminal DNA-binding domain of

VtrA and ToxR fused with the ZIP domain of yeast GCN4 for dimerization: $VtrA^{N}$-ZIP and Vp-$ToxR^{N}$-ZIP, given that DNA-binding activity of both proteins is activated by dimerization of the cytoplasmic DNA-binding domains (Dziejman & Mekalanos, 1994; R. Okada et al., 2017). Meanwhile, chimeric proteins of $VtrA^{N}$ and Vp-$ToxR^{N}$ with a ZIP mutant domain (ZIP^{m}) were also constructed, yielding monomeric proteins: $VtrA^{N}$-ZIP^{m} and Vp-$ToxR^{N}$-ZIP^{m}. First, I examined the binding of these chimeric proteins to the *vtrB* promoter using EMSA. As expected, the dimeric $VtrA^{N}$-ZIP but not the monomeric $VtrA^{N}$-ZIP^{m} induced the shift of the *vtrB* promoter probe (**Fig. 14A**, top panel). The dimeric Vp-$ToxR^{N}$-ZIP also shifted the *vtrB* promoter probe (**Fig. 14A**, bottom panel), indicating the direct binding of Vp-ToxR in the *vtrB* promoter. Then, the DNase footprinting assay was performed to determine the binding regions of VtrA and Vp-ToxR in the *vtrB* promoter (**Fig. 14B**). The VtrA-protected region (-55 to -30) contained a short T-tract (4 bases) and overlapped with -35 element within the *vtrB* promoter (**Fig. 14C**). The Vp-ToxR protected region (-85 to -58) was upstream of the VtrA-protected region and on the repetitive T-rich elements within *vtrB* promoter. Taken together, these results indicate that VtrA and Vp-ToxR bind to the AT-rich regions within the *vtrB* promoter, which overlapped with the binding region of H-NS (**Fig. 14C**), suggesting that H-NS might block the binding of VtrA and Vp-ToxR to the *vtrB* promoter.

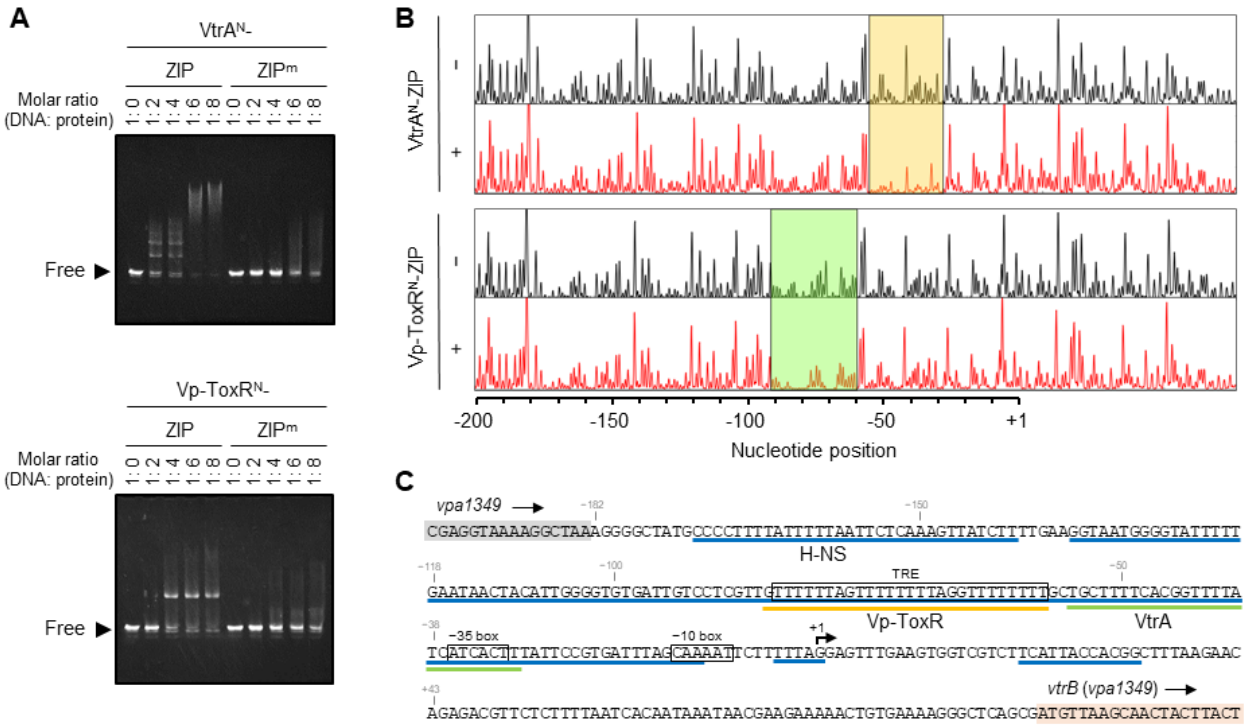

Figure 14. VtrA and Vp-ToxR also bind to AT-rich regions within the *vtrB* promoter. (**A**) EMSA using the *vtrB* promoter probe with dimeric ZIP or monomeric ZIP^{m}-fused N-terminal DNA binding domains of VtrA (VtrA^{N}; top) and Vp-ToxR (Vp-ToxR^{N} bottom). The *vtrB* promoter probe (Pro*vtrB*: 50 nM) was incubated with indicated concentrations of each fusion protein and subjected to composite gel electrophoresis followed by the EtBr staining. (**B**) DNase footprinting by ZIP-fused VtrA^{N} (VtrA^{N}-GCN4-ZIP) or ZIP-fused Vp-ToxR^{N} (Vp-ToxR^{N}-GCN4-ZIP) on the *vtrB* promoter. The 6-FAM labeled promoter region of *vtrB* (50 nM) with BSA (−) or fusion proteins (+) was incubated with DNase I, and was then subjected to the capillary electrophoresis. VtrA^{N}-GCN4-ZIP for 100 nM, Vp-ToxR^{N}-GCN4-ZIP for 600 nM. Orange and green shadings indicate the regions protected by VtrA^{N} (top) and ToxR^{N} (bottom), respectively. (**C**) The DNA sequence of *V. parahaemolyticus* of the *vtrB* promoter region. The approximate nucleotides number of footprint region are based on GeneScan^{TM} 500 LIZ® as an internal standard of mobility in capillary electrophoresis.

Next, I addressed whether H-NS blocks the transcriptional activation activity of VtrA and Vp-ToxR. The deletion of *vtrA* or *Vp-toxR* from the Δ*hns* of *V. parahaemolyticus* eliminated the production of VtrB (**Fig. 15A**), indicating that VtrA and Vp-ToxR are required for *vtrB* activation even in the absence of H-NS. I then examined whether overexpressing VtrA or Vp-

ToxR could antagonize H-NS-mediated repressive effects on VtrB. Overexpression of VtrA under the non-permissive conditions activated VtrB production, indicating that VtrA could outcompete with H-NS in a concentration-dependent manner (**Fig. 15B**). In contrast, VtrB was not expressed by overexpression of Vp-ToxR. Taken together, these findings suggest that H-NS silences *vtrB* transcription under non-permissive conditions through repression of the VtrA-mediated transcriptional activation.

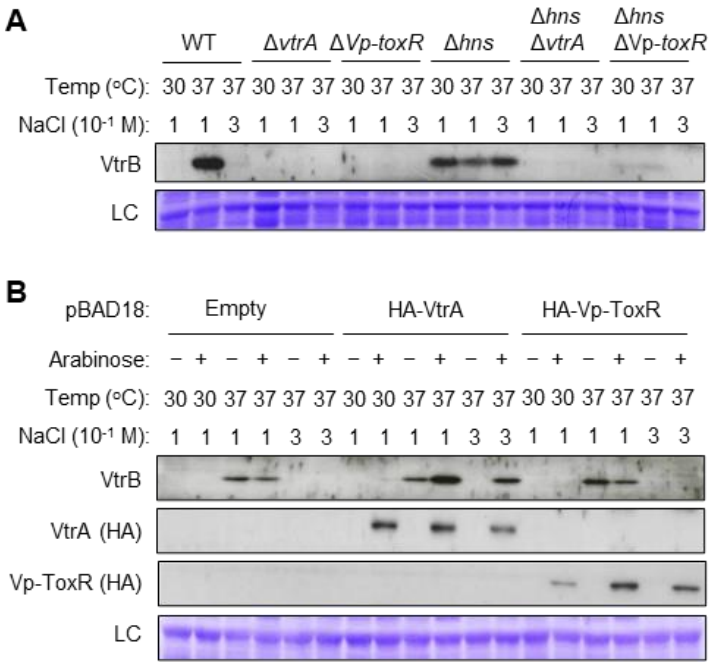

Figure 15. VtrA is able to outcompete with HNS-mediated repression of VtrB production. (**A**) VtrB production in *V. parahaemolyticus* strains WT, Δ*vtrA*, Δ*toxR*, Δ*hns,* Δ*hns* Δ*vtrA* and Δ*hns* Δ*toxR* was examined by immunoblotting. LC, loading control. (**B**) The effects of the P_{BAD}-driven overexpression of hemagglutinin (HA)-tagged VtrA and Vp-ToxR in *V. parahaemolyticus* WT with final arabinose concentration of 0.1% on VtrB production under indicated conditions. Bacterial whole-cell lysates were analyzed by immunoblotting for indicated antibodies. LC, loading control.

3.5 Multimerization of H-NS is needed to repress VtrB production

To examine the H-NS-mediated silencing of VtrB in more detail, I first tried to complement the Δ*hns* mutant of *V. parahaemolyticus* with H-NS of *Escherichia coli* (hereinafter referred as to Ec H-NS), which has been extensively studied in greater detail. Even though Ec H-NS have 54.41% identity with H-NS of *V. parahaemolyticus* (hereinafter referred as to Vp H-NS to distinguish from Ec H-NS and H-NS of other bacteria), Ec H-NS could substitute Vp H-NS in *V. parahaemolyticus*, indicating a conserved feature of H-NS (**Fig. 16A** and **B**). In Ec H-NS, two residues, L30 and I70, are critical for the oligomerization of H-NS (C et al., 1997; Lim et al., 2012; Yamanaka et al., 2018). These residues were also conserved in Vp H-NS (**Fig. 16A** and **B**). I created point mutations in Vp H-NS: L30P and I70C (**Fig. 16B**). These mutations caused de-repression of VtrB production under the non-permissive conditions (**Fig. 17A**), suggesting that multimerization of Vp H-NS is important to repress *vtrB* transcriptional activation under the non-permissive conditions. Higher expression of these mutants compared to the wild-type Vp H-NS was reasonable because the mutation of these residues disturb the repressive activity of H-NS, and H-NS also regulates its own promoter (Falconi et al., 1993; Ueguchi et al., 1993). Next, I examined the DNA-binding ability of these point mutants using EMSA with the *vtrB* promoter probe. Like Ec H-NS (Lim et al., 2012; Yamanaka et al., 2018), these mutations retained binding ability *in vitro* (**Fig. 17B**).

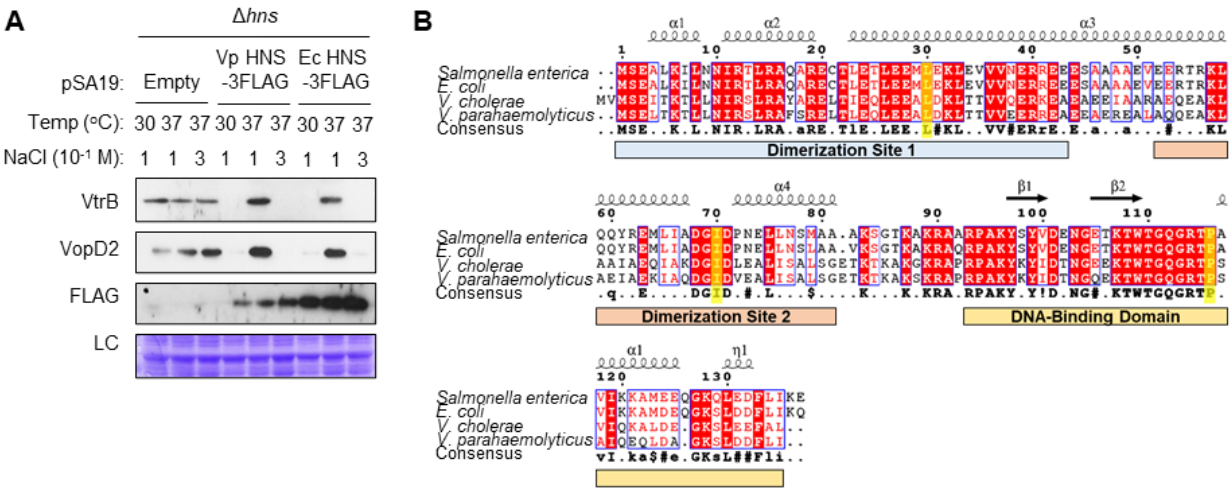

Figure 16. Ec H-NS is able to substitute Vp H-NS for the repressive effect on VtrB production.

(**A**) *V. parahaemolyticus* Δ*hns* harboring pSA19 empty vector, pSA19-Vp H-NS-3×FLAG or pSA19-Ec H-NS-3×FLAG were grown at indicated temperature and concentrations of NaCl. Bacterial whole-cell lysates were analyzed by immunoblotting for indicated antibodies. H-NS production was determined by immunoblotting with an anti-FLAG antibody. LC, loading control. (**B**) Sequence alignment of H-NS from *Salmonella* (STM1751), *E. coli* (b1237), *V. cholera* (VC0395_A0700), and *V. parahaemolyticus* (VP1133). Residues of dimerization domains, L30 (site 1) and I70 (site 2), as well a residue of DNA binding domain, P116 (P117 in *V. parahaemolyticus*), are conserved among H-NS homologs, as indicated by the yellow highlight. The secondary structure of H-NS from *Salmonella* was shown on the top of sequences (PDB: 3nr7 and 2L93).

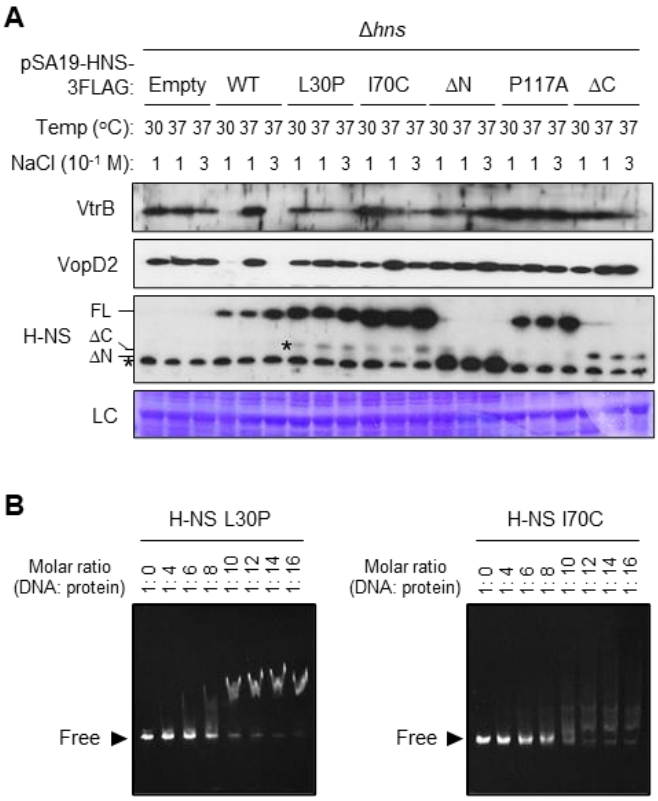

Figure 17. H-NS requires its multimerization for the repressive activity against VtrB production under the non-permissive conditions.

(**A**) *V. parahaemolyticus* were expressing 3×FLAG-tagged Vp H-NS (WT) and its variants; L30P (a point mutation in site 1), I70C (a point mutation in site 2), ΔN (lacking the N-terminal oligomerization domain), P117A (a point mutation in DNA-binding domain), and ΔC (lacking the C-terminal DNA-binding domain), from the pSA19 plasmid with the endogenous promoter of Vp H-NS. Bacterial whole-cell lysates were analyzed by immunoblotting for indicated antibodies. H-NS production was examined by immunoblotting with an anti-FLAG antibody. LC, loading control. An asterisk indicates the non-specific band. (**B**) Vp H-NS variants having point mutations at dimerization site 1 and site 2 retained the binding ability to the *vtrB* promoter *in vitro*. EMSA was performed using the *vtrB* promoter probe with purified proteins of Vp H-NS having point mutation L30P and I70C.

3.6 Ionic conditions are responsible for the Vp H-NS mediated salinity-dependent repression of VtrB production

Several studies have shown that temperature directly affects the dimerization stability of H-NS (Hameed et al., 2019; Stella et al., 2006; Zhao et al., 2020, 2021), whereas osmolarity modulates H-NS's activity through the ionic strength (Qin et al., 2020). Therefore, I examined the effect of another monovalent salt in the salinity-dependent T3SS2 regulation. When *V. parahaemolyticus* WT was grown in LB medium with KCl instead of NaCl, VtrB production was observed at 0.1 M KCl but not at above 0.2 M KCl, a result similar to those at NaCl (**Fig. 18A**). An increase in salts affects ionic strength and osmotic pressure; therefore, I examined which condition is responsible for the observed repression. To this end, a neutral osmolyte, sucrose, is supplemented with LB medium because of no usage by *V. parahaemolyticus* as a carbon source. Due to the requirement of minimal salts for *V. parahaemolyticus* to grow (Morishita & Takada, 2011; Palasuntheram, 1981), NaCl at a low concentration of 0.04 M was added to the culture medium. When *V. parahaemolyticus* WT was grown in LB medium with minimal NaCl and increased concentrations of sucrose, VtrB production was observed even at 0.6 M sucrose, whose osmolarity is equivalent to 0.3 M NaCl (**Fig. 18A**). These results suggest that ionic strength, rather than the osmotic pressure, is responsible for the observed Vp H-NS mediated VtrB production repression.

It has been reported that both low and high ionic strengths of salts influence the silencing

activity of H-NS by affecting the DNA stiffening and bridging with H-NS (Qin et al., 2019). Because *V. parahaemolyticus* is a moderate halophile bacterium that can adapt to higher salinity by maintaining its sodium homeostasis through Na efflux pumps (35, 36) or synthesis compatible solute (Naughton et al., 2009; Ongagna-Yhombi & Boyd, 2013), I increased the salinity of the culture medium to 1.4 M NaCl, which is the upper limit of salinity for *V. parahaemolyticus* to grow, to examine whether higher salinity also affects the VtrB production in *V. parahaemolyticus*. Expectedly, VtrB production was observed at NaCl concentrations greater than 1 M (**Fig. 18B**), indicating that both low and high ionic strength affects the repressive activity of Vp H-NS against VtrB production in *V. parahaemolyticus*.

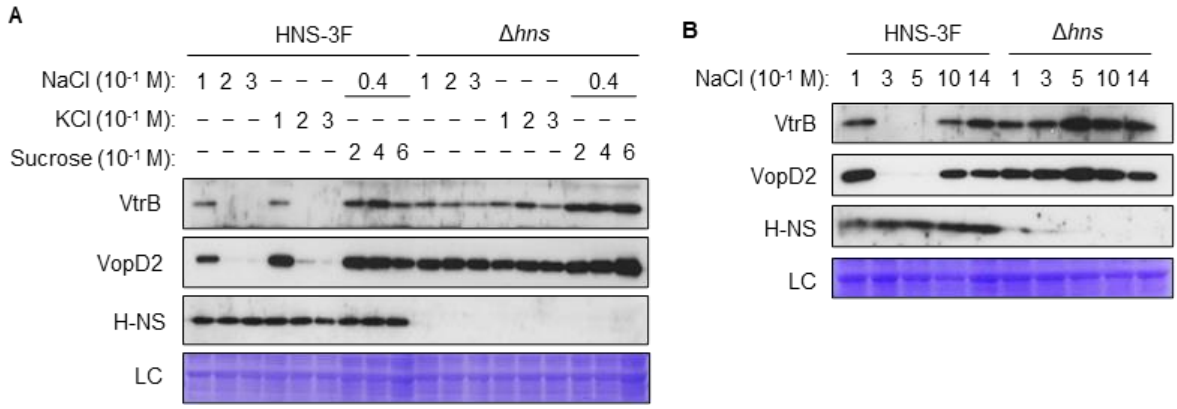

Figure 18. Ionic conditions are responsible for the H-NS mediated VtrB repression.
(**A, B**) *V. parahaemolyticus* strains HNS-3F and Δ*hns* strains were grown in LB medium with indicated concentrations of NaCl, KCl or sucrose at 37°C. In the case of sucrose supplementation, 40 mM NaCl was added to allow the growth of *V. parahaemolyticus*. The production of VtrB and VopD2 were analyzed by immunoblotting. H-NS production was examined by immunoblotting with an anti-FLAG antibody. LC, loading control.

CHAPTER 4
DISCUSSION

In this study, first I revealed that VtrB production underlies the temperature- and salinity-dependent expression of T3SS2-related genes. VtrA and Vp-ToxR, both upstream regulators of VtrB, are membrane-spanning transcriptional regulators consisting of the N-terminal DNA-binding domain, the central transmembrane domain and the C-terminal periplasmic domain. The periplasmic domains of these regulators are thought to be involved in sensing environmental signals such as bile acids (Lembke et al., 2020; Midgett et al., 2020; Okada et al., 2017). The periplasmic domain of VtrA forms a complex with the periplasmic domain of VtrC, a co-transcribed factor of VtrA, which binds to bile acids (Li et al., 2016). This binding presumably alters the state of VtrA, inducing multimerization of its DNA-binding domain and subsequent transcriptional activation of *vtrB*. However, my results show that VtrA and Vp-ToxR are constitutively expressed at various temperatures and NaCl concentrations, and their transcriptional activation activities are not affected. These results suggest that the two positive regulators of VtrB do not transmit physical cues from the external environment. Here, I identified H-NS, a global transcriptional repressor, as a negative regulator of VtrB production. It has been reported that H-NS binds to the *vtrA* promoter and represses *vtrA* expression (Sun et al., 2014). However, the *hns* mutation did not affect the VtrA protein level in my results, and this was also the case for *vtrA* transcript analysis by RNA-seq. Under the permissive condition,

VtrB protein levels were comparable between the *hns*-deleted and its parental strains, and the *hns*-deleted strain produced a similar amount of VtrB protein under the non-permissive conditions as under the permissive condition. This observation indicates that the H-NS-mediated suppression of VtrB is restricted to the non-permissive conditions. Similar results were observed with the *vtrB* mRNA transcript, suggesting that this regulation occurs at the transcriptional level. VtrA binds near the -35 element of the *vtrB* promoter, and Vp-ToxR binds to a more upstream region called the T-rich repetitive element (TRE), which is important for *vtrB* transcriptional activation (Okada et al., 2017), overlapping with the broad binding region of H-NS within the *vtrB* promoter. These binding regions have low GC content and are suitable targets for transcriptional repression of H-NS, which prefers AT-rich sequences (Gordon et al., 2011).

Many virulence genes of pathogenic bacteria are thought to have been acquired by horizontal gene transfer during evolution (Gal-Mor & Finlay, 2006). In prokaryotes, the GC content of horizontally acquired genes is often lower than that of the entire genome, and such regions are likely to be targeted for H-NS mediated transcriptional repression (Navarre, 2016). Bacteria can overcome H-NS silencing by altering H-NS activity in response to environmental signals (temperature, pH, osmotic pressure) and/or counteracting its repression using transcriptional regulators. In *Salmonella*, two pathogenicity islands, SPI-1 and SPI-2, encode different T3SSs, T3SS-1 and T3SS-2, respectively, which are essential for its virulence.

Salmonella counteracts H-NS silencing by the SPI-1 master regulators HilC, HilD, and RtsA for activating T3SS-1 expression at 37°C, which is required for entry into epithelial cells (Olekhnovich & Kadner, 2007; Ono et al., 2005). Once internalized into epithelial cells, the expression of T3SS-2, which is required for intracellular survival and replication, is stimulated by the host environment conditions, including low magnesium and low pH. The acidic environment is a signal for the two-component system SsrA-SsrB, in which the sensor kinase SsrA phosphorylates the response regulator SsrB, and in turn, the phosphorylated SsrB counteracts H-NS silencing and activates transcription of multiple operons within SPI-2 (Walthers et al., 2007, 2011). Another example in EPEC is that the locus of enterocyte effacement (LEE) pathogenicity island encoding the T3SS required for A/E lesion, is silenced by H-NS at 27ºC (Umanski et al., 2002). The transcriptional activator of the LEE pathogenicity island, Ler, has the C-terminal DNA-binding domain similar to that of H-NS and the N-terminal oligomerization domain which promotes toroidal Ler-DNA structure formation (García et al., 2012; Mellies et al., 2011). Both H-NS and Ler bind overlapping regions within LEE pathogenicity island, where H-NS acts as a silencer and Ler acts as an anti-silencer that can counteract the H-NS mediated gene silencing at 37ºC (Bustamante et al., 2001). The competition between Ler and H-NS is thought to be an important factor in LEE genes expression, in which environmental factors such as temperature and ionic conditions might directly affect the DNA binding activities of both regulators (Winardhi et al., 2014).

In *V. cholerae*, the species more closely related to *V. parahaemolyticus*, H-NS silences the gene expression of the pathogenicity island 1 (VPI-1), which contains the toxin-coregulated pilus (TCP) operon encoding the TCP pilus essential for intestinal colonization of *V. cholerae*, and the CTXΦ genetic island, which encodes the genes for cholera toxin (Ayala et al., 2015; Kazi et al., 2016). ToxT, a transcriptional activator encoded by VPI-1, positively regulates the VPI-1 and CTXΦ gene expression. The one target site of H-NS in these two genetic islands for transcriptional repression is on the *toxT* promoter, where its repression is counteracted by Vc-ToxR followed by activation by the transcriptional activator TcpP. Interestingly, the relationship between TcpP, Vc-ToxR, and H-NS on the *toxT* promoter in *V. cholerae* is quite similar to that of VtrA, Vp-ToxR, and H-NS on the *vtrB* promoter in *V. parahaemolyticus*. Like VtrA, TcpP is a membrane-spanning transcriptional regulator that binds near the -35 element in the *toxT* promoter and directly activates *toxT* transcription, whereas Vc-ToxR binds to the TNAAA-N5-TNAAA direct repeat sequence upstream of the TcpP-binding region and functions as a co-regulator to promote transcriptional activation of *toxT* (Goss et al., 2013). It has been also proposed that Vc-ToxR promotes the interaction between TcpP and the *toxT* promoter by replacing H-NS and altering DNA topology (Goss et al., 2013).

In *V. parahaemolyticus*, Vp-ToxR is a co-activator required to activate *vtrB* transcription by VtrA. Overexpression of Vp-ToxR did not cancel the silencing of *vtrB* by H-NS under the non-permissive conditions, suggesting that it might not serve for recruiting VtrA.

Recently, it has been shown that TcpP binds to the *toxT* promoter independently of Vc-ToxR in *V. cholerae* (Calkins et al., 2021). Ectopic expression of VtrA in *E. coli* increases *vtrB* promoter activity (Kodama et al., 2010), indicating that VtrA is a direct transcriptional activator of *vtrB*. The binding region of VtrA overlapped with the -35 element of the *vtrB* promoter, suggesting its direct interaction with RNA polymerase. Some studies have reported that in the absence of H-NS, the positive regulators are no longer needed in transcription activation in the cases of *ctx* expression by ToxT or Vc-ToxR in *V. cholerae* (Nye et al., 2000) and LEE operon activation by Ler in EPEC (Bustamante et al., 2001). However, the mutant in which *vtrA* or *vp-toxR* is deleted from the *hns*-deleted strain did not produce VtrB protein even under the permissive condition (**Fig. 15A**), indicating that these positive regulators are necessary for the *vtrB* transcriptional activation even in the absence of H-NS, possibly by recruiting RNA polymerase.

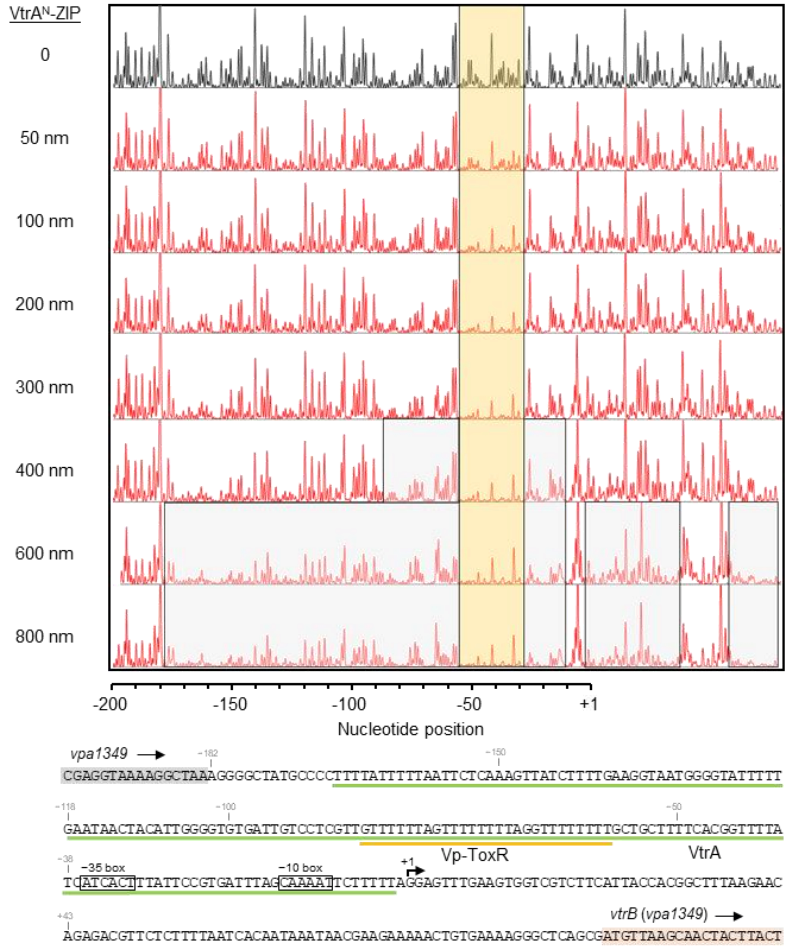

Figure 19. Higher concentrations of VtrA^{N}-ZIP covered a broad region within the *vtrB* promoter, including Vp-ToxR binding region.

The silencing of *vtrB* by H-NS under the non-permissive conditions was overcome by overexpression of VtrA in contrast to that of Vp-ToxR (**Fig. 15B**). The deletion of the gene for Vp-ToxR abolishes *vtrB* expression, which is also restored by overexpression of VtrA (Hubbard et al., 2016). Moreover, ectopic expression of VtrA in *E. coli*, which is relatively overexpressed under the control of the P_{BAD} promoter, does not require Vp-ToxR for *vtrB* induction (Okada et al., 2017). These observations suggest that excess VtrA can replace the function of Vp-ToxR. Intriguingly, in my DNase footprinting assay, higher concentrations of

VtrA ware found to bind to a broader region within the *vtrB* promoter, including the TRE, which is the Vp-ToxR binding region (**Fig. 19B**). Consistent with this, ectopic expression of VtrA in *E. coli* does not increase the transcriptional activity of the *vtrB* promoter lacking the TRE (Okada et al., 2017). However, the exact role of Vp-ToxR in transcriptional activation of *vtrB* is still unclear. Transcriptional activators facilitate RNA polymerase recruitment on the promoter of the gene to stimulate transcription through different mechanisms: class I and class II activation (Lee et al., 2012). Class I activators bind the upstream of -35 element of the promoter and interact with α-CTD subunits of RNA polymerase for the recruitment of the polymerase. Class II activators bind close to or overlaps with the -35 element of the promoter and recruits the RNA polymerase to the promoter by interacting with α-NTD and/or the domain 4 of σ subunit. Considering the binding sites of VtrA and Vp-ToxR within the *vtrB* promoter (**Fig. 14C**), VtrA may act as a class II activator while Vp-ToxR would be assigned to a class I activator. The combination of class I and class II activation is defined as class III activation, in which two transcription activators make independent contacts with RNA polymerase and both factors need each other for transcription activation (Lee et al., 2012). Given that both VtrA and ToxR are required in *vtrB* transcription activation, the transcriptional activation of *vtrB* might be classified as class III activation.

The expression of VtrB under the permissive condition suggests that H-NS mediated silencing of *vtrB* transcription can be canceled at a certain temperature of 37°C and a salt

concentration of 0.1 M NaCl. The H-NS mediated transcription silencing is based on its ability to multimerize with its DNA targets (Lim et al., 2012). H-NS dimerization sites 1 and 2 are involved in this multimerization, with both sites mediating dimerization of H-NS monomers, which then associate as protomers via the vacant site to form multimers. In *E. coli*, mutations at these sites (site 1: L30P, site 2: I70C) reduce the silencing activity of H-NS *in vivo* (Lim et al., 2012; Yamanaka et al., 2018). In *V. parahaemolyticus*, mutations in these sites of H-NS also canceled silencing of T3SS2 gene expression (**Fig. 17A**), suggesting that multimerization is also responsible for the silencing activity of H-NS in *V. parahaemolyticus*. Overexpression of VtrA activated VtrB expression at 37°C and a high salt concentration of 0.3 M NaCl, but not at the low temperature of 30°C, even at a permissive salt concentration of 0.1 M NaCl (**Fig. 15B**), suggesting that temperature has a stronger effect on the silencing activity of H-NS than salt concentrations. Furthermore, unlike high concentrations of NaCl or KCl, the neutral osmolyte sucrose did not silence T3SS2 gene expression (**Fig. 18A**). This indicates that ionic strength, rather than osmotic pressure, affects silencing activity of H-NS in *V. parahaemolyticus*, supporting the hypothesis that ionic strength alters the DNA-binding properties of the H-NS family proteins, as proposed by Qin and colleagues (Qin et al., 2020).

The H-NS silencing is initiated by DNA binding of H-NS to the nucleation sites with AT-rich sequences for the high binding affinity of H-NS to DNA at its targets (Bouffartigues et al., 2007), and then H-NS multimerizes and spreads along the DNA strand to form the

filamented and stiffened H-NS–DNA complex (Amit et al., 2003; Winardhi et al., 2012). Under certain concentrations of salts such as NaCl, KCl and $MgCl_2$, the filamented H-NS–DNA complex can bridge between two DNA duplexes by binding of H-NS with a DNA duplex to a second DNA duplex, to form the DNA–H-NS–DNA bridged complex (Liu et al., 2010; Qin et al., 2020). The stiffened filament and bridged DNA formation by H-NS is thought to be responsible for the H-NS-mediated gene silencing because several *in vitro* studies have shown that both complex formations could inhibit the action of RNA polymerase and transcriptional activators (Amit et al., 2003; Chen et al., 2005; Dame et al., 2002). A recent study of MvaT, an H-NS family protein of *Pseudomonas aeruginosa,* has shown that the stiffened and bridged formation can be switched between different salt concentrations (Qin et al., 2020). The N-terminal dimerization domain of MvaT contains a cluster of negatively charged residues, whereas the C-terminal DNA-binding domain and the central linker region of MvaT consist of positively charged residues. The ionic strength of salts can modulate the electrostatic interaction between these oppositely charged domains of MvaT and change the conformation of MvaT protomer to half-open or fully open conformers. Under low ionic strength due to low salt concentrations, one DNA-binding domain of the MvaT protomer binds to the target DNA, while the other DNA-binding domain is sequestered by the N-terminal dimerization domain through the electrostatic interaction (half-open), forming the lateral filament of the MvaT–DNA complex along the DNA strand. On the other hand, increase in ionic strength due to high

salt concentrations weakens the electrostatic interaction between the second DNA-binding domain and the N-terminal dimerization domain, releasing the second DNA-binding domain free (full open) to bind to another DNA duplex for the bridged formation. It is not yet clear which formation, DNA stiffening or DNA bridging, can cause more robust silencing activity. One study have reported that SsrB, the *Salmonella* T3SS2 regulator, could outcompete the silencing by H-NS in the stiffened filament but not in bridged complex (Walthers et al., 2011). Another study showed that bridged, not filamented H-NS nucleoprotein complex promotes Rho-dependent termination (Kotlajich et al., 2015). These studies suggest that DNA bridging by H-NS might show more potent silencing activity of H-NS. Here, I demonstrated that H-NS multimerization is important for the transcriptional silencing of *vtrB* by H-NS in *V. parahaemolyticus*, the details of H-NS–DNA complex formation for *vtrB* silencing remains unclear at this stage. This issue will be addressed in future research as described in the next chapter.

The *vtrB* gene is encoded within the Vp-PAI region with low GC content, which is thought to be acquired by horizontal gene transfer (Makino et al., 2003). Given the property that H-NS silences foreign gene expression, it would be possible that H-NS might not only target the *vtrB* promoter for the T3SS2 silencing but serve as the transcriptional repressor for multiple genes within the Vp-PAI region; H-NS might bind to several nucleation sites in Vp-PAI, forming the broad filamented H-NS–DNA complex and the DNA–H-NS–DNA complex

throughout this genomic island. This hypothetical scenario might be supported by the observation that the plasmid-borne inducible expression of VtrB under the non-permissive conditions broke T3SS2 silencing by H-NS, but the level of VtrB protein was around 10-fold higher than that of VtrB protein under the permissive condition (**Fig. 9D**), but warrants validation in the future study: the genome-wide mapping of the H-NS binding sites under various conditions, including the permissive and non-permissive conditions using chromatin immunoprecipitation (ChIP)-sequencing.

In *Enterobacteriaceae*, it is known that StpA and Hha/Ydgt/Ymoa interact with H-NS and that this interaction modulates the activity of H-NS (Boudreau et al., 2018; Ellison & Miller, 2006; Paytubi et al., 2004; Ueda et al., 2013). However, no such paralogs or co-regulators have been found in *Vibrio* spp. including *V. parahaemolyticus* (Singh et al., 2016). In *V. cholerae*, a small protein called TsrA has recently been reported as a transcriptional repressor similar to H-NS. The regulation of TsrA on genome-wide gene expression is strongly correlated with that of H-NS. Although TsrA does not have a DNA-binding domain, it may interact with H-NS because of its structural similarity to the dimerization domain of H-NS. A TsrA homologue is also found in *V. parahaemolyticus*. Although there is no direct evidence that TsrA interacts with H-NS and affects its activity at the moment, it will be interesting to further explore whether this homologue is involved as a co-regulator in the regulation of T3SS2 gene expression via H-NS in *V. parahaemolyticus*.

CHAPTER 5
CONCLUSION AND FUTURE PERSPECTIVES

*V. parahaemolyticu*s requires T3SS2 for its enteropathogenicity to humans, and the T3SS2 gene cluster is encoded in Vp-PAI spanning 80 kb on the chromosome 2. The T3SS2 expression is regulated in a temperature- and salinity-dependent manner, which seems to mimic the virulence regulation of *V. parahaemolyticu*s in the host environment during its infection, but its underlying mechanism has been elusive over 10 years. In this study, I demonstrated that H-NS regulates the entire T3SS2 gene expression in *V. parahaemolyticus* by silencing the transcription of the *vtrB* gene, which encodes one of the transcriptional master regulators of the T3SS2 gene cluster, under the non-permissive conditions of low temperature and/or high salt concentrations. H-NS binds to the AT-rich sequence in the *vtrB* promoter, where is shared by two positive regulators of *vtrB*, VtrA and Vp-ToxR. The silencing activity of H-NS was related to its activity for multimerization, and changes in physical conditions such as temperature and salinity may alter the DNA-binding properties of H-NS and affect its silencing activity. Thus, my findings suggest that competition between activation of *vtrB* transcription by VtrA and Vp-ToxR and silencing of *vtrB* transcription by H-NS might underlie the temperature- and salinity-dependent T3SS2 gene regulation (**Fig. 20**). The H-NS regulatory mechanism may be responsible for the appropriate expression of the Vp-PAI genes in *V. parahaemolyticus*: silencing in the habitat and expressing in the host environment. Overall, my

findings demonstrate the bedrock role H-NS in the temperature- and salinity-dependent regulation of T3SS2, and expand our understanding of the virulence regulation in *V. parahaemolyticus*.

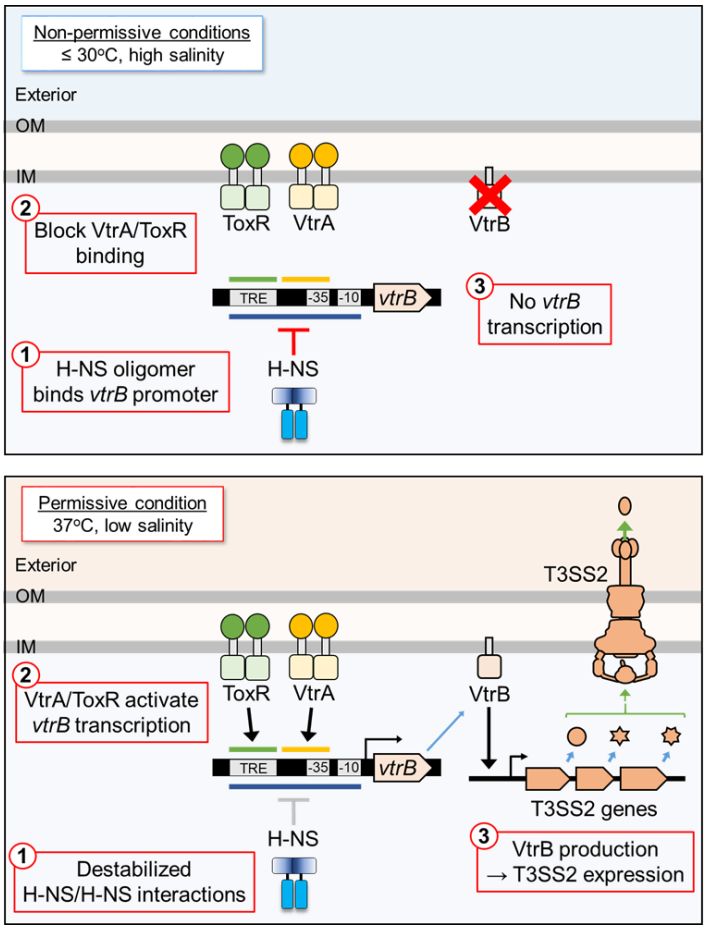

Figure 20. The working hypothesis depicting temperature- and salinity-dependent T3SS2 silencing by H-NS. Upper panel: T3SS2 gene expression is silenced under the non-permissive conditions, in which H-NS silences *vtrB* transcription through the overlapping binding with VtrA and Vp-ToxR. Bottom panel: T3SS2 silencing is canceled under the permissive condition, in which VtrA and/or Vp-ToxR might outcompete H-NS with reduced silencing activity, resulting in the production of VtrB and activation of T3SS2 gene expression.

This study also raises some issues to be experimentally validated in the further study. First, the competitive situation in which the *vtrB* promoter is being occupied by H-NS under

the non-permissive condition while VtrA and Vp-ToxR are dominant over H-NS on the *vtrB* promoter under the permissive condition, has not yet been verified. To examine this, I performed the EMSA assay in which the *vtrB* promoter probe was co-incubated with H-NS and VtrA or Vp-ToxR. However, even at 25°C, H-NS could not block the binding of VtrA or Vp-ToxR to the *vtrB* promoter probe. It might be possible that H-NS forms the stiffened complex with DNA on the *vtrB* promoter but the formation of the bridged complex may require a wider region around Vp-PAI. The silencing activity of the bridged complex with H-NS and DNA has been suggested more potent than that of the stiffened complex (Walthers et al. 2011; Kotlajich et al. 2015). Therefore, the complex state of H-NS with DNA may not be fully reproduced in the EMSA assay *in vitro*. Alternatively, this issue will be examined using a different approach: ChIP-qPCR, in which DNA corresponding to the *vtrB* promoter region that co-immunoprecipitates with H-NS, VtrA or Vp-ToxR from *V. parahaemolyticus* grown under the permissive and non-permissive conditions is analyzed by qPCR. This method will allow us to quantitatively evaluate the interaction between the *vtrB* promoter and each protein under various conditions, and would inform the competitive state *in vivo* (predictably, on the *vtrB* promoter, the dominance of H-NS under the non-permissive conditions and the dissociation of H-NS under the permissive condition). The second issue is that the complex status of H-NS with the *vtrB* promoter under the permissive and non-permissive conditions is not yet determined. To date, it is technically challenging to determine the exact state of the H-NS–

DNA complex *in vivo*; hence, *in vitro* experiments have been relied on to observe the H-NS–DNA complex formation. The silencing activity of H-NS family proteins is suggested to be correlated with the complex status of H-NS–DNA complex (Hameed et al. 2019; Qin et al. 2020). Qin et al. have proposed a model in which H-NS forms the stiffened DNA complex at low ionic strength, and it forms the bridged DNA complex at high ionic strength, and the H-NS–DNA complex collapses when the ionic strength threshold is exceeded. Given that the potential potent silencing activity of the bridged DNA complex than the stiffened DNA complex, this model is consistent with our observations that T3SS2 is expressed at low ionic strength, repressed at high ionic strength, and expressed at extreme higher ionic strength (**Fig. 18B**). This issue might be addressed by atomic force microscopy, which is often employed to image the H-NS–DNA complex *in vitro* (Lim et al. 2012; Yamanaka et al. 2018) to observe the filamented or bridged formation of H-NS within *vtrB* promoter or larger DNA fragment including Vp-PAI region under the permissive and non-permissive conditions. Thus, these future efforts would provide the detailed mechanistic insight into the potential change in the competitive state between H-NS and VtrA or Vp-ToxR on the *vtrB* promoter under the permissive and non-permissive conditions.

REFERENCE

Amit, R., Oppenheim, A. B., & Stavans, J. (2003). Increased bending rigidity of single DNA molecules by H-NS, a temperature and osmolarity sensor. *Biophysical Journal*, *84*(4), 2467–2473. https://doi.org/10.1016/S0006-3495(03)75051-6

Anders, S., Pyl, P. T., & Huber, W. (2014). HTSeq—a Python framework to work with high-throughput sequencing data. *Bioinformatics*, *31*(2), 166–169. https://doi.org/10.1093/bioinformatics/btu638

Ansaruzzaman, M., Lucas, M., Deen, J. L., Bhuiyan, N. A., Wang, X. Y., Safa, A., Sultana, M., Chowdhury, A., Balakrish Nair, G., Sack, D. A., Von Seidlein, L., Puri, M. K., Ali, M., Chaignat, C. L., Clemens, J. D., & Barreto, A. (2005). Pandemic serovars (O3:K6 and O4:K68) of *Vibrio parahaemolyticus* associated with diarrhea in Mozambique: Spread of the pandemic into the African continent. *Journal of Clinical Microbiology*, *43*(6), 2559–2562. https://doi.org/10.1128/JCM.43.6.2559-2562.2005

Arold, S. T., Leonard, P. G., Parkinson, G. N., & Ladbury, J. E. (2010). H-NS forms a superhelical protein scaffold for DNA condensation. *Proceedings of the National Academy of Sciences of the United States of America*, *107*(36), 15728–15732. https://doi.org/10.1073/pnas.1006966107

Ayala, J. C., Silva, A. J., & Benitez, J. A. (2017). H-NS: an overarching regulator of the *Vibrio cholerae* life cycle. *Research in Microbiology*, *168*(1), 16. https://doi.org/10.1016/J.RESMIC.2016.07.007

Ayala, J. C., Wang, H., Benitez, J. A., & Silva, A. J. (2015). RNA-Seq analysis and whole genome DNA-binding profile of the *Vibrio cholerae* histone-like nucleoid structuring protein (H-NS). *Genomics Data*, *5*, 147–150. https://doi.org/10.1016/J.GDATA.2015.05.039

Baker-Austin, C., Oliver, J. D., Alam, M., Ali, A., Waldor, M. K., Qadri, F., & Martinez-Urtaza, J. (2018). *Vibrio* spp. infections. *Nature Reviews Disease Primers 2018 4:1*,

4(1), 1–19. https://doi.org/10.1038/s41572-018-0005-8

Barker, W. H., Mackowiak, P. A., Fishbein, M., Morris, G. K., D'alfonso, J. A., Hauser, G. H., & Felsenfeld, O. (1974). *Vibrio parahaemolyticus* gastroenteritis outbreak in covington, Louisiana, in August 1972. *American Journal of Epidemiology*, *100*(4), 316–323. https://doi.org/10.1093/OXFORDJOURNALS.AJE.A112040

Bina, T. F., Kunkle, D. E., Bina, X. R., Mullett, S. J., Wendell, S. G., & Bina, J. E. (2021). Bile salts promote ToxR regulon activation during growth under virulence-inducing conditions. *Infection and Immunity*, *89*(12), e0044121. https://doi.org/10.1128/IAI.00441-21

Bockemühl, J., Amédomé, A., & Triemer, A. (1972). A cholera-like gastroenteritis due to *Vibrio parahaemolyticus* on the coast of Togo (West Africa). *Zeitschrift fur Tropenmedizin und Parasitologie*, *23*(3), 308–315.

Böhme, K., Steinmann, R., Kortmann, J., Seekircher, S., Heroven, A. K., Berger, E., Pisano, F., Thiermann, T., Wolf-Watz, H., Narberhaus, F., & Dersch, P. (2012). Concerted actions of a thermo-labile regulator and a unique intergenic RNA thermosensor control *Yersinia* virulence. *PLoS Pathogens*, *8*(2), e1002518. https://doi.org/10.1371/journal.ppat.1002518

Boudreau, B. A., Hron, D. R., Qin, L., Van Der Valk, R. A., Kotlajich, M. V., Dame, R. T., & Landick, R. (2018). StpA and Hha stimulate pausing by RNA polymerase by promoting DNA–DNA bridging of H-NS filaments. *Nucleic Acids Research*, *46*(11), 5525–5546. https://doi.org/10.1093/NAR/GKY265

Bouffartigues, E., Buckle, M., Badaut, C., Travers, A., & Rimsky, S. (2007). H-NS cooperative binding to high-affinity sites in a regulatory element results in transcriptional silencing. *Nature Structural & Molecular Biology*, *14*(5), 441–448. https://doi.org/10.1038/nsmb1233

Browning, D. F., & Busby, S. J. W. (2016). Local and global regulation of transcription

initiation in bacteria. *Nature Reviews. Microbiology*, *14*(10), 638–650. https://doi.org/10.1038/nrmicro.2016.103

Bryan, F. L. (1980). Epidemiology of foodborne diseases transmitted by fish, shellfish and marine crustaceans in the United States, 1970–1978. *Journal of Food Protection*, *43*(11), 859–876. https://doi.org/10.4315/0362-028X-43.11.859

Bustamante, V. H., Santana, F. J., Calva, E., & Puente, J. L. (2001). Transcriptional regulation of type III secretion genes in enteropathogenic *Escherichia coli*: Ler antagonizes H-NS-dependent repression. *Molecular Microbiology*, *39*(3), 664–678. https://doi.org/10.1046/j.1365-2958.2001.02209.x

Cabanillas-Beltrán, H., Llausás-Magaña, E., Romero, R., Espinoza, A., García-Gasca, A., Nishibuchi, M., Ishibashi, M., & Gomez-Gil, B. (2006). Outbreak of gastroenteritis caused by the pandemic *Vibrio parahaemolyticus* O3:K6 in Mexico. *FEMS Microbiology Letters*, *265*(1), 76–80. https://doi.org/10.1111/J.1574-6968.2006.00475.X

Calkins, A. L., Demey, L. M., Karslake, J. D., Donarski, E. D., Biteen, J. S., & DiRita, V. J. (2021). Independent promoter recognition by TcpP precedes cooperative promoter activation by TcpP and ToxR. *mBio*. https://doi.org/10.1128/MBIO.02213-21

Carlson-Banning, K. M., & Sperandio, V. (2018). Enterohemorrhagic *Escherichia coli* outwits hosts through sensing small molecules. *Current Opinion in Microbiology*, *41*, 83–88. https://doi.org/10.1016/j.mib.2017.12.002

Chatterjee, B. D., Neogy, K. N., & Gorbach, S. L. (1970). Study of *Vibrio parahaemolyticus* from cases of diarrhoea in Calcutta. *The Indian Journal of Medical Research*, *58*(2), 234–238.

Chen, C.-C., Chou, M.-Y., Huang, C.-H., Majumder, A., & Wu, H.-Y. (2005). A cis-spreading nucleoprotein filament is responsible for the gene silencing activity found in the promoter relay mechanism. *The Journal of Biological Chemistry*, *280*(6), 5101–5112. https://doi.org/10.1074/jbc.M411840200

Crawford, J. A., Kaper, J. B., & DiRita, V. J. (1998). Analysis of ToxR-dependent transcription activation of ompU, the gene encoding a major envelope protein in *Vibrio cholerae*. *Molecular Microbiology*, *29*(1), 235–246. https://doi.org/10.1046/j.1365-2958.1998.00925.x

Dame, R. T., Wyman, C., Wurm, R., Wagner, R., & Goosen, N. (2002). Structural basis for H-NS-mediated trapping of RNA polymerase in the open initiation complex at the rrnB P1. *The Journal of Biological Chemistry*, *277*(3), 2146–2150. https://doi.org/10.1074/jbc.C100603200

Deng, W., Marshall, N. C., Rowland, J. L., McCoy, J. M., Worrall, L. J., Santos, A. S., Strynadka, N. C. J., & Finlay, B. B. (2017). Assembly, structure, function and regulation of type III secretion systems. *Nature Reviews Microbiology*, *15*(6), 323–337. https://doi.org/10.1038/nrmicro.2017.20

DiRita, V. J., Parsot, C., Jander, G., & Mekalanos, J. J. (1991). Regulatory cascade controls virulence in *Vibrio cholerae*. *Proceedings of the National Academy of Sciences of the United States of America*, *88*(12), 5403–5407. https://doi.org/10.1073/pnas.88.12.5403

Dziejman, M., & Mekalanos, J. J. (1994). Analysis of membrane protein interaction: ToxR can dimerize the amino terminus of phage lambda repressor. *Molecular Microbiology*, *13*(3), 485–494. https://doi.org/10.1111/J.1365-2958.1994.TB00443.X

Echeverria, P., Pitarangsi, C., Eampokalap, B., Vibulbandhitkit, S., Boonthai, P., & Rowe, B. (1983). A longitudinal study of the prevalence of bacterial enteric pathogens among adults with diarrhea in Bangkok, Thailand. *Diagnostic Microbiology and Infectious Disease*, *1*(3), 193–204. https://doi.org/10.1016/0732-8893(83)90018-4

Ellison, D. W., & Miller, V. L. (2006). H-NS represses inv transcription in *Yersinia enterocolitica* through competition with RovA and interaction with YmoA. *Journal of Bacteriology*, *188*(14), 5101–5112. https://doi.org/10.1128/JB.00862-05

Enos-Berlage, J. L., Guvener, Z. T., Keenan, C. E., & McCarter, L. L. (2005). Genetic

determinants of biofilm development of opaque and translucent *Vibrio parahaemolyticus*. *Molecular Microbiology*, *55*(4), 1160–1182. https://doi.org/10.1111/J.1365-2958.2004.04453.X

Falconi, M., Higgins, N. P., Spurio, R., Pon, C. L., & Gualerzi, C. O. (1993). Expression of the gene encoding the major bacterial nucleoid protein H-NS is subject to transcriptional auto-repression. *Molecular Microbiology*, *10*(2), 273–282. https://doi.org/10.1111/J.1365-2958.1993.TB01953.X

Fang, F. C., Frawley, E. R., Tapscott, T., & Vázquez-Torres, A. (2016). Discrimination and integration of stress signals by pathogenic bacteria. *Cell Host & Microbe*, *20*(2), 144–153. https://doi.org/10.1016/j.chom.2016.07.010

Faruque, S. M., & Mekalanos, J. J. (2003). Pathogenicity islands and phages in *Vibrio cholerae* evolution. *Trends in Microbiology*, *11*(11), 505–510. https://doi.org/10.1016/j.tim.2003.09.003

Faruque, S. M., & Nair, G. B. (2006). Epidemiology. In *The Biology of Vibrios* (pp. 383–398). John Wiley & Sons, Ltd. https://doi.org/https://doi.org/10.1128/9781555815714.ch27

Fleischmann, R. D., Adams, M. D., White, O., Clayton, R. A., Kirkness, E. F., Kerlavage, A. R., Bult, C. J., Tomb, J. F., Dougherty, B. A., & Merrick, J. M. (1995). Whole-genome random sequencing and assembly of *Haemophilus influenzae* Rd. *Science (New York, N.Y.)*, *269*(5223), 496–512. https://doi.org/10.1126/science.7542800

Fujino, T., Okuno, Y., Nakada, D., Aoyama, A., Fukai, K., Mukai, T., & Ueho, T. (1953). On the bacteriological examination of Shirasu-food poisoning. *Med Jour Osaka Univ*, *4*(2/3), 299–304. https://eurekamag.com/research/025/150/025150755.php

Gal-Mor, O., & Finlay, B. B. (2006). Pathogenicity islands: a molecular toolbox for bacterial virulence. *Cellular Microbiology*, *8*(11), 1707–1719. https://doi.org/10.1111/j.1462-5822.2006.00794.x

García, J., Cordeiro, T. N., Prieto, M. J., & Pons, M. (2012). Oligomerization and DNA binding of Ler, a master regulator of pathogenicity of enterohemorrhagic and enteropathogenic *Escherichia coli*. *Nucleic Acids Research*, *40*(20), 10254–10262. https://doi.org/10.1093/nar/gks846

Gaytán, M. O., Martínez-Santos, V. I., Soto, E., & González-Pedrajo, B. (2016). Type three secretion system in attaching and effacing pathogens. *Frontiers in Cellular and Infection Microbiology*, *6*, 129. https://doi.org/10.3389/fcimb.2016.00129

Ge, X. (2021). iDEP Web application for RNA-Seq data analysis. *Methods in Molecular Biology (Clifton, N.J.)*, *2284*, 417–443. https://doi.org/10.1007/978-1-0716-1307-8_22

Ghosh, H. K., & Bowen, T. E. (1980). Halophilic *vibrios* from human tissue infections on the pacific coast of Australia. *Pathology*, *12*(3), 397–402. https://doi.org/10.3109/00313028009077102

Goh, K. T., & Lam, S. (1981). *Vibrio* infections in Singapore. *Annals of the Academy of Medicine, Singapore*, *10*(1), 2–10.

Gonzalez-Escalona, N., Jolley, K. A., Reed, E., & Martinez-Urtaza, J. (2017). Defining a core genome multilocus sequence typing scheme for the global epidemiology of *Vibrio parahaemolyticus*. *Journal of Clinical Microbiology*, *55*(6), 1682–1697. https://doi.org/10.1128/JCM.00227-17

Gordon, B. R. G., Li, Y., Cote, A., Weirauch, M. T., Ding, P., Hughes, T. R., Navarre, W. W., Xia, B., & Liu, J. (2011). Structural basis for recognition of AT-rich DNA by unrelated xenogeneic silencing proteins. *Proceedings of the National Academy of Sciences of the United States of America*, *108*(26), 10690–10695. https://doi.org/10.1073/pnas.1102544108

Goss, T. J., Morgan, S. J., French, E. L., & Krukonisa, E. S. (2013). ToxR recognizes a direct repeat element in the toxT, ompU, ompT, and ctxA promoters of *Vibrio cholerae* to regulate transcription. *Infection and Immunity*, *81*(3), 884–895.

https://doi.org/10.1128/IAI.00889-12

Gotoh, K., Kodama, T., Hiyoshi, H., Izutsu, K., Park, K.-S. S., Dryselius, R., Akeda, Y., Honda, T., & Iida, T. (2010). Bile acid-induced virulence gene expression of *Vibrio parahaemolyticus* reveals a novel therapeutic potential for bile acid sequestrants. *PLOS ONE*, *5*(10), e13365. https://doi.org/10.1371/JOURNAL.PONE.0013365

Guiney, D. G. (1997). Regulation of bacterial virulence gene expression by the host environment. *The Journal of Clinical Investigation*, *99*(4), 565–569. https://doi.org/10.1172/JCI119196

Guzman, L. M., Belin, D., Carson, M. J., & Beckwith, J. (1995). Tight regulation, modulation, and high-level expression by vectors containing the arabinose PBAD promoter. *Journal of Bacteriology*, *177*(14), 4121–4130. https://doi.org/10.1128/JB.177.14.4121-4130.1995

Hacker, J., & Kaper, J. B. (2000). Pathogenicity islands and the evolution of microbes. *Annual Review of Microbiology*, *54*, 641–679. https://doi.org/10.1146/annurev.micro.54.1.641

Hameed, U., Liao, C., Radhakrishnan, A. K., Huser, F., Aljedani, S. S., Zhao, X., Momin, A. A., Melo, F. A., Guo, X., Brooks, C., Li, Y., Cui, X., Gao, X., Ladbury, J. E., Jaremko, Ł., Jaremko, M., Li, J., & Arold, S. T. (2019). H-NS uses an autoinhibitory conformational switch for environment-controlled gene silencing. *Nucleic Acids Research*, *47*(5), 2666–2680. https://doi.org/10.1093/NAR/GKY1299

Häse, C. C., & Mekalanos, J. J. (1998). TcpP protein is a positive regulator of virulence gene expression in *Vibrio cholerae*. *Proceedings of the National Academy of Sciences of the United States of America*, *95*(2), 730–734. https://doi.org/10.1073/pnas.95.2.730

Henriksen, S. D. (1978). Chapter I Serotyping of Bacteria. *Methods in Microbiology*, *12*(C), 1–13. https://doi.org/10.1016/S0580-9517(08)70355-6

Hiyoshi, H., Kodama, T., Iida, T., & Honda, T. (2010). Contribution of *Vibrio*

parahaemolyticus virulence factors to cytotoxicity, enterotoxicity, and lethality in mice. *Infection and Immunity*, *78*(4), 1772–1780. https://doi.org/10.1128/IAI.01051-09

Hiyoshi, H., Kodama, T., Saito, K., Gotoh, K., Matsuda, S., Akeda, Y., Honda, T., & Iida, T. (2011). VopV, an F-actin-binding type III secretion effector, is required for *Vibrio parahaemolyticus*-induced enterotoxicity. *Cell Host and Microbe*, *10*(4), 401–409. https://doi.org/10.1016/j.chom.2011.08.014

Honda, S. I., Goto, I., Minematsu, I., Ikeda, N., Asano, N., Ishibashi, M., Kinoshita, Y., Nishibuchi, M., Honda, T., & Miwatani, T. (1987). Gastroenteritis due to kanagawa negative *Vibrio parahaemolyticus*. *The Lancet*, *329*(8528), 331–332. https://doi.org/10.1016/S0140-6736(87)92062-9

Honda, T., Goshima, K., Takeda, Y., Sugino, Y., & Miwatani, T. (1976). Demonstration of the cardiotoxicity of the thermostable direct hemolysin (lethal toxin) produced by *Vibrio parahaemolyticus*. *Infection and Immunity*, *13*(1), 163–171. https://doi.org/10.1128/iai.13.1.163-171.1976

Honda, T., & Iida, T. (1993). The pathogenicity of *Vibrio parahaemolyticus* and the role of the thermostable direct haemolysin and related haemolysins. *Reviews and Research in Medical Microbiology*, *4*(2). https://journals.lww.com/revmedmicrobiol/Fulltext/1993/04000

Honda, T., Ni, Y. X., & Miwatani, T. (1988). Purification and characterization of a hemolysin produced by a clinical isolate of Kanagawa phenomenon-negative *Vibrio parahaemolyticus* and related to the thermostable direct hemolysin. *Infection and Immunity*, *56*(4), 961–965. https://doi.org/10.1128/iai.56.4.961-965.1988

Honda, T., Taga, S., Takeda, T., Hasibuan, M. A., Takeda, Y., & Miwatani, T. (1976). Identification of lethal toxin with the thermostable direct hemolysin produced by *Vibrio parahaemolyticus*, and some physicochemical properties of the purified toxin. *Infection and Immunity*, *13*(1), 133–139. https://doi.org/10.1128/iai.13.1.133-139.1976

Hsu, S. T., Liu, C. H., Wang, T. K., & Liu, T. P. (1977). Food poisoning due to *Vibrio parahaemolyticus*. *Zhonghua Minguo Wei Sheng Wu Xue Za Zhi = Chinese Journal of Microbiology*, *10*(3), 87–89.

Hubbard, T. P., Chao, M. C., Abel, S., Blondel, C. J., Wiesch, P. A. zur, Zhou, X., Davis, B. M., & Waldor, M. K. (2016). Genetic analysis of *Vibrio parahaemolyticus* intestinal colonization. *Proceedings of the National Academy of Sciences*, *113*(22), 6283–6288. https://doi.org/10.1073/PNAS.1601718113

Hueck, C. J. (1998). Type III protein secretion systems in bacterial pathogens of animals and plants. *Microbiology and Molecular Biology Reviews : MMBR*, *62*(2), 379–433. https://doi.org/10.1111/j.1365-2958.2006.05301.x

Hughes, J. M., Boyce, J. M., Aleem, A. R. M. A., Wells, J. G., Rahman, A. S., & Curlin, G. T. (1978). *Vibrio parahaemolyticus* enterocolitis in Bangladesh: report of an outbreak. *The American Journal of Tropical Medicine and Hygiene*, *27*(1 Pt 1), 106–112. https://doi.org/10.4269/AJTMH.1978.27.106

Hung, D. T., & Mekalanos, J. J. (2005). Bile acids induce cholera toxin expression in *Vibrio cholerae* in a ToxT-independent manner. *Proceedings of the National Academy of Sciences of the United States of America*, *102*(8), 3028–3033. https://doi.org/10.1073/pnas.0409559102

Hurley, C. C., Quirke, A. M., Reen, F. J., & Boyd, E. F. (2006). Four genomic islands that mark post-1995 pandemic *Vibrio parahaemolyticus* isolates. *BMC Genomics*, *7*(1), 1–19. https://doi.org/10.1186/1471-2164-7-104/FIGURES/7

Iguchi, T., Kondo, S., & Hisatsune, K. (1995). *Vibrio parahaemolyticus* O serotypes from O1 to O13 all produce R-type lipopolysaccharide: SDS-PAGE and compositional sugar analysis. *FEMS Microbiology Letters*, *130*(2–3), 287–292. https://doi.org/10.1111/j.1574-6968.1995.tb07733.x

Izutsu, K., Kurokawa, K., Tashiro, K., Kuhara, S., Hayashi, T., Honda, T., & Iida, T. (2008).

Comparative genomic analysis using microarray demonstrates a strong correlation between the presence of the 80-kilobase pathogenicity island and pathogenicity in Kanagawa phenomenon-positive *Vibrio parahaemolyticus* strains. *Infection and Immunity*, *76*(3), 1016–1023. https://doi.org/10.1128/IAI.01535-07

Janda, J. M., Powers, C., Bryant, R. G., & Abbott, S. L. (1988). Current perspectives on the epidemiology and pathogenesis of clinically significant *Vibrio spp. Clinical Microbiology Reviews*, *1*(3), 245–267. https://doi.org/10.1128/CMR.1.3.245

Jegathesan, M., & Paramasivam, T. (1976). Emergence of *Vibrio Parahaemolyticus* as an important cause of diarrhea in Malaysia. *The American Journal of Tropical Medicine and Hygiene*, *25*(1), 201–202. https://doi.org/10.4269/AJTMH.1976.25.201

Jennings, E., Thurston, T. L. M., & Holden, D. W. (2017). Salmonella SPI-2 Type III secretion system effectors: Molecular mechanisms and physiological consequences. *Cell Host and Microbe*, *22*(2), 217–231. https://doi.org/10.1016/j.chom.2017.07.009

Kazi, M. I., Conrado, A. R., Mey, A. R., Payne, S. M., & Davies, B. W. (2016). ToxR antagonizes H-NS regulation of horizontally acquired genes to drive host colonization. *PLOS Pathogens*, *12*(4), e1005570. https://doi.org/10.1371/JOURNAL.PPAT.1005570

Kodama, T., Akeda, Y., Kono, G., Takahashi, A., Imura, K., Iida, T., & Honda, T. (2002). The EspB protein of enterohaemorrhagic *Escherichia coli* interacts directly with alpha-catenin. *Cellular Microbiology*, *4*(4), 213–222. https://doi.org/10.1046/j.1462-5822.2002.00176.x

Kodama, T., Gotoh, K., Hiyoshi, H., Morita, M., Izutsu, K., Akeda, Y., Park, K. S., Cantarelli, V. V., Dryselius, R., Iida, T., & Honda, T. (2010). Two regulators of *Vibrio parahaemolyticus* play important roles in enterotoxicity by controlling the expression of genes in the Vp-PAI Region. *PLOS ONE*, *5*(1), e8678. https://doi.org/10.1371/JOURNAL.PONE.0008678

Kodama, T., Yamazaki, C., Park, K.-S., Akeda, Y., Iida, T., & Honda, T. (2010).

Transcription of *Vibrio parahaemolyticus* T3SS1 genes is regulated by a dual regulation system consisting of the ExsACDE regulatory cascade and H-NS. *FEMS Microbiology Letters*, *311*(1), 10–17. https://doi.org/10.1111/J.1574-6968.2010.02066.X

Kotlajich, M. V., Hron, D. R., Boudreau, B. A., Sun, Z., Lyubchenko, Y. L., & Landick, R. (2015). Bridged filaments of histone-like nucleoid structuring protein pause RNA polymerase and aid termination in bacteria. *ELife*, *2015*(4). https://doi.org/10.7554/ELIFE.04970

Kourany, M., & Vasquez, M. A. (1975). The first reported case from Panamá of acute gastroenteritis caused by *Vibrio parahaemolyticus. The American Journal of Tropical Medicine and Hygiene*, *24*(4), 638–640. https://doi.org/10.4269/AJTMH.1975.24.638

Kuroda, T., Mizushima, T., & Tsuchiya, T. (2005). Physiological roles of three Na+/H+ antiporters in the halophilic bacterium *Vibrio parahaemolyticus*. *Microbiology and Immunology*, *49*(8), 711–719. https://doi.org/10.1111/J.1348-0421.2005.TB03662.X

Langmead, B., & Salzberg, S. L. (2012). Fast gapped-read alignment with Bowtie 2. *Nature Methods*, *9*(4), 357–359. https://doi.org/10.1038/nmeth.1923

Leal, N. C., Da Silva, S. C., Cavalcanti, V. O., De, Â. C. T., Nunes, V. V. F., Miralles, I. S., & Hofer, E. (2008). *Vibrio parahaemolyticus* serovar O3:K6 gastroenteritis in northeast Brazil. *Journal of Applied Microbiology*, *105*(3), 691–697. https://doi.org/10.1111/J.1365-2672.2008.03782.X

Lee, D. J., Minchin, S. D., & Busby, S. J. W. (2012). Activating transcription in bacteria. *Annual Review of Microbiology*, *66*, 125–152. https://doi.org/10.1146/annurev-micro-092611-150012

Lembke, M., Höfler, T., Walter, A. N., Tutz, S., Fengler, V., Schild, S., & Reidl, J. (2020). Host stimuli and operator binding sites controlling protein interactions between virulence master regulator ToxR and ToxS in *Vibrio cholerae*. *Molecular Microbiology*, *114*(2), 262–278. https://doi.org/10.1111/MMI.14510

Letchumanan, V., Chan, K. G., & Lee, L. H. (2014). *Vibrio parahaemolyticus*: A review on the pathogenesis, prevalence, and advance molecular identification techniques. *Frontiers in Microbiology*, *5*(DEC), 705. https://doi.org/10.3389/FMICB.2014.00705/

Li, P., Rivera-Cancel, G., Kinch, L. N., Salomon, D., Tomchick, D. R., Grishin, N. V., & Orth, K. (2016). Bile salt receptor complex activates a pathogenic type III secretion system. *ELife*, *5*(2016JULY), 1–26. https://doi.org/10.7554/eLife.15718

Lim, C. J., Lee, S. Y., Kenney, L. J., & Yan, J. (2012). Nucleoprotein filament formation is the structural basis for bacterial protein H-NS gene silencing. *Scientific Reports 2012 2:1*, *2*(1), 1–6. https://doi.org/10.1038/srep00509

Lin, Z., Kumagai, K., Baba, K., Mekalanos, J. J., & Nishibuchi, M. (1993). *Vibrio parahaemolyticus* has a homolog of the *Vibrio cholerae* toxRS operon that mediates environmentally induced regulation of the thermostable direct hemolysin gene. *Journal of Bacteriology*, *175*(12), 3844–3855. https://doi.org/10.1128/jb.175.12.3844-3855.1993

Liu, Y., Chen, H., Kenney, L. J., & Yan, J. (2010). A divalent switch drives H-NS/DNA-binding conformations between stiffening and bridging modes. *Genes & Development*, *24*(4), 339–344. https://doi.org/10.1101/GAD.1883510

Lustri, B. C., Sperandio, V., & Moreira, C. G. (2017). Bacterial chat: Intestinal metabolites and signals in host-microbiota-pathogen interactions. *Infection and Immunity*, *85*(12). https://doi.org/10.1128/IAI.00476-17

Madan Babu, M., Teichmann, S. A., & Aravind, L. (2006). Evolutionary dynamics of prokaryotic transcriptional regulatory networks. *Journal of Molecular Biology*, *358*(2), 614–633. https://doi.org/10.1016/j.jmb.2006.02.019

Makino, K., Oshima, K., Kurokawa, K., Yokoyama, K., Uda, T., Tagomori, K., Iijima, Y., Najima, M., Nakano, M., Yamashita, A., Kubota, Y., Kimura, S., Yasunaga, T., Honda, T., Shinagawa, H., Hattori, M., & Iida, T. (2003). Genome sequence of *Vibrio parahaemolyticus*: a pathogenic mechanism distinct from that of *V. cholerae*. *Lancet*,

361(9359), 743–749. https://doi.org/10.1016/S0140-6736(03)12659-1

Martinez-Urtaza, J., & Baker-Austin, C. (2020). *Vibrio parahaemolyticus*. *Trends in Microbiology*, *28*(10), 867–868. https://doi.org/10.1016/J.TIM.2020.02.008

Martinez-Urtaza, J., Simental, L., Velasco, D., DePaola, A., Ishibashi, M., Nakaguchi, Y., Nishibuchi, M., Carrera-Flores, D., Rey-Alvarez, C., & Pousa, A. (2005). Pandemic *Vibrio parahaemolyticus* O3:K6, Europe. *Emerging Infectious Diseases*, *11*(8), 1319. https://doi.org/10.3201/EID1108.050322

Matsuda, S., Hiyoshi, H., Tandhavanant, S., & Kodama, T. (2020). Advances on *Vibrio parahaemolyticus* research in the postgenomic era. *Microbiology and Immunology*, *64*(3), 167–181. https://doi.org/10.1111/1348-0421.12767

Matsuda, S., Okada, R., Tandhavanant, S., Hiyoshi, H., Gotoh, K., Iida, T., & Kodama, T. (2019). Export of a *Vibrio parahaemolyticus* toxin by the Sec and type III secretion machineries in tandem. *Nature Microbiology 2019 4:5*, *4*(5), 781–788. https://doi.org/10.1038/s41564-019-0368-y

Matsumoto, C., Okuda, J., Ishibashi, M., Iwanaga, M., Garg, P., Rammamurthy, T., Wong, H. C., Depaola, A., Kim, Y. B., Albert, M. J., & Nishibuchi, M. (2000). Pandemic spread of an O3:K6 clone of *Vibrio parahaemolyticus* and emergence of related strains evidenced by arbitrarily primed PCR and toxRS sequence analyses. *Journal of Clinical Microbiology*, *38*(2), 578–585. https://doi.org/10.1128/JCM.38.2.578-585.2000/

Mellies, J. L., Benison, G., McNitt, W., Mavor, D., Boniface, C., & Larabee, F. J. (2011). Ler of pathogenic *Escherichia coli* forms toroidal protein-DNA complexes. *Microbiology (Reading, England)*, *157*(Pt 4), 1123–1133. https://doi.org/10.1099/mic.0.046094-0

Merson, M. H., Morris, G. K., Sack, D. A., Wells, J. G., Feeley, J. C., Sack, R. B., Creech, W. B., Kapikian, A. Z., & Gangarosa, E. J. (1976). Travelers' Diarrhea in Mexico. *Http://Dx.Doi.Org/10.1056/NEJM197606102942401*, *294*(24), 1299–1305. https://doi.org/10.1056/NEJM197606102942401

Midgett, C. R., Swindell, R. A., Pellegrini, M., & Jon Kull, F. (2020). A disulfide constrains the ToxR periplasmic domain structure, altering its interactions with ToxS and bile-salts. *Scientific Reports 2020 10:1*, *10*(1), 1–11. https://doi.org/10.1038/s41598-020-66050-5

Miller, J. H. (1972). *Experiments in molecular genetics*. https://doi.org/10.3/JQUERY-UI.JS

Miller, V. L., & Mekalanos, J. J. (1984). Synthesis of cholera toxin is positively regulated at the transcriptional level by toxR. *Proceedings of the National Academy of Sciences of the United States of America*, *81*(11), 3471–3475. https://doi.org/10.1073/pnas.81.11.3471

Miyamoto, Y., Kato, T., Obara, Y., Akiyama, S., Takizawa, K., & Yamai, S. (1969). In vitro hemolytic characteristic of *Vibrio parahaemolyticus*: its close correlation with human pathogenicity. *Journal of Bacteriology*, *100*(2), 1147–1149. https://doi.org/10.1128/jb.100.2.1147-1149.1969

Molenda, J. R., Johnson, W. G., Fishbein, M., Wentz, B., Mehlman, I. J., & Thoburn A. Dadisman, J. (1972). *Vibrio parahaemolyticus* gastroenteritis in Maryland: Laboratory Aspects. *Applied Microbiology*, *24*(3), 444–448. https://doi.org/10.1128/AM.24.3.444-448.1972

Morishita, H., & Takada, H. (2011). Sparing effect of lithium ion on the specific requirement for sodium ion for growth of *Vibrio parahaemolyticus*. *Https://Doi.Org/10.1139/M76-187*, *22*(9), 1263–1268. https://doi.org/10.1139/M76-187

Muthuramalingam, M., Whittier, S. K., Picking, W. L., & Picking, W. D. (2021). The *Shigella* type III secretion system: An overview from top to bottom. *Microorganisms*, *9*(2). https://doi.org/10.3390/microorganisms9020451

Naughton, L. M., Blumerman, S. L., Carlberg, M., & Boyd, E. F. (2009). Osmoadaptation among *Vibrio* species and unique genomic features and physiological responses of *Vibrio parahaemolyticus*. *Applied and Environmental Microbiology*, *75*(9), 2802–2810. https://doi.org/10.1128/AEM.01698-08

Navarre, W W. (2016). The impact of gene silencing on horizontal gene transfer and bacterial evolution. *Advances in Microbial Physiology*, *69*, 157–186. https://doi.org/10.1016/bs.ampbs.2016.07.004

Navarre, William Wiley, Porwollik, S., Wang, Y., McClelland, M., Rosen, H., Libby, S. J., & Fang, F. C. (2006). Selective silencing of foreign DNA with low GC content by the H-NS protein in *Salmonella. Science*, *313*(5784), 236–238. https://doi.org/10.1126/SCIENCE.1128794/

Nishimura, M., Fujii, T., Hiyoshi, H., Makino, F., Inoue, H., Motooka, D., Kodama, T., Ohkubo, T., Kobayashi, Y., Nakamura, S., Namba, K., & Iida, T. (2015). A repeat unit of *Vibrio* diarrheal T3S effector subverts cytoskeletal actin homeostasis via binding to interstrand region of actin filaments. *Scientific Reports 2015 5:1*, *5*(1), 1–8. https://doi.org/10.1038/srep10870

Nye, M. B., Pfau, J. D., Skorupski, K., & Taylor, R. K. (2000). *Vibrio cholerae* H-NS silences virulence gene expression at multiple steps in the ToxR regulatory cascade. *Journal of Bacteriology*, *182*(15), 4295–4303. https://doi.org/10.1128/JB.182.15.4295-4303.2000

Okada, K., Iida, T., Kita-Tsukamoto, K., & Honda, T. (2005). Vibrios commonly possess two chromosomes. Journal of bacteriology, 187(2), 752–757. https://doi.org/10.1128/JB.187.2.752-757.2005

Okada, N., Iida, T., Park, K.-S. S., Goto, N., Yasunaga, T., Hiyoshi, H., Matsuda, S., Kodama, T., Honda, T., Lida, T., Park, K.-S. S., Goto, N., Yasunaga, T., Hiyoshi, H., Matsuda, H., Kodama, T., Honda, T., Iida, T., Park, K.-S. S.,Honda, T. (2009). Identification and characterization of a novel type III secretion system in trh-positive *Vibrio parahaemolyticus* strain TH3996 reveal genetic lineage and diversity of pathogenic machinery beyond the species level. *Infection and Immunity*, *77*(2), 904–913. https://doi.org/10.1128/IAI.01184-08

Okada, N., Matsuda, S., Matsuyama, J., Park, K.-S., de los Reyes, C., Kogure, K., Honda, T., & Iida, T. (2010). Presence of genes for type III secretion system 2 in *Vibrio mimicus* strains. *BMC Microbiology*, *10*, 302. https://doi.org/10.1186/1471-2180-10-302

Okada, R., Matsuda, S., & Iida, T. (2017). *Vibrio parahaemolyticus* VtrA is a membrane-bound regulator and is activated via oligomerization. *PLoS ONE*, *12*(11), 1–16. https://doi.org/10.1371/journal.pone.0187846

Okuda, J., Ishibashi, M., Hayakawa, E., Nishino, T., Takeda, Y., Mukhopadhyay, A. K., Garg, S., Bhattacharya, S. K., Nair, G. B., & Nishibuchi, M. (1997). Emergence of a unique O3:K6 clone of *Vibrio parahaemolyticus* in Calcutta, India, and isolation of strains from the same clonal group from Southeast Asian travelers arriving in Japan. *Journal of Clinical Microbiology*, *35*(12), 3150–3155. https://doi.org/10.1128/JCM.35.12.3150-3155.1997

Olekhnovich, I. N., & Kadner, R. J. (2007). Role of nucleoid-associated proteins Hha and H-NS in expression of *Salmonella enterica* activators HilD, HilC, and RtsA required for cell invasion. *Journal of Bacteriology*, *189*(19), 6882–6890. https://doi.org/10.1128/JB.00905-07

Ongagna-Yhombi, S. Y., & Boyd, F. E. (2013). Biosynthesis of the osmoprotectant ectoine, but not glycine betaine, is critical for survival of osmotically stressed *Vibrio parahaemolyticus* cells. *Applied and Environmental Microbiology*, *79*(16), 5038–5049. https://doi.org/10.1128/AEM.01008-13

Ono, S., Goldberg, M. D., Olsson, T., Esposito, D., Hinton, J. C. D., & Ladbury, J. E. (2005). H-NS is a part of a thermally controlled mechanism for bacterial gene regulation. *Biochemical Journal*, *391*(2), 203–213. https://doi.org/10.1042/BJ20050453

Ottaviani, D., Leoni, F., Rocchegiani, E., Santarelli, S., Canonico, C., Masini, L., DiTrani, V., & Carraturo, A. (2008). First clinical report of pandemic *Vibrio parahaemolyticus* O3:K6 infection in Italy. *Journal of Clinical Microbiology*, *46*(6), 2144–2145.

https://doi.org/10.1128/JCM.00683-08/

Palasuntheram, C. (1981). The halophilic properties of *Vibrio parahaemolyticus*. *Journal of General Microbiology*, *127*(2), 427–428. https://doi.org/10.1099/00221287-127-2-427

Parales, R. E., & Harwood, C. S. (1993). Construction and use of a new broad-host-range lacZ transcriptional fusion vector, pHRP309, for Gram − bacteria. *Gene*, *133*(1), 23–30. https://doi.org/10.1016/0378-1119(93)90220-W

Park, K.-S., Ono, T., Rokuda, M., Jang, M.-H., Iida, T., & Honda, T. (2004). Cytotoxicity and enterotoxicity of the thermostable direct hemolysin-deletion mutants of *Vibrio parahaemolyticus*. *Microbiology and Immunology*, *48*(4), 313–318. https://doi.org/10.1111/j.1348-0421.2004.tb03512.x

Park, K. S., Ono, T., Rokuda, M., Jang, M. H., Okada, K., Iida, T., & Honda, T. (2004). Functional characterization of two type III secretion systems of *Vibrio parahaemolyticus*. *Infection and Immunity*, *72*(11), 6659–6665. https://doi.org/10.1128/IAI.72.11.6659-6665.2004

Paytubi, S., Madrid, C., Forns, N., Nieto, J. M., Balsalobre, C., Uhlin, B. E., & Juárez, A. (2004). YdgT, the Hha paralogue in *Escherichia coli*, forms heteromeric complexes with H-NS and StpA. *Molecular Microbiology*, *54*(1), 251–263. https://doi.org/10.1111/J.1365-2958.2004.04268.X

Petassi, M. T., Hsieh, S.-C., & Peters, J. E. (2020). Guide RNA categorization enables target site choice in Tn7-CRISPR-Cas transposons. *Cell*, *183*(7), 1757-1771.e18. https://doi.org/10.1016/j.cell.2020.11.005

Peters, J. E., Makarova, K. S., Shmakov, S., & Koonin, E. V. (2017). Recruitment of CRISPR-Cas systems by Tn7-like transposons. *Proceedings of the National Academy of Sciences of the United States of America*, *114*(35), E7358–E7366. https://doi.org/10.1073/pnas.1709035114

Pha, K., & Navarro, L. (2016). *Yersinia* type III effectors perturb host innate immune

responses. *World Journal of Biological Chemistry*, *7*(1), 1–13. https://doi.org/10.4331/wjbc.v7.i1.1

Pienkoß, S., Javadi, S., Chaoprasid, P., Nolte, T., Twittenhoff, C., Dersch, P., & Narberhaus, F. (2021). The gatekeeper of *Yersinia* type III secretion is under RNA thermometer control. *PLoS Pathogens*, *17*(11), e1009650. https://doi.org/10.1371/journal.ppat.1009650

Pinaud, L., Sansonetti, P. J., & Phalipon, A. (2018). Host cell targeting by enteropathogenic bacteria T3SS effectors. *Trends in Microbiology*, *26*(4), 266–283. https://doi.org/10.1016/j.tim.2018.01.010

Piñeyro, P., Zhou, X., Orfe, L. H., Friel, P. J., Lahmers, K., & Call, D. R. (2010). Development of two animal models to study the function of *Vibrio parahaemolyticus* type III secretion systems. *Infection and Immunity*, *78*(11), 4551–4559. https://doi.org/10.1128/IAI.00461-10

Plaza, N., Urrutia, I. M., Garcia, K., Waldor, M. K., & Blondel, C. J. (2021). Identification of a Family of *Vibrio* Type III Secretion System Effectors That Contain a Conserved Serine/Threonine Kinase Domain . *mSphere*, *6*(4). https://doi.org/10.1128/MSPHERE.00599-21

Provenzano, D., Schuhmacher, D. A., Barker, J. L., & Klose, K. E. (2000). The virulence regulatory protein ToxR mediates enhanced bile resistance in *Vibrio cholerae* and other pathogenic *Vibrio* species. *Infection and Immunity*, *68*(3), 1491–1497. https://doi.org/10.1128/IAI.68.3.1491-1497.2000

Qin, L, Erkelens, A. M., Bdira, F. Ben, & Dame, R. T. (2019). The architects of bacterial DNA bridges: a structurally and functionally conserved family of proteins. https://doi.org/10.1098/rsob.190223

Qin, Liang, Bdira, F. Ben, Sterckx, Y. G. J., Volkov, A. N., Vreede, J., Giachin, G., van Schaik, P., Ubbink, M., & Dame, R. T. (2020). Structural basis for osmotic

regulation of the DNA binding properties of H-NS proteins. *Nucleic Acids Research*, *48*(4), 2156–2172. https://doi.org/10.1093/NAR/GKZ1226

Radics, J., Königsmaier, L., & Marlovits, T. C. (2014). Structure of a pathogenic type 3 secretion system in action. *Nature Structural and Molecular Biology*, *21*(1), 82–87. https://doi.org/10.1038/nsmb.2722

Ritchie, J. M., Rui, H., Zhou, X., Iida, T., Kodoma, T., Ito, S., Davis, B. M., Bronson, R. T., & Waldor, M. K. (2012). Inflammation and disintegration of intestinal villi in an experimental model for *Vibrio parahaemolyticus*-induced diarrhea. *PLOS Pathogens*, *8*(3), e1002593. https://doi.org/10.1371/JOURNAL.PPAT.1002593

Sakurai, J., Bahavar, M. A., Jinguji, Y., & Miwatani, T. (1975). Interaction of thermostable direct hemolysin of *Vibrio parahaemolyticus* with human erythrocytes. *Biken Journal*, *18*(4), 187–192.

Sakurai, J., Honda, T., Jinguji, Y., Arita, M., & Miwatani, T. (1976). Cytotoxic effect of the thermostable direct hemolysin produced by *Vibrio parahaemolyticus* on FL cells. *Infection and Immunity*, *13*(3), 876–883. https://doi.org/10.1128/iai.13.3.876-883.1976

Sakurai, J., Matsuzaki, A., & Miwatani, T. (1973). Purification and characterization of thermostable direct hemolysin of *Vibrio parahaemolyticus*. *Infection and Immunity*, *8*(5), 775–780. https://doi.org/10.1128/iai.8.5.775-780.1973

Salomon, D., Klimko, J. A., & Orth, K. (2014). H-NS regulates the *Vibrio parahaemolyticus* type VI secretion system *1*. *160*, 1867–1873. https://www.microbiologyresearch.org/content/journal/micro/10.1099/mic.0.080028-0

Shinoda, S. (2011). Sixty years from the discovery of *Vibrio parahaemolyticus* and some recollections. *Biocontrol Science*, *16*(4), 129–137. https://doi.org/10.4265/BIO.16.129

Singh, K., Milstein, J. N., & Navarre, W. W. (2016). Xenogeneic silencing and its impact on bacterial genomes, *70*, 199–213. https://doi.org/10.1146/ANNUREV-MICRO-102215-095301

Sriratanaban, A., & Reinprayoon, S. (1982). *Vibrio parahaemolyticus*: a major cause of travelers' diarrhea in Bangkok. *The American Journal of Tropical Medicine and Hygiene*, *31*(1), 128–130. https://doi.org/10.4269/ajtmh.1982.31.128

Stella, S., Falconi, M., Lammi, M., Gualerzi, C. O., & Pon, C. L. (2006). Environmental control of the *In vivo* oligomerization of nucleoid protein H-NS. *Journal of Molecular Biology*, *355*(2), 169–174. https://doi.org/10.1016/J.JMB.2005.10.034

Sturm, A., Heinemann, M., Arnoldini, M., Benecke, A., Ackermann, M., Benz, M., Dormann, J., & Hardt, W.-D. (2011). The cost of virulence: retarded growth of *Salmonella Typhimurium* cells expressing type III secretion system 1. *PLoS Pathogens*, *7*(7), e1002143. https://doi.org/10.1371/journal.ppat.1002143

Sugiyama, T., Iida, T., Izutsu, K., Park, K. S., & Honda, T. (2008). Precise region and the character of the pathogenicity island in clinical *Vibrio parahaemolyticus* strains. *Journal of Bacteriology*, *190*(5), 1835–1837. https://doi.org/10.1128/JB.01293-07

Sun, F., Zhang, Y., Qiu, Y., Yang, H., Yang, W., Yin, Z., Wang, J., Yang, R., Xia, P., & Zhou, D. (2014). H-NS is a repressor of major virulence gene loci in *Vibrio parahaemolyticus*. *Frontiers in Microbiology*, *0*(DEC), 675. https://doi.org/10.3389/FMICB.2014.00675

Thompson, F. L., Iida, T., & Swings, J. (2004). Biodiversity of *Vibrios*. *Microbiology and Molecular Biology Reviews*, *68*(3), 403–431. https://doi.org/10.1128/MMBR.68.3.403-431.2004

Tobe, T., Yoshikawa, M., Mizuno, T., & Sasakawa, C. (1993). Transcriptional control of the invasion regulatory gene *virB* of *Shigella flexneri*: Activation by VirF and repression by H-NS. *Journal of Bacteriology*, *175*(19), 6142–6149. https://doi.org/10.1128/JB.175.19.6142-6149.1993/

Todd, E. C. D. (1981). Foodborne and waterborne disease in Canada - 1976 Annual Summary. *Journal of Food Protection*, *44*(10), 787–795. https://doi.org/10.4315/0362-

028X-44.10.787

Tsuchiya, T., & Shinoda, S. (1985). Respiration-driven Na+ pump and Na+ circulation in *Vibrio parahaemolyticus*. *Journal of Bacteriology*, *162*(2), 794–798. https://doi.org/10.1128/JB.162.2.794-798.1985

Ueda, T., Takahashi, H., Uyar, E., Ishikawa, S., Ogasawara, N., & Oshima, T. (2013). Functions of the Hha and YdgT Proteins in transcriptional silencing by the nucleoid proteins, H-NS and StpA, in *Escherichia coli*. *DNA Research*, *20*(3), 263–271. https://doi.org/10.1093/DNARES/DST008

Ueguchi, C., Kakeda, M., & Mizuno, T. (1993). Autoregulatory expression of the *Escherichia coli* hns gene encoding a nucleoid protein: H-NS functions as a repressor of its own transcription. *Molecular and General Genetics MGG 1993 236:2*, *236*(2), 171–178. https://doi.org/10.1007/BF00277109

Ueguchi, C., Seto, C., Suzuki, T., & Mizuno, T. (1997). Clarification of the dimerization domain and its functional significance for the *Escherichia coli* nucleoid protein H-NS. *Journal of Molecular Biology*, *274*(2), 145–151. https://doi.org/10.1006/JMBI.1997.1381

Umanski, T., Rosenshine, I., & Friedberg, D. (2002). Thermoregulated expression of virulence genes in enteropathogenic *Escherichia coli*. *Microbiology*, *148*(9), 2735–2744. https://doi.org/10.1099/00221287-148-9-2735

Varshavsky, A. J., Nedospasov, S. A., Bakayev, V. V., Bakayeva, T. G., & Georgiev, G. P. (1977). Histone-like proteins in the purified *Escherichia coli* deoxyribonucleoprotein. *Nucleic Acids Research*, *4*(8), 2725–2746. https://doi.org/10.1093/NAR/4.8.2725

Velazquez-Roman, J., León-Sicairos, N., Hernández-Díaz, L. de J., & Canizalez-Roman, A. (2014). Pandemic *Vibrio parahaemolyticus* O3: K6 on the American continent. *Frontiers in Cellular and Infection Microbiology*, *3*(JAN), 110. https://doi.org/10.3389/FCIMB.2013.00110

Walthers, D., Carroll, R. K., Navarre, W. W., Libby, S. J., Fang, F. C., & Kenney, L. J. (2007). The response regulator SsrB activates expression of diverse *Salmonella* pathogenicity island 2 promoters and counters silencing by the nucleoid-associated protein H-NS. *Molecular Microbiology*, *65*(2), 477–493. https://doi.org/10.1111/J.1365-2958.2007.05800.X

Walthers, D., Li, Y., Liu, Y., Anand, G., Yan, J., & Kenney, L. J. (2011). *Salmonella enterica* response regulator SsrB relieves H-NS silencing by displacing H-NS bound in polymerization mode and directly activates transcription. *Journal of Biological Sciences*. https://doi.org/10.1074/jbc.M110.164962

Wang, Y., Zhang, Y., Yin, Z., Wang, J., Zhu, Y., Peng, H., Zhou, D., Qi, Z., & Yang, W. (2017). H-NS represses transcription of the flagellin gene lafA of lateral flagella in *Vibrio parahaemolyticus*, *64*(1), 69–74. https://doi.org/10.1139/CJM-2017-0315

Whitaker, W. B., Parent, M. A., Boyd, A., Richards, G. P., & Boyd, E. F. (2012). The *Vibrio parahaemolyticus* ToxRS regulator is required for stress tolerance and colonization in a novel orogastric streptomycin-induced adult murine model. *Infection and Immunity*, *80*(5), 1834–1845. https://doi.org/10.1128/IAI.06284-11

Winardhi, R. S., Fu, W., Castang, S., Li, Y., Dove, S. L., & Yan, J. (2012). Higher order oligomerization is required for H-NS family member MvaT to form gene-silencing nucleoprotein filament. *Nucleic Acids Research*, *40*(18), 8942–8952. https://doi.org/10.1093/nar/gks669

Winardhi, R. S., Gulvady, R., Mellies, J. L., & Yan, J. (2014). Locus of enterocyte effacement-encoded regulator (Ler) of pathogenic *Escherichia coli* competes off histone-like nucleoid-structuring protein (H-NS) through noncooperative DNA binding. *The Journal of Biological Chemistry*, *289*(20), 13739–13750. https://doi.org/10.1074/jbc.M113.545954

Xu, M., Yamamoto, K., Honda, T., & Ming X. (1994). Construction and characterization of

an isogenic mutant of *Vibrio parahaemolyticus* having a deletion in the thermostable direct hemolysin-related hemolysin gene (trh). *Journal of Bacteriology*, *176*(15), 4757–4760. https://doi.org/10.1128/jb.176.15.4757-4760.1994

Yamanaka, Y., Winardhi, R. S., Yamauchi, E., Nishiyam, S. I., Sowa, Y., Yan, J., Kawagishi, I., Ishihama, A., & Yamamoto, K. (2018). Dimerization site 2 of the bacterial DNA-binding protein H-NS is required for gene silencing and stiffened nucleoprotein filament formation. *Journal of Biological Chemistry*, *293*(24), 9496–9505. http://www.jbc.org/article/S0021925820389195/

Yang, M., Liu, Z., Hughes, C., Stern, A. M., Wang, H., Zhong, Z., Kan, B., Fenical, W., & Zhu, J. (2013). Bile salt-induced intermolecular disulfide bond formation activates *Vibrio cholerae* virulence. *Proceedings of the National Academy of Sciences of the United States of America*, *110*(6), 2348–2353. https://doi.org/10.1073/pnas.1218039110

Yother, J., Chamness, T. W., & Goguen, J. D. (1986). Temperature-controlled plasmid regulon associated with low calcium response in *Yersinia pestis*. *Journal of Bacteriology*, *165*(2), 443–447. https://doi.org/10.1128/jb.165.2.443-447.1986

Yu, X.-J., McGourty, K., Liu, M., Unsworth, K. E., & Holden, D. W. (2010). pH sensing by intracellular *Salmonella* induces effector translocation. *Science (New York, N.Y.)*, *328*(5981), 1040–1043. https://doi.org/10.1126/science.1189000

Zakhariev, Z. A. (1976). The spread of parahemolytic *vibrios* in humans in the Burgass Region (Bulgaria). *Zhurnal mikrobiologii, epidemiologii i immunobiologii*, *7*, 46–48.

Zhao, X., Kharchenko, V., Hameed, U., Liao, C., Huser, F., Remington, J., Radhakrishnan, A., Jaremko, M., Jaremko, Ł., Arold, S., & Li, J. (2020). Molecular basis for the adaptive evolution of environment sensing by H-NS proteins. 1–18. https://doi.org/10.1101/2020.04.21.053520

Zhao, X., Remington, J. M., Schneebeli, S. T., Arold, S. T., & Li, J. (2021). Molecular basis for environment sensing by a nucleoid-structuring bacterial protein filament. *The*

Journal of Physical Chemistry Letters, *12*(32), 7878–7884. https://doi.org/10.1021/ACS.JPCLETT.1C01710

Zhou, D., & Galán, J. (2001). *Salmonella* entry into host cells: the work in concert of type III secreted effector proteins. *Microbes and Infection*, *3*(14–15), 1293–1298. https://doi.org/10.1016/s1286-4579(01)01489-7

Zhou, X., Gewurz, B. E., Ritchie, J. M., Takasaki, K., Greenfeld, H., Kieff, E., Davis, B. M., & Waldor, M. K. (2013). A *Vibrio parahaemolyticus* T3SS effector mediates pathogenesis by independently enabling intestinal colonization and inhibiting TAK1 activation. *Cell Reports*, *3*(5), 1690–1702. https://doi.org/10.1016/j.celrep.2013.03.039

Zhou, X., Massol, R. H., Nakamura, F., Chen, X., Gewurz, B. E., Davis, B. M., Lencer, W., & Waldor, M. K. (2014). Remodeling of the intestinal brush border underlies adhesion and virulence of an enteric pathogen. m*Bio*, *5*(4). https://doi.org/10.1128/MBIO.01639-14

Zingl, F. G., Kohl, P., Cakar, F., Leitner, D. R., Mitterer, F., Bonnington, K. E., Rechberger, G. N., Kuehn, M. J., Guan, Z., Reidl, J., & Schild, S. (2020). Outer Membrane vesiculation facilitates surface exchange and *In Vivo* adaptation of *Vibrio cholerae*. *Cell Host & Microbe*, *27*(2), 225-237.e8. https://doi.org/10.1016/j.chom.2019.12.002

ACKNOWLEDGMENTS

I would like to express my deepest gratitude to my supervisor, Prof. Tetsuya Iida, who accepted me to be in his lab and gave me the opportunity to learn about a historically important pathogenic bacterium in Japan, *Vibrio parahaemolyticus*. I am fortunate to be standing on the shoulder of one of the giants in *V. parahaemolyticus research*. I appreciate his support and guidance over these past three years.

I am also very fortunate to have a great mentor in the field, Dr. Shigeaki Matsuda, who always supported me in every situation, research and life matter, throughout my years of study. He made me fall in love with the pathogenic bacteria research and how clever those small creatures can make devastating diseases in humans. He taught me how to crack the code about the way they can harm us. I appreciate his patience and tirelessness in teaching, advising and directing me in experiments inside the lab, as well as guiding me in presenting and writing my research work. His support is priceless, and I am lucky to be his apprentice.

I sincerely thank Dr. Eiji Ishii and Dr. Pranee Somboonthum for their help in my lab life. I would also like to thank other students in the Iida lab (dr. Delly Chipta Lestari, Dhira Saraswati Anggramukti, Mohamad Imad Al Kadi and Tan Paramita Wibowo), who shared the journey of student life and fought to finish the study along with me. Also, I must thank Ms. Junko Hirosato (Iida lab secretary) and Ms. Mariko Okazaki (office for research promotion in RIMD) for their support in my life inside and outside the lab, especially in getting paperwork done due to my limitation in Japanese language.

I am grateful to my family and friends for their support, especially my wife, Nur Humaidah Muwafiqi, who was always on my side when I was up and down throughout the process of researching and writing this thesis. In Japan, she has already worked hard to give birth and raise our first child, Ayumi Kaina Lashira. Forgive me, my love, if sometimes I were absent from raising our daughter to get my study done.

Last but not least, this story of my Ph.D. journey in Japan would not have been possible without the support of the BIKEN Foundation through the Taniguchi scholarship program. I hope this Ph.D. study experience will provide enough knowledge for me to become an excellent independent researcher.

AUTHOR'S ACHIEVEMENT

Publication

Andre Pratama, Eiji Ishii, Toshio Kodama, Tetsuya Iida, Shigeaki Matsuda. Xenogeneic silencing-mediated regulation of T3SS2 in *Vibrio parahaemolyticus*. (The author is preparing the manuscript and is willing to publish it within one year after graduation)

Conference

Andre Pratama, Eiji Ishii, Toshio Kodama, Tetsuya Iida, Shigeaki Matsuda. Xenogeneic silencing-mediated regulation of T3SS2 in *Vibrio parahaemolyticus*. The 95th Annual Meeting of Japanese Society of Bacteriology. 29-31 March 2022. On-demand oral presentation. (Accepted to be a presenter)